MECHANICS OF SOFT TISSUES AND BODY LOADING: EXPERIMENTAL RESEARCH FOR THE PURPOSE OF PRESSURE INJURY PREVENTION AND MODELING

By

Justin D. Scott

A DISSERTATION

Submitted to
Michigan State University
in partial fulfillment of the requirements
for the degree of

Engineering Mechanics – Doctor of Philosophy

2021

ABSTRACT

MECHANICS OF SOFT TISSUES AND BODY LOADING: EXPERIMENTAL RESEARCH FOR THE PURPOSE OF PRESSURE INJURY PREVENTION AND MODELING

By

Justin D. Scott

Over 3 million people in the United States rely on wheelchairs, spending about 12 hours in a wheelchair every day to carry out tasks of daily living [1], [2]. A common and expensive side effect of wheelchair use is the formation of pressure injuries, which are a result of sustained normal and shear pressures on the body, such as those experienced in the buttocks and thighs while seated [3]–[6]. The prevalence of pressure injuries in wheelchair users in care facilities is as high as 47%, and treatment costs up to $120,000 per incident [7], [8]. Because pressure injuries are destructive, both in terms of quality of life and financially, there is a clear need for strategies to prevent them.

Despite advances in technology used to prevent pressure injuries and models that assess risk, both the new technology and models have limitations. Even with the implementation of new wheelchairs, wheelchair cushions, and other pressure injury prevention tools, pressure injury prevalence only declined by one third over the past decade [9]. From the modeling perspective, the most advanced buttock and thigh models still use limited data from humans, excluding critical data from wheelchair users, the population most at risk for developing pressure injuries [10].

As such, the goals of this dissertation were to 1) determine the material properties of wheelchair users' buttocks and thighs and compare them to those of able-bodied people, 2) to design an articulating chair that can reduce the seated normal pressure on the buttocks, and 3) to evaluate the ability of several seat pan covers to reduce shear pressure on the buttocks while seated.

The first task was to create a protocol to determine the material properties of the buttocks and thighs in a position representative of the seated position and accessible to wheelchair users.

Force and deflection data of the buttocks and thighs of able-bodied people were obtained in seated, quadruped, and prone positions. It was found that the buttocks and thighs were similar in the seated and quadruped positions. As the quadruped position was accessible, it was used to test wheelchair users; and data collected from the buttocks to the middle regions of the thighs were softer in wheelchair users than able-bodied people, while the distal thighs of wheelchair users were stiffer.

An accessible articulating chair was created with independently rotating parts, including seat pan, back, pelvic support, and thoracic support. The chair was used to collect seated interface pressure data during induced back recline, seat pan tilt, and changes to back articulation in able-bodied individuals and wheelchair users. Recline increased pressure on the buttocks, while seat pan tilt decreased pressure on the buttocks, and changes in back articulation changed pressure patterns on the back.

Three seat pan covers were evaluated for their coefficients of friction when paired with materials used to make pants and their abilities to reduce shear pressure on the buttocks of seated individuals. A sled was used to determine the coefficients of friction of pants materials on vinyl, one-layer nylon, and two-layer nylon seat pan covers. Coefficients of friction were compared to values found using human participants, and finally it was shown that the two-layer nylon seat pan cover reduced shear on seated individuals in the articulating chair while undergoing back recline.

The material property data from the buttocks and thighs and the interface pressure data collected represent advances in both pressure injury risk assessment and prevention. The material property data from wheelchair users were the first of their kind and can be used in finite element models. Data collected from the articulating chair and seat pan covers yielded interface and boundary conditions for models of the seated buttocks and thighs as well as strategies to reduce the normal and shear pressures on the buttocks and thighs, reducing the risk of pressure injuries.

This work is dedicated to Alexander Spaulding Hobbs,
a man who is more inspirational than he can know,
who taught us that nobody should ever be left behind or forgotten
and to treat everyone and everything with respect and dignity.
His benevolence is an ideal for which we all can strive.
Without him, this dissertation would not have been possible.
Thank you.

ACKNOWLEDGEMENTS

This dissertation is the result of a joint effort by so many individuals that it is difficult to give credit to everyone who deserves it. So many people have guided me in my development, allowed me into their spaces to do research, and helped me conduct the research as well.

To everyone who supported me in my journey to graduate school, this would not have been possible without you. My parents and friends from Rutgers have all helped me become literate in the language of academia, which opened up the opportunity that brought me to Michigan.

Since I have been at Michigan State, Dr. Bush has been a constant source of inspiration and has helped me refine myself into a better person and researcher. Her contributions to my work cannot be overstated, and she has cultivated an environment in the Biomechanical Design Research Lab that fosters student growth. Neither can the contributions of my committee, including Dr. Grimm, Dr. Roccabianca, and Dr. Slade, be ignored. All have taught me and contributed to my growth, whether formally in the classroom, by asking the right questions in meetings, or by offering their expertise when needed.

My experience has also been shaped by the people who have facilitated my research and become my friends in the process. Piotr Pasik's tolerance of my oft strange requests and openness in allowing me to participate in the Adaptive Sports Club has been a blessing. Brian Sheridan and the staff at Level 11 are some of the most competent and caring people I have met. And, of course, the undergraduates I have had the privilege of working with have made this dissertation possible.

Last, but not least, Ania and I have been partners through a lot. A lot of late nights and a lot of life development over the past few years. But we have given each other a lot of support and a lot of love. I could not have done this without you.

TABLE OF CONTENTS

LIST OF TABLES

LIST OF FIGURES

INTRODUCTION

Pressure injuries (PIs) are a dire issue for populations who use wheelchairs, including people with spinal cord injuries, surgery patients, and elderly individuals [7], [11], [12]. The prevalence of PIs in these populations can be as high as 47% in persons with spinal cord injuries and 61% in elderly individuals [7], [11]. Not only are PIs prevalent across several populations, but they are expensive to treat and can require a lengthy recovery. The average cost of treatment is approximately $35,000, and PIs can take up to 22 weeks to heal [13], [14]. These factors contribute to the $27 billion annual expenditure for PI treatment in the United States and motivate research efforts for methods to reduce the incidence of PIs [15].

Among the risk factors associated most intimately with PI formation are sustained normal and shear pressures on soft tissues and the internal stresses and strains they cause [16]. Such pressures, stresses, and strains are common in the buttocks, thighs, and lower back while seated; and over half of PIs in wheelchair users occur around bony prominences in the buttocks, thighs, and lower back, such as the greater trochanters, ischial tuberosities, and sacrum [17]. Therefore, efforts have been made to quantify and reduce pressure, tissue stresses, and tissue strains in those regions. Finite element models have been created to estimate the internal stresses and strains in the buttocks and thighs under seated loading conditions [18]–[20]. Meanwhile, common practices to reduce normal and shear pressures on the body while seated include repositioning strategies—such as reclining the back of a chair, and the use of specialized cushions [2], [21]. In these ways, clinicians and researchers have been working to understand and reduce to risk of PI formation.

Even with the progress in modeling research and clinical practices related to PI prevention, there are still consistent limitations in each area. From a modeling perspective, several inputs are needed to determine the stresses and strains in the buttocks and thighs under seated loading. The

seated load itself, the geometry of the buttocks and thighs, and accurate material properties of the buttocks and thighs are required to estimate internal stresses and strains. Though models have attempted to estimate internal stresses and strains of humans in the seated position, the models used to do so included material properties from animals [18]–[20]. While some studies reported material properties of the human buttocks and thighs, those studies investigated able-bodied people lying down [22], [23]. Thus, they represent able-bodied people lying down and not seated wheelchair users, a crucial difference for models of the buttocks and thighs.

From a clinical perspective, incidence of PIs is still a significant issue. Specialized cushions are able to reduce, but not eliminate, the incidence of PIs, leaving room to improve patient outcomes [21]. Further, the evidence supporting the use of recline as a pressure relieving strategy is inconclusive [4]. Recline decreases the normal load on the seat pan overall. However, there is a need to determine if the overall reduction translates to a pressure reduction on the bony regions of the buttocks. Furthermore, back recline shifts loading from the seat pan to the back, which may increase the risk of PI formation on the lower back (sacrum). Finally, back recline can increase shear force on the buttocks, which is another risk factor for PI development [4]. This makes strategies to reduce shear load on the buttocks critical to reducing PI risk in reclined positions.

Overall, this research aimed to develop and use novel technology to address the above limitations in clinical practices and more accurately characterize the mechanical responses of wheelchair users' soft tissues to external load. This was done by achieving five goals, addressed in chapters 2 through 6. The motivation of this work is further explained in **Chapter 1**, along with an in-depth literature review.

Chapter 2 determines and compares the material properties of the soft tissues in the buttocks and thighs of able-bodied people in the seated, quadruped, and prone positions.

Chapter 3 determines the material properties of the soft tissues in the buttocks and thighs of individuals with spinal cord injuries while in the quadruped position and compares them to the material properties of tissues in able-bodied people.

Chapter 4 evaluates the ability of an articulating chair design to redistribute pressure on the body of able-bodied people using back recline, seat pan tilt, and changes in back articulation. Changes in blood perfusion over the ischial tuberosity of the pelvis are also investigated as an additional factor associated with PI risk.

Chapter 5 evaluates the effects of back recline, seat pan tilt, and back articulation on interface pressures and perfusion over the ischial tuberosities of wheelchair users.

Chapter 6 determines the coefficients of friction between three seat pan covers (vinyl, one-layer nylon, and two-layer nylon) and common clothing fabrics using a sled, compares those coefficients of friction to those found with human participants, and finally evaluates the ability of the three seat pan covers to reduce shear load on the buttocks and thighs while seated.

A synopsis of the impact of this work is presented in the **Conclusions**.

As with many scientific writings, sections of this research either have been published or have been submitted to various academic journals. Chapters 2 and 3 have been published, and the citation information for the journal articles are included at the beginning of each chapter. Chapters 4 and 5 have been submitted and are awaiting review. Because each chapter is written as a standalone journal article, the motivations of this work, including the statistics, risk factors, and prevention strategies with respect to PIs are stated within each chapter. The research included in this dissertation was funded by NSF Grant CBET-1603646.

CHAPTER 1: A REVIEW OF THE STATISTICS, RISKS, PATHOPHYSIOLOGY, AND TREATMENT OF PRESSURE INJURIES IN THE BUTTOCKS AND THIGHS

Pressure Injury Definition

PIs are defined as localized damage to the skin and underlying soft tissue, usually over a bony prominence. Many times PIs are related to a medical devices, such as wheelchairs [24], [25]. PIs can either start in the skin or deeper tissue below the skin [26]–[28].

If the PI starts in the skin, a stage 1 injury is defined as the presence of a redness that blanches when pressed on by a finger. Stage 2 of an injury includes partial skin-loss, exposing the dermis. A stage 3 injury includes full skin-loss, exposing subcutaneous fat. A stage 4 injury has full skin and tissue loss, exposing the underlying bone. If there is significant debris in the injury, it can be deemed unstageable [24], [25].

PIs that start in deeper tissue versus the skin, termed deep tissue pressure injuries (DPTIs), are difficult to detect because of the lack of an external wound. A potential indicator for a DPTI is non-blanching redness. The stages for DPTIs are defined similarly to injuries that start in the skin, however the extent of the tissue damage is unknown until the wound opens. Thus, these injuries tend to have more layers of tissue damage before the injury is detected. Injuries may start in the deep tissue due to the loss of the epidermis' elasticity and decreased resilience in hypoxic conditions [27], [29]. The most common areas for PI formation are the buttocks, sacrum, greater trochanter, foot, and heel [16]. However, PIs may also form in other regions of the body, including the popliteal fossa, scapulae, and back of the head [30]–[33].

Prevalence and Statistics of Pressure Injuries

PIs are a stubborn medical problem in the United States healthcare system. Incidence in general hospital populations has been reported between 3% and 36% [34], [35]. In high risk populations, such as surgery patients post-operation or wheelchair using patients, the prevalence of PIs can be as high as 47% [7].

In addition to pervading the United States healthcare system, PIs are an issue all over the world. A recent global review showed that the prevalence of PIs in adults and children in hospital settings were shown to be 11% and 8%, respectively [36]. In Europe, PI prevalence rates can vary between 6% and 54% [30], [31], [37]–[43]. Several countries in Asia have reported prevalence rates between 8% and 29% [44]–[48]. Prevalence studies in South Africa, Brazil, and Australia reported 30%, 14%, and 12% prevalence as well [49]–[51]. PIs have been shown to be an issue in every care setting on almost every continent, demonstrating the global nature of the problem.

The prevalence of PIs in the United States has decreased since 2006, yet PIs have remained a significant issue for individuals in hospitals as well as those who use assistive devices [9], [12]. PIs affect as many as 10% to 27% of individuals in general hospitals and over a third of surgery patients [52], [53]. Depending on the type of facility at which the patient is being treated, the prevalence of PIs can vary. The prevalence of PIs is 15% of those in community care facilities, 19% of those in rehabilitative care, 27% of people in acute care facilities, and 47% in long-term acute care facilities acquire PIs [13], [54], [55].

Individuals with a spinal cord injury (SCI) are at a particularly high risk of developing PIs. The incidence of SCIs in the United States is about 50 people per million each year, leading to about 17,500 new cases of SCI each year [56]–[58]. This is in addition to the estimated 285,000 individuals currently living with a SCI in the United States [57]. The incidence of PIs in patients

with SCIs over four years of care can be as high as 30%, with a prevalence as high as 47% for those in long-term care [6], [7]. Additionally, 40% of patients with SCIs develop a PI during post-injury rehabilitation [17], [56], [59]. These factors contribute to a 80% lifetime incidence of PIs in individuals with SCIs [60], [61].

Individuals in community living facilities or nursing homes also experience high rates of PIs, even without SCIs. As many as 61% of individuals in nursing homes have PIs [11]. Even with the use of pressure relieving cushions, the incidence of PIs is as high as 40% per year for elderly individuals using wheelchairs. Moreover, those who experience PIs tend to have higher peak pressures beneath their buttocks than those who do not experience them [62]. Increased pressure under the buttocks is important, because almost 25% of all PIs occur in the soft tissue in that region [16], [63].

Financial Cost of Treating Pressure Injuries

Not only are PIs painful wounds that can greatly affect the quality of an individual's life, they are also expensive to treat. An average PI incurs total healthcare costs exceeding $35,000 per PI incident [13]. If a PI reaches stage 4 (bone exposed), the total healthcare cost can be greater than $120,000 for a single PI [8]. If a PI is acquired while being hospitalized for a separate issue, the treatment of the injury adds over $8,500 to the total cost of treatment for the individual [64]. These treatment costs add up to a total of $26.8 billion annually in the United States [15], [16]. The cost to society is clearly high, and the goal of preventing PIs entirely is the best solution.

Common Locations for Pressure Injuries

PIs commonly develop in the regions around bony prominences. While supine or seated, PIs are common around the calcanei, malleoli, greater trochanters, ischial tuberosities, coccyx, sacrum, and scapulae (Figure 1.1) [17], [21], [30]–[33], [37], [50], [51], [65], [66]. Three of those bony prominences, the ischial tuberosities, coccyx, and sacrum, are located in the buttocks and lower back, where about half of PIs occur [6], [65]. These regions in or near the buttocks are regions that experience large amounts of external pressure while supine or seated [20], [67], [68]. Blood perfusion in the those regions decreases as a result of the external pressure applied while in the supine or seated positions [69]. Additionally, PIs may form in or near the popliteal fossae of the knees while seated due to external pressure [70]–[74]. As will be discussed later, external pressure and decreased blood perfusion are two factors that facilitate the development of PIs; and they ultimately contribute to the risk of PI development in tissues near the bony prominence in and around the buttocks.

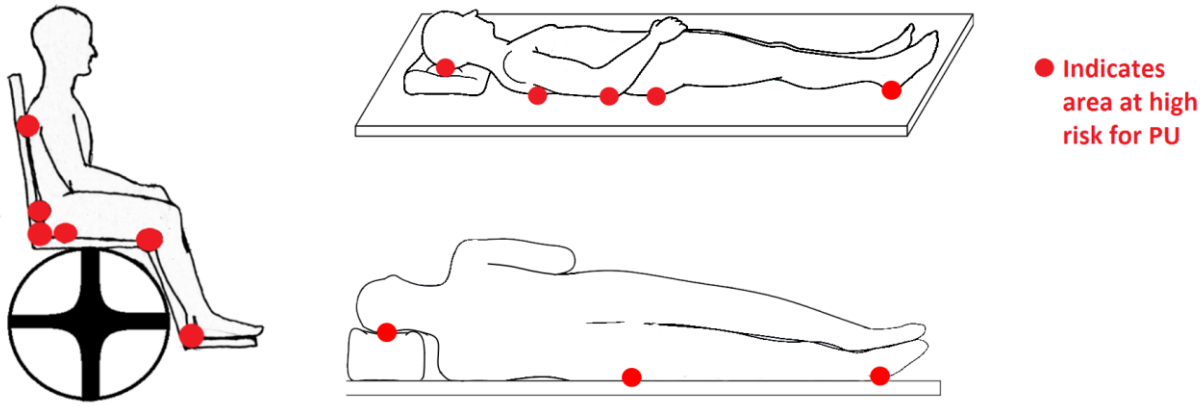

Figure 1.1 Left) Lateral view of a seated individual, with PI prone regions highlighted by red circles, including the calcaneus, popliteal fossa, ischial tuberosity, coccyx, sacrum, and scapulae. Top right) Lateral view of a supine individual with PI prone regions highlighted, including the occiput, scapulae, sacrum, ischial tuberosity, and calcaneus. Bottom right) Lateral view of an individual lying on their side with PI prone regions highlighted, including the ear, greater trochanter, and malleolus

Lower Back, Buttock and Thigh Anatomy

The lower back, buttocks and thighs are regions of the body that may experience PIs while seated. As mentioned in the previous section, PIs can occur near the sacrum, coccyx, ischial tuberosities, and near the popliteal fossae of the knees. Although PIs may form in other regions while lying down, these regions are at risk while seated. Because of the prevalence of PIs, it is important to understand the anatomy in these regions.

The lower back and buttocks regions consist of the pelvis and inferior aspects of the sacrum and coccyx encompassed by several layers of muscle, fat, and skin. The three regions of the pelvis are the ilium, pubis, and ischium. There are several bony landmarks on the pelvis. In the ilium, there is the anterior superior iliac spine (ASIS), anterior inferior iliac spine (AIIS), posterior superior iliac spine (PSIS), and posterior inferior iliac spine (PIIS). In the pubis, there is the pubic tubercle. The ischial tuberosity is on the ischium (Figure 1.2).

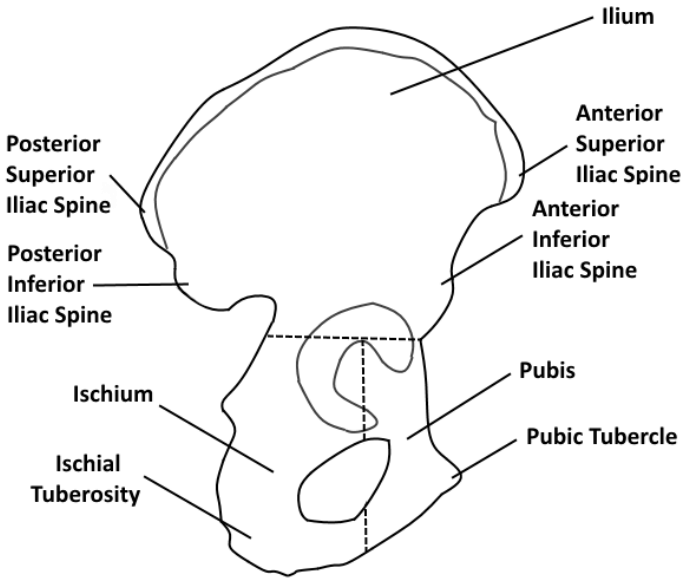

Figure 1.2 Lateral view of the right half of the pelvis with bony prominences labelled within their respective regions. The ilium is on the top, the pubis is in the bottom right, and the ischium is in the bottom left. PIs commonly form around bony prominences, such as the ischial tuberosity

Origins of the muscles in the buttocks are on the ilium and ischium of the pelvis, as well as the sacrum. Buttocks muscles originating on the ilium include the gluteus maximus, medius, and minimus. The gluteus minimus and medius insert on the greater trochanter, while the gluteus maximus inserts on the posterior femur. Muscles deep to the gluteal muscles that originate on the ischium (called lateral hip rotators) are the superior and inferior gemelli, quadratus femoris, and obturator internus, which insert on the greater trochanter. The piriformis originates on the sacrum, ultimately inserting on the greater trochanter as well (Figure 1.3). The gluteus maximus is the only muscle that overlays the ischial tuberosity and carries the most load while in the seated posture. Though there is adipose tissue as well, it is the only layer of muscle separating bone and skin over the ischial tuberosity [75]. The sacrum also has only a thin layer of muscle overlaying the bone.

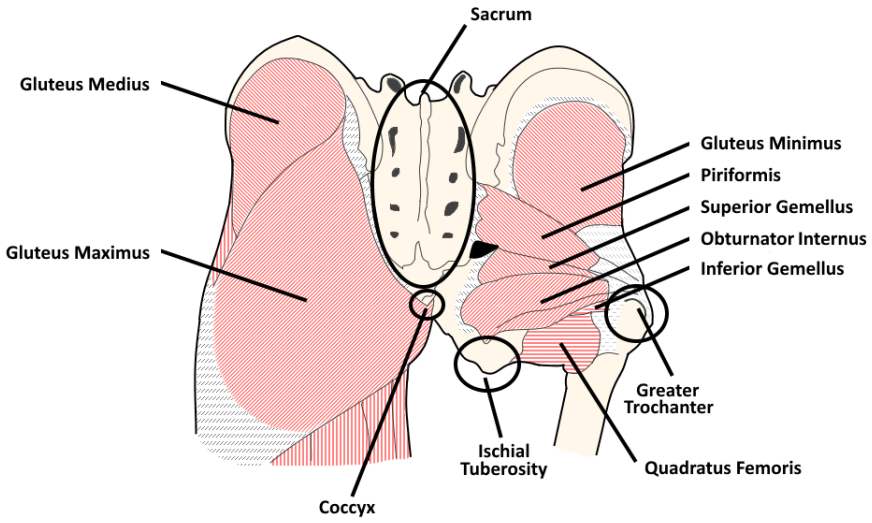

Figure 1.3 Buttock muscle origins and insertions. The regions around the ischial tuberosity, coccyx, greater trochanter, and sacrum, circled, carry the most load while seated and are especially prone to PIs

Origins of the muscles in the thighs are on the ilium, pubis, ischium, femurs, and ischial tuberosities (Figure 1.4). Several of the muscles have multiple origins and/or insertions. As mentioned before, the gluteus medius and maximus originate on the ilium and insert on the femur.

Adductor magnus and gracilis originate on both the pubis and ischium and insert on the femur and tibia, respectively. Vastus lateralis originates on the femur and inserts on the tibia, while one head of the biceps femoris originates on the femur and inserts on the fibula. The second head of the biceps femoris, the semitendinosus, the semimembranosus, and part of the adductor magnus originate on the ischial tuberosity and insert on the fibula, tibia (both semitendinosus and semimembranosus), and femur, respectively. The ischial tuberosities are bony prominences of the buttocks that are covered by or attached to muscles in the buttocks and thighs, and the surrounding tissues are prone to PI formation [17], [33]. Though there is not muscle tissue covering the popliteal fossae of the knees, the tendons of the gracilis, vastus lateralis, biceps femoris, semitendinosus, and semimembranosus all cover the region, where PIs may also occur [70]–[74].

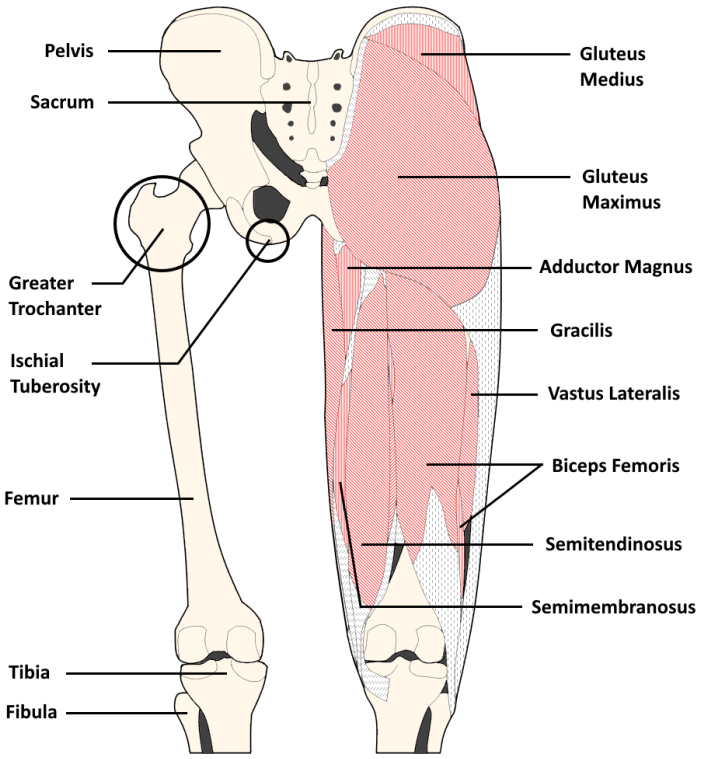

Figure 1.4 Thigh muscle origins and insertions. The ischial tuberosities and greater trochanter (circled) are prone to PI formation and are covered by the thigh muscles, as shown

Anatomical Changes in the Buttock and Thigh Soft Tissue

Spinal Cord Injury

Anatomical changes to the tissue in the lower limbs (buttocks and thighs) have been documented for those who have a SCI. Changes in skeletal muscle cross sectional area are rapid in patients with SCIs, whether they have complete or incomplete injuries. While both types of injuries cause muscle atrophy, it is exacerbated in people with complete SCIs, with as much as a 45% decrease in the area of skeletal muscle within the first six weeks post injury [76], [77]. These changes in cross sectional area have been confirmed using both MRIs and CT scans [78]. SCI also leads to adipose tissue infiltrating lower limb muscles, which can affect their ability to contract regardless of the classification of the SCI [79], [80]. Further changes to lower limb muscle tissue include a gradual change of type 1 (oxidative) muscle fibers to type 2 (glycolytic) muscle fibers post-injury [81]. All these tissue changes, especially the deterioration of muscle in terms of quantity and quality, increase internal tissue stresses when the tissue is loaded and increase the risk of PI formation [82], [83].

Aging

As people age, the soft tissue in their buttocks undergoes changes in structure. X-ray scans have shown that the cross-sectional area of skeletal muscles peaks between the ages of 30 and 50, after which muscle size generally decreases due to decreases in hormonal production and physical activity [84], [85]. The skeletal muscle cross sectional area of elderly individuals is about 40% smaller than the area of individuals in the peak age range [86]. In addition to the muscles physically getting smaller as individuals age, their ability to exert forces diminishes as well, which is in part a result of the reduction in size and number of type 2 muscle fibers with aging [87]–[89]. Similarly

to individuals with SCIs, these tissue changes put the tissue at risk of PI formation due to increased tissue stresses when loaded.

Risk Factors for Pressure Injuries

Scales have been created to assess the risk of PI development. These include the Norton, Waterlow, and Braden Q scales, but by far the most widely used tool is the Braden Scale [90], [91]. The Braden Scale has six risk categories, where lower scores in each of the categories indicates a higher risk of PI development. Figure 1.5 shows the six categories: sensory perception, mobility, activity, moisture, nutrition, and friction/shear [33], [66]. Research into the prevention of PIs has largely focused on reducing the risk in those six areas. Thus, reducing PI risk involves increasing sensory perception, mobility, activity, and nutrition levels while decreasing moisture and friction/shear. This section focuses on the mechanical aspects of the Braden Scale, namely mobility, activity, and friction/shear, which are directly linked to the research conducted for this dissertation. Moisture will be discussed briefly as part of current research into the effects of microclimate on PI development.

Individuals with decreased mobility are at an increased risk of developing PIs. Elderly people are at an increased risk, particularly wheelchair users and the bedridden individuals [60]. Those with SCIs have an elevated risk of experiencing PIs as well; and the risk of developing a PI scales with the severity of the injury. Studies show that there are not just two categories, “low risk” and “high risk”; rather, mobility is a continuous spectrum and that less mobility leads to higher risk of PI formation.

Sensory Perception – ability to respond meaningfully to pressure-related discomfort			
1. Completely Limited – Unresponsive to painful stimuli, due to diminished level of consciousness	**2. Very Limited –** Responds only to painful stimuli. Conveys discomfort only by restlessness	**3. Slightly Limited –** Responds to verbal commands but cannot always convey discomfort	**4. No Impairment –** Responds to verbal commands. Has no sensory deficit
Moisture – degree to which skin is exposed to moisture			
1. Constantly Moist – Skin is moist constantly by sweat, urine, etc. Dampness every time the patient is moved	**2. Very Moist –** Skin is often, but not always moist. Linen must be changed at least once a shift	**3. Occasionally Moist –** Skin is occasionally moist, requiring an extra linen change once a day	**4. Rarely Moist –** Skin is usually dry, linen only requires changing at routing intervals
Activity – degree of physical activity			
1. Bedfast – Confined to bed	**2. Chairfast –** Ability to walk severely limited or non-existent. Cannot bear own weight and/or must be assisted into chair or wheelchair	**3. Walks occasionally –** walks occasionally during day, but short distances, with or without assistance. Spends most time in bed or chair	**4. Walks frequently –** Walks outside room at least twice a day and inside room at least once every two hours during waking hours.
Mobility – ability to change and control body position			
1. Completely Immobile – Does not make any changes in body position without assistance	**2. Very Limited –** Makes occasional slight changes in body position but unable to make frequent changes	**3. Slightly Limited –** Makes frequent though slight changes in body or extremity position independently	**4. No Limitation –** Makes major and frequent changes in position without assistance
Nutrition – usual food intake pattern			
1. Very Poor – Never eats a complete meal. Rarely eats more than ½ of any food offered. Eats 2 servings or less of protein per day. Does not take a liquid supplement	**2. Probably Inadequate –** Rarely eats a complete meal and generally eats ½ of food offered. 3 servings of protein per day. Occasionally takes a supplement	**3. Adequate –** Eats over ½ of most meals. Eats 4 servings of protein per day. Occasionally will refuse a meal, but will usually take a supplement when offered	**4. Excellent –** Eats most of every meal. Usually eats 4 or more servings of protein per day. Occasionally eats between meals. Does not require supplementation.
Friction & Shear			
1. Problem – Needs at least moderate help to move. Cannot lift without sliding against sheets. Slides in bed or chair, needing repositioning with help. Spasticity, contractures or agitation leads to constant friction.	**2. Potential Problem –** Moves feebly or requires help. While moving, skin slides to some extent against sheets, chair, etc. Maintains relatively good position in chair or bed most of the time but occasionally slides.	**3. No Apparent Problem –** Moves in bed and in chair independently and has sufficient muscle strength to lift up completely during move. Maintains good position in bed or chair.	**4. N/A**

Figure 1.5 Sample Braden Scale assessment sheet. Lowers in any of the six categories indicate higher risk for developing a PI. Categories shaded in blue are addressed in this research

Activity level is another factor that affects the risk of an individual acquiring a PI. Reduced activity, such as that seen in individuals with chronic pain, can increase the likelihood of obtaining a PI [92]. Using an assistive device may also directly contribute to PI risk [24]. Over half of elderly individuals and people with SCIs report chronic pain. Further, a quarter of elderly people use an assistive device to ambulate and experience some trouble walking, while almost every individual with a SCI uses an assistive device [93]–[95]. Therefore, both chronic pain and assistive device use are factors that contribute PI risk in both populations via decreased mobility. This decrease in mobility has led to deceased activity levels in both populations, which contributes to the high PI prevalence [96], [97].

Friction and shear force (force parallel to the skin) are cited as risk factors for the development of PIs in 1) the Braden scale, 2) literature that predates the Braden scale, and 3) in subsequent literature [98], [99]. This is in part due to the reduction in blood perfusion in the tissue when shear force is applied [28], [100]–[102]. Yet both normal forces (forces perpendicular to the skin) and shear forces are capable of reducing the blood perfusion in the loaded tissue, so both should be considered as risk factors for PI development [100]. Animal research has shown that soft tissues are able to sustain normal loads greater than 45 kilopascals as long as they are intermittently relieved, whereas loads as small as 9 kilopascals have been shown to cause tissue damage if sustained for two hours without relief [103]–[107]. Pressures of 32 kilopascals can start causing tissue damage if they are sustained for longer than 15 minutes [106]. This value of pressure is clinically significant because the peak normal pressures on the buttocks of seated individuals is about 28 kilopascals, indicating a risk of tissue damage within the first two hours if the pressure is not relieved [108]–[112].

Microclimate is a relatively new area of study that describes the environment surrounding a PI, with particular emphasis on the humidity and temperature of the region around the wound. The microclimate around the wound has several effects on the tissue. For example, increasing either the temperature or humidity of the microclimate increases the coefficient of friction between skin and fabric [113]–[116]. In addition to increasing the coefficient of friction, increasing the temperature and humidity decreases the stiffness and ultimate strength of skin. Because of these effects of temperature and humidity, there have been several attempts to control the microclimate around areas that are prone to PI formation. One such study investigated the use of Dartex, spandex, and incontinence (moisture-blocking) covers to control temperature and moisture of the ischial region of the buttocks but found no clear benefits [117]. Another study investigated the use of an insert between the buttocks and cushion, which had limited effects on both temperature and humidity [118]. As there has yet to be any cushion, insert, or cover that significantly decreases temperature and moisture, there is still a need for equipment that keeps the ischial region cool and dry.

Mechanisms of PI Development

Multiple theories have been proposed to explain the mechanism of tissue death. There is evidence that the origins of PIs within tissues are related to the normal and shear pressures applied to the tissue. Shear pressures have been stated to cause superficial injuries in the skin, and normal pressures are believed to cause deep tissue injuries in the muscle [27]. Within the affected tissue, there are several mechanisms by which the pressures can cause necrosis.

Occlusion of blood perfusion to soft tissue has been observed with normal pressures as small as 12 kilopascals [119]. Including shear pressure in addition to normal pressure augments

the effect of normal pressure on blood perfusion occlusion [101], [120]. Without blood perfusion, the tissue does not receive oxygen and thus undergoes anaerobic respiration to produce energy. Anaerobic respiration produces lactic acid as waste, which builds up in the tissue since there is no blood perfusion to carry the lactic acid away from the tissue, lowering the pH of the tissue. This lack of oxygen and lowered pH causes tissue necrosis over time, even with relatively small applied pressures [121].

In the same way that blood perfusion may be occluded by sustained pressures, the lymphatic system is also affected. Cellular waste that is not transported through the cardiovascular system may be transported through the lymphatic system. However, this system is also disrupted by applied pressures. Interstitial fluid is the fluid in the body that is neither within the cells nor the cardiovascular system. The lymphatic system normally maintains the interstitial fluid when the soft tissue is not loaded. However, a 10% increase of interstitial fluid per unit of muscle volume has been seen in subjects with external load sustained on their soft tissue. The pressures on the tissues result in reduced interstitial fluid flow, leaving more cellular waste in the tissue, eventually causing tissue damage [26].

PI development can occur quickly with direct compression of the tissue as well. Large amounts (greater than 32 kilopascals) of normal pressure on the tissue can initiate changes in the tissue within as little as 15 minutes. When tissue is compressed to 40% of its original size for one hour, necrosis can occur; and when tissue is compressed to 55% of its original size, necrosis can happen in less than five hours [26]. These results align with those previously reported, giving a time frame for cell death between one and two hours [105], [106].

Regardless of the mechanism of tissue necrosis, the underlying cause of it is the presence of external loads. These loads result in internal stresses, which in turn cause occlusion of the cardiovascular and lymphatic systems as well as tissue deformation [26].

Shear Forces

While the effects of normal forces on the soft tissue have been widely studied with respect to the issue of PIs, shear forces have been examined in a relatively small number of studies. The idea that shear forces may have a role in PI formation has been around for over half a century, and has been reaffirmed by its inclusion in the Braden Scale and recent studies that suggest reducing shear force may be the most effective way to reduce PIs [91], [98], [101], [122], [123]. There were numerous studies that investigated the effects of external shear force on the perfusion and vasculature of the skin [28], [101], [120], [124]. However, none of these studies focused on the perfusion of thigh and buttock tissue while seated.

Studies investigating the effects of seated shear load on the buttocks and thighs are lacking. One study investigated the effects of posture on the shear forces on the buttocks and thighs while seated [125]. Yet this study only investigated the gross shear force on the buttocks and thighs together while seated, so the shear on individual regions could not be estimated. Even in the most advanced experimental chair designs used to quantify the seat pan-soft tissue interaction have limitations with regards to their ability to measure shear force [126]. There has yet to be an investigation into the effects of shear forces on the blood perfusion in the buttocks and thighs while seated; and this includes shear forces in different postures. Posture change has been shown to affect both normal and shear forces, but the effects on blood perfusion due to those changes is not available in the literature [125]. Therefore, it is necessary to describe the interaction between

posture change, shear force measurements, and blood perfusion measurements and then leverage that interaction to prevent PIs.

Medical Attention for Pressure Injuries

Treatment

Several methods have been used clinically to treat PIs. Stage one injuries heal the fastest (16.9 days on average), and stage four injuries can take up to 22 weeks on average to heal [14], [16]. Regardless of the type of treatment, the wound area is always offloaded [127]. Wounds are first cleaned and debrided of any dead tissue [128]. After cleaning, antibiotics and several topical treatments are applied to reduce the amount of time needed for healing to occur [129]. Among them are collagen, hydrofoam, hydropolymer, and hydrocolloid dressings, which have been shown to decrease time to healing for injuries [130]–[132]. Alginate and silver nano particle dressings have been used, although less frequently. Negative pressures and electric stimulation have also been applied topically to wounds to create a more hospitable healing environment [133]. In addition to surface treatments, nutritional supplements like collagen peptides have shown some benefit to PI recovery [134]. In serious cases, surgery may be used to excise the injured tissue surrounding the PI, and the wound may be covered by a flap of healthy tissue from the surrounding area [128], [135].

Prevention

There are several measures that are currently taken to prevent the occurrence of PIs, as prevention is more desirable than treatment. The cost of PI prevention in inpatient facilities is actually less expensive than treatment [136]. Further, prevention of a PI is more desirable than

treatment from a patient care perspective. In a clinical setting, prevention includes a daily risk assessment, nutrition assessment, consistent repositioning, the use of specialized support surfaces, prophylactic dressing, and moisture/incontinence control [129], [133], [137]–[142]. Some of these prevention strategies were shown to lead to lower PI incidence and reduced healthcare costs [90], [136], [143]. If carefully implemented, prevention measures have, in some cases, been shown to eliminate the incidence of PIs in inpatient settings [54], [144]. These strategies become especially important after surgery, when the risk of PI development can be mitigated by properly dressing the area on which the operation occurred as well as areas that commonly experience large loads [145]. Pressure relieving equipment (such as an adjustable bed) has also been introduced in inpatient settings, however the equipment is not as effective as increased time with nurses [138], [146]. Prevention not only reduces the cost of healthcare, but it saves the patients time in the hospital because they do not have to recover from a PI.

Outpatient modalities of PI prevention have focused on pressure relieving wheelchair cushions, wheelchairs adjustments, and pressure-relieving movements carried out by the user. Specialized cushions have shown promise in reducing the incidence of PI in wheelchair users but have not eliminated the issue altogether [21], [133], [147]. Among the innovations in pressure reducing seat cushions are developments in contoured cushions that are molded to the wheelchair users' buttocks, modular cushions with areas of varying stiffness or materials, and dynamic cushions with air bladders that inflate sections of the cushion to be loaded while deflating sections of the cushion to be offloaded [148]–[157]. Common measurements used to determine the effectiveness of cushions are contact area, mean pressure, and peak pressure [5], [111], [158]. Increasing area of contact and decreasing mean and peak pressure are generally considered desirable to reduce the risk of PIs. Pressure relieving cushions have been able to reduce the peak

pressures in the buttocks by up to 40%, but they have been unable to reduce the pressure on the buttocks to less than 32 millimeters of mercury, which is the intra-arteriolar pressure [159], [160]. Thus, these cushions have not eliminated the risk of blood vessel occlusion nor the risk of PIs.

In general, chair adjustments such as whole body tilt and back recline are the most utilized ways of relieving pressure on the buttocks [2]. Whole body tilt describes a simultaneous rotation of the chair back and seat pan that results in the seated individual facing upward. Tilting has been shown to decrease pressures and improve blood perfusion in the buttocks if the whole body is tilted by at least 35° [161]. However, this angle of tilt is often impractical for everyday tasks and makes interactions with other people more difficult for the chair user. Furthermore, it increases the pressure on the lower back, another location where PIs often occur [16], [63], [125]. Recline has been shown to reduce the normal force on the buttocks while seated, but has also shown an increase in shear force on the same area, thus decreasing one risk factor for PI development while increasing another [108], [162].

Load relieving movements carried out by the seated individual have also been evaluated for use in outpatient settings and daily life, provided that the person has enough strength and mobility to perform them. Movements like forward and lateral trunk tilt have been introduced as a means by which chair occupants may offload regions of their buttocks. Forward bending of the trunk has been shown to reduce peak pressures on the buttocks by approximately 10% [125]. Meanwhile, lateral trunk tilt offloads the contralateral side of the body, but tissues in the ipsilateral side of the body experience pressures that can put them at risk for PI development [20], [108], [163]. Other movements that completely offload the buttocks, such as the wheelchair user lifting themselves off of their cushion (a wheelchair pushup), have been proposed. But the lift has to be

held for almost two minutes for blood perfusion to return to pre-loaded levels, and can thus be difficult to perform [164].

Experimental Methods for Pressure Reduction

Existing PI prevention strategies have reduced the prevalence of PIs, however they have not been able to eliminate the risk of PIs altogether [9], [12]. As PIs are still a significant issue for many people, there are ongoing efforts to further diminish the risk of PI development. Many of these efforts are focused on modifications of the chairs on which people sit or changing the interfaces between the seated people and the chairs. In many cases, these modifications are tantamount to updates to currently existing technologies and PI prevention strategies.

Pressure Relieving Cushions

Cushions affect the peak pressure on the buttocks and thighs while seated. Peak pressure on the soft tissue in the buttocks and thighs while seated has been an indicator of the risk for PI development, and two cushion-dependent mechanisms have been found to increase the peak pressure on those regions while seated [62]. If a cushion is too stiff, the cushion will not distribute the pressure on the buttocks and thighs, creating a pressure concentration near the bony prominences. If a cushion is too soft, bony areas sink into the cushion until it "bottoms out", or is not able to be compressed anymore. Once the cushion "bottoms out", it will no longer distribute pressure over the compressed areas, once again creating a pressure concentration near bony prominences on the buttocks and thighs. Therefore, there is an optimal stiffness for a cushion used in seating, where the cushion distributes pressure without bottoming out [165]. A limitation of the optimal stiffness found in this study is that all the participants in the study were able-bodied. This

limitation is significant because studies have shown individuals with SCIs have larger pressure concentrations on bony prominences and different anatomies while seated relative to able-bodied individuals [77], [79], [108], [160]. Because of this, it is imperative to optimize cushion material properties to reduce the risk of PIs in high-risk populations, such as those with SCIs.

Shear pressure has also been noted as a risk factor for PI development, and there is a need to reduce shear pressure on the buttocks and thighs while seated [91], [143], [166]. One avenue by which shear pressure can be reduced is by the introduction of a shear reducing cushion cover. Though reducing shear with a cushion cover may be a viable strategy, research on new shear reducing cushion covers is limited. There have been studies on the effects of seated posture on shear [4], [167]. There have been studies on the effects of skin microclimate on shear [113]–[115]. Yet there have been very few studies on the effects of shear reducing cushion covers. To the extent that shear reducing cushion covers have been studied, one recent cover mechanism was able to reduce shear pressure *while adjusting* to a reclined posture relative to a control cover [168]. However, the mechanism actually increased shear pressure *while in* the reclined posture relative to the control cover. Since seated individuals spend more time in a static posture than switching between postures, this mechanism is limited. Due to the lack of research in shear reducing cushion covers, there is a clear need to improve upon existing cushion covers to reduce the shear, and thus the PI risk, in seated individuals.

Finite Element Evaluations of Internal Stress

Finite element models evaluate the effects of normal and shear forces by considering the entire model as a group of smaller, connected pieces that transmit load to one another. Each piece in the model deforms based on inputs, such as the geometry of the model, the material of the model,

and the normal and shear forces applied. Finite element models have been used to evaluate PI prevention strategies. Such models investigated the effects of changing the material properties or shapes of the specialized cushions used to prevent PIs [169]–[173]. There have been vast improvements in some model inputs, like anatomically correct 3-D model geometry. However, accurate *in-vivo* material properties of tissues are still needed to improve models' accuracy.

Advances in Geometry

There have been improvements in the techniques used to create the geometry of finite element models, which have advanced from two-dimensional to three-dimensional models [18], [174], [175]. Two-dimensional models were used to show how slices of the thighs and buttocks responded while under seated load and evaluated how changes in posture affected the load [20], [174]. However, it has been shown that material properties and internal stress of the tissue differ when considering two dimensional slices and a full three-dimensional model [10], [19]. Patient-specific three-dimensional finite element models either used a homogeneous material to represent the soft tissue or utilized a more detailed geometry captured by MRI [18], [175]–[182]. Regardless of the model geometry, there was a noted lack of realistic material properties for *in-vivo* human soft tissues in the seated position.

A relatively new consideration in finite element modeling has been to investigate how external pressures affected internal anatomical structures, such as vasculature. Previously, the geometry of the vasculature had been ignored, but recently one area under investigation has been the skin and its blood vessels. Numerous finite element models investigated the change in cross sectional area and blood flow of blood vessels after normal stress was applied by using fractal patterns to model the geometry of the vasculature [183]–[185]. Some models evaluated the effect

of shear force and friction on vessel size and blood flow [183]. However, authors of these studies noted that the properties of skin varied greatly depending on the storage and testing conditions, highlighting again the need for accurate material properties. Despite the lack of appropriate material properties for skin, models provided insight into the amount of external pressure that may cause blood flow occlusion.

Descriptions of Soft Tissue: Linear Elastic Models

The behaviors of materials, such as soft tissues, are described by material models when using finite element programs. The choice of material models used to represent materials is of the utmost importance when the goal is to have accurate evaluations of internal stresses and deformations via finite element modeling.

The simplest material model used is a linear elastic model, where the internal stress is directly proportional to strain in the material. Strain is represented by Ɛ and defined as follows:

$$strain = \epsilon = \frac{new\ material\ thickness - old\ material\ thickness}{old\ material\ thickness} \quad \text{(Eq. 1.1)}$$

This type of material behavior was popular due to its simplicity. Because of its simplicity, investigators used linear elastic behavior to represent the tissue in the thighs and buttocks in models dating back to the 1970s [186]. Models used linear elastic representations of tissue to determine stresses in the buttocks while lying in the supine position [187]. Further, investigations using linear elastic material properties for tissues obtained results like those showing an increase in the thickness of a cushion to more than eight centimeters did not improve the pressure distribution abilities of the cushion [188]. More recent uses of linear elastic materials to represent the soft tissue took advantage of the material's simplicity to monitor the internal stresses in the soft tissue in real-

time [189]. However, it was largely determined that soft tissue was not accurately represented by linear elastic materials, meaning that most recent finite element models did not consider linear elastic materials to represent soft tissue [190].

Descriptions of Soft Tissue: Hyperelastic Models

Most researchers started using hyperelastic material models to represent soft tissues. The equations that represent common hyperelastic models can be found in Table 1.1. To determine the relationship between the stress and the deformation for any hyperelastic material, the derivative of the potential function must be taken with respect to the stretch of the material. Eqs. 1.2 and 1.3 show how the stretch and the stress are determined, respectively:

$$stretch = \lambda = \frac{new\ length}{original\ length} \quad \text{(Eq. 1.2)}$$

$$stress = \ \sigma_i = J^{-1}\lambda_i \frac{d\Psi}{d\lambda_i} \quad \text{(Eq. 1.3)}$$

In the equation for stress, the subscript ‘i’ is used to denote that the stress can be found in any of the three principle directions by substituting either 1, 2, or 3 in for ‘i', J is the determinant of the Right Cauchy Green Strain tensor, and λ is a stretch in a principle direction. σ is the stress in a given direction, and Ψ is the strain energy function of the material model. When considering soft tissues with these material models, the Yeoh, Ogden, and Martins models were shown to best fit the uniaxial compression data from soft tissues, supporting their use for soft tissue representation [10], [191].

Despite their relatively poor performances with respect to the other material models, the Neo-Hookean and Mooney-Rivlin materials have been employed in several situations. Both Neo-

Hookean and Mooney-Rivlin representations of soft tissue were used to show that the highest stresses in the buttocks while seated were found in the muscle tissue near the ischial tuberosity [192]–[194]. Neo-Hookean materials were further used to show that stresses in the buttock tissue were in general lower for individuals within a normal body mass index range versus those in the low or high range [195]. Modifications to Neo-Hookean materials included damage components to show how the stiffening of the soft tissue as it encounters injury can create further stress concentrations in the surrounding tissue [196].

The Odgen material model performed well in describing the behavior of soft tissue, and has also been used in various investigations into the response of soft tissue while seated [10], [197]. Ogden materials have been used for over twenty years, spanning models that have been two dimensional up until recent models that use anatomically accurate three-dimensional geometries gathered from magnetic resonance images [18], [174]. A sensitivity analysis showed that the internal stresses evaluated by finite element models strongly relied on the material parameters used to inform the material [198]. This last study indicated the importance of carefully selected material parameters based on accurate experimental data to achieve realistic internal stress values.

Descriptions of Soft Tissue: Poro/Viscoelastic Models

Poroelastic and viscoelastic material models considered the time-dependent properties of materials. Like other types of materials, poroelastic and viscoelastic materials showed that the largest stresses in the buttocks and thighs while seated were in the muscle layers near the ischial tuberosities [199], [200]. Poroelastic and viscoelastic models also showed the benefits of using contoured versus flat cushions [201], that individuals with SCI experience larger stresses and

stretches in the buttocks while seated [82], and were used to explore the response of muscle tissue to vibration [202].

Table 1.1 Material models and their strain energy functions, with their parameters and dependence on the material deformation listed [191]

Material Name	Potential Function	Material Parameters	Dependence on Deformation
Mooney-Rivlin	$\Psi = \frac{\mu_1}{2}(I_1 - 3) - \frac{\mu_2}{2}(I_2 - 3)$	μ_1 and μ_2	Invariants of Right Cauchy Green Strain Tensor
Yeoh	$\Psi = \sum_{i=1}^{3} c_i (I_1 - 3)^i$	c_1, c_2, and c_3	First invariant of Right Cauchy Green Strain Tensor
Neo-Hookean	$\Psi = c_1(I_1 - 3)$	c_1	First invariant of Right Cauchy Green Strain Tensor
Ogden	$\Psi = \sum_{i=1}^{N} \frac{\mu_i}{\alpha_i}(\lambda_1^{\alpha_i} + \lambda_2^{\alpha_i} + \lambda_3^{\alpha_i} - 3)$	μ and α	Principle stretches
Humphrey	$\Psi = c(e^{Q} - 1)$	Q	Right Cauchy Green Stretch Tensor
Martins	$\Psi = c\left(e^{b(I_1-3)} - 1\right) + A(e^{a(\lambda_1-1)^2} - 1)$	a, b, c, and A	Principle stretch and first invariant of Right Cauchy Green Stretch Tensor
Veronda-Westmann	$\Psi = c_1\left[e^{\alpha(I_1-3)} - 1\right] - c_2(I_2 - 3) + g(I_3)$	c_1, c_2, and α	Invariants of Right Cauchy Green Stretch Tensor

Experimental Determination of Material Parameters

Regardless of the material model used to describe the soft tissue in the human body, experimental data were needed to verify the material properties of the tissue used in the models. Several of the finite element studies in the previous sections noted the dependence of internal stress evaluations on the appropriate selection of material model and material properties [191], [195], [198]. Of particular importance to the research performed for this dissertation is the need for material properties that accurately represent *in-vivo* human tissue while seated. These properties

are critical to represent the internal stresses in wheelchair users, however current material property data were collected from animals or humans in limited, specific situations.

Animal Studies

Material properties obtained from the mechanical testing of animal tissue were commonly used to inform finite element models that evaluate stresses in human tissue. Particularly common were studies that determined the material properties of soft tissue in rats and pigs. Investigations into the material properties of the rat soft tissue were able to determine the properties of rat muscle tissue independently [177], [203]. Additionally, material properties from rat soft tissue were used in several finite element models [175], [198]. Material property data from pigs were also collected and used in some of the most recent finite element models [18], [195], [204]. These animal data have been used to inform finite element models. But it has been noted that changes in the material parameter values, especially relative changes between fat and muscle, significantly impacted stresses and deformations in the respective tissues [204]. Therefore, there is a need to determine the material properties of human soft tissue to improve the accuracy of evaluations made with finite element models.

Human Studies

Data on the force and deflection of human soft tissue has been collected using various methods. However, there have been limitations in terms of their usefulness in representing the buttocks and thighs while seated. A few investigations of the force and deflection responses of the buttocks occurred while participants were laying down. There were indentation tests of the buttocks as well as force and deflection measurements taken through digital image correlation

[23], [205]–[209]. These data are limited in their usefulness in the seated position due to the fact that both the muscle thickness and tension in the gluteal muscles are different in the seated position with respect to lying down [210], [211]. An additional limitation to the data collected through digital image correlation was that the data were collected included only a few points, meaning there were not many (in some cases, only two) data points with which to fit the material model's parameters. Given that tissue is a nonlinear material, numerous data points are required to accurately fit parameters. The most recent investigations into the deformation of soft tissue in the buttocks while seated used magnetic resonance images to collect soft tissue deflection while in the seated position while loaded versus unloaded. While the deflections seen were accurate, there were only two load states considered, and only six males were included in the study [212]. So, a major flaw in this investigation was its attempt to characterize a nonlinear material using two data points and the single gender represented by the data. To more accurately represent the soft tissue of the buttocks while seated, more participants are required, particularly including both males and females, and more data points are needed while people are in the seated position. More data points per individual will allow for more accurate recreations of force-deflection curves in soft tissue while seated.

CHAPTER 2: THE EFFECTS OF BODY POSITION ON THE MATERIAL PROPERTIES OF SOFT TISSUE IN THE HUMAN THIGH

The contents of this chapter were originally published in the Journal of Mechanical Behavior of Biomedical Materials.

J. Scott, S. Chen, S. Roccabianca, and T. R. Bush, "The effects of body position on the material properties of soft tissue in the human thigh," *J. Mech. Behav. Biomed. Mater.*, vol. 110, 2020, doi: 10.1016/j.jmbbm.2020.103964.

Introduction

The number of people who have experienced PIs is staggering, creating a substantial financial burden for both individuals and society at large. Prevalence rates of PIs have been shown to be extremely high, depending on the setting. Approximately 40% of patients with spinal cord injuries (SCI) experienced PIs during rehabilitation [17]. 47% of wheelchair users in long-term care facilities had PIs [7]. Furthermore, over 60% of individuals who were admitted into geriatric care facilities had at least one pre-existing PI [11]. Because an average PI incurs over $35,000 in healthcare costs, PIs have added as much as $1.3 billion to medical expenses each year in the United States [13], [64], [111]. Half of these injuries were on the thigh or buttock regions, meaning that understanding the conditions leading to PIs in those areas is critical to reducing the risk and the cost [6], [16], [62], [147].

While the cellular mechanism of PI development is still undetermined, it has been generally agreed upon that internal stresses in the tissue were factors in PI development [26], [106], [213], [214]. Such stresses were reported in the thighs and buttocks while seated [106], [213]. Over time,

these stresses may cause stress-induced necrosis, vascular damage, reduced interstitial flow, and hypoxia due to a reduced volume of blood in the tissue. All of these potential mechanisms of PI formation are caused by internal stress [26], [27], [102], [215].

Finite element models have used the material properties of the buttocks and thighs to predict internal stresses that occur under seated loading conditions. Yet, determining appropriate material properties for use in these has been difficult. Some finite element models used tissue properties obtained from experiments on animals [191], [192], [198], [203], [216], [217]. More recently, *in vivo* indentation tests have been conducted to find the strains caused by forces applied to the human thighs and buttocks [207], [208]. However, there are significant limitations to these studies. Some used only two load states, unloaded and fully loaded, to obtain the material properties of the tissue. Two load states are not adequate because soft biological tissues are nonlinear materials, meaning that more than two load points are necessary for accurate material descriptions [191], [218]. However, there have been several models that have utilized material descriptions based on two loading states [18], [192], [216]. Other experimental studies have collected data with individuals in the prone or supine position [23], [205], [208], [219]. These positions have different knee and hip articulations as compared to the seated position; and joint articulations have been shown to affect the tensions in the tendons and the muscles, so it is likely that *in vivo* material properties will differ with body position [211], [220]. Furthermore, tissue thickness in the buttock region depends on the hip articulation, meaning that the same external loading on the soft tissue will not result in the same internal loading pattern when seated versus laying down [210].

Because wheelchair users are at an elevated risk for PI development in their thighs and buttocks while seated, accurate *in vivo* material descriptions for these tissues are needed. Testing

in the seated position is ideal, yet significant challenges exist with respect to obtaining the material properties of wheelchair users in a seated position. The authors conducted force-deflection testing on the buttocks and thighs in an elevated lab chair [10], [221]. That protocol required removing sections of the seat pan to expose the regions of interest, which reduced the stability of the person in the chair and called for balance and core strength that not every wheelchair user has. In addition, repeatedly transferring into and out of the elevated lab chair, as required by the mechanical testing protocol, was problematic for this population. The combination of those challenges makes testing in the seated position impossible for some wheelchair users, so developing a protocol for an alternative position is imperative.

The supported quadruped (crawling) position is common in physical therapy for wheelchair users and has the same knee and hip articulations as the seated position, making it a candidate for the data collection from wheelchair users. This position has the thigh and buttocks regions exposed for taking measurements, has a similar body configuration relative to the seated position, and many wheelchair users have experienced it while in physical therapy. Therefore, the supported quadruped position was included with the prone and seated positions for our experimental tests.

A need exists for *in vivo* material property data representing the thigh and buttocks region while in a seated or "seat-like" position. Previous work has obtained material property data for the thighs and buttocks with able-bodied individuals in the prone or supine positions, and these data have been used as an analog for the seated thighs and buttocks despite potential discrepancies [207], [208]. As such, the goals of this research were to determine and compare the material properties of the soft tissue in the thigh in the seated, quadruped, and prone positions.

Methods

Participant Recruitment

20 able-bodied individuals (10 males and 10 females) volunteered to participate in this study, which was approved by the Biomedical and Health Institutional Review Board at Michigan State University. Exclusion criteria for this study included active wounds on the buttocks or thighs, osteoporosis, occult bone disease, musculoskeletal diseases, and pregnancy.

Test positions

All participants wore snug-fitting, but stretchy pants or shorts to permit testing. The participants were tested in each of three positions: seated, quadruped (crawling), and prone (Figure 2.1). In the seated position, the participants sat on a chair with removable slats, each of which exposed a body region where the tissue testing was performed. In the quadruped position, participants faced the floor with their knees and hips flexed at ninety degrees and a support under their chest. In this position, their thighs were also blocked by a padded vertical barrier.

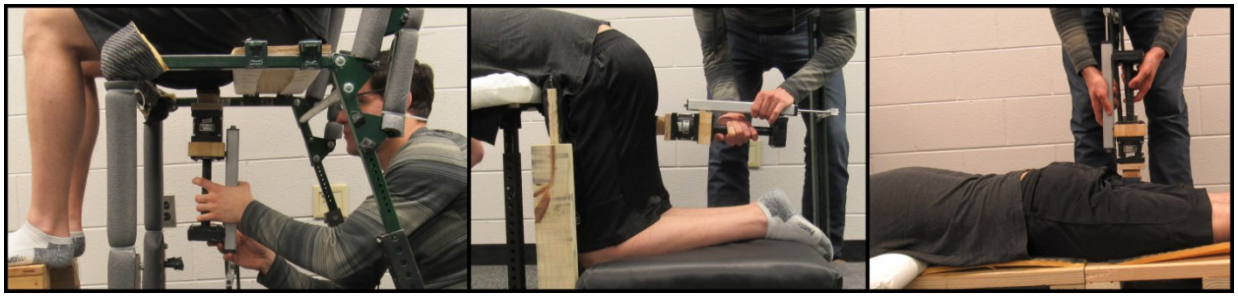

Figure 2.1 Indentation test setups for every position. The seated position (left) has a segment of the chair removed to expose the middle thigh region, the quadruped position (middle) allows access to the entire thigh without obstruction, as does the prone (right) position. In the seated position, the stand was placed beneath the participants, while it was placed behind them in the quadruped position, and above them in the prone position

Test Regions

The three test regions were all determined by their positions relative to the greater trochanter and lateral epicondyle of the femur (Figure 2.2a). The femoral length was defined as the distance between the greater trochanter and lateral epicondyle. The proximal thigh region was 10% of the femoral length distal to the greater trochanter. This region was just distal to the ischial tuberosity of the pelvis, which has been shown to be one of the most common regions for PI development [70]. Although this region is near the ischial tuberosity and could be termed the buttocks region, this region will be referred to as the proximal thigh region throughout the paper. The middle thigh region was 50% of the femoral length distal to the greater trochanter. And the distal region was 90% of the femoral length distal to the greater trochanter, another region where PIs form [71]. Thus, three regions were tested in all participants and are referred to as the proximal, middle and distal thigh regions.

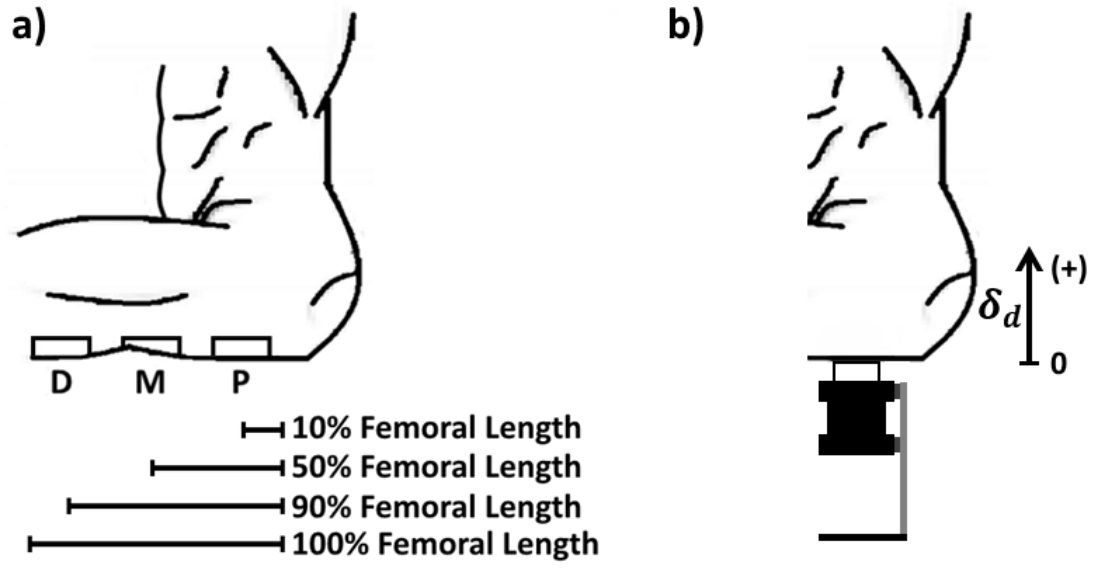

Figure 2.2 Regions of interest for the thigh tissue testing. The region labeled 'P' is the proximal region, 'M' is the middle region, and 'D' is the distal region. b) Zero deflection was determined by placing the indenting tool flush against skin. As the tissue was compressed a positive deflection was obtained

Tissue Testing Protocol

Force and deflection measurements of the soft tissue were collected via a custom-built indenter. The indenter was designed to collect force and deflection data continuously. The indenting surface was embedded with a load cell that obtained the force measures (AMTI, Watertown, MA). The tool was connected to a linear potentiometer, which collected linear displacement data (Honeywell, Morris Plains, NJ). These instruments were synchronized and used to generate a continuous force-deflection curve to characterize the non-linearity of the tissue response to external force. The surface area of the indenter was a five centimeter by five centimeter square. One end of the potentiometer was attached to the load cell, while the other was attached to a reference structure that remained stationary throughout testing (Figure 2.1).

To start each test, a reference distance measurement was taken. The indenting tool was positioned near the test region, and the load cell was zeroed. The reference measurement was the largest distance recorded by the potentiometer with no force recorded by the load cell (Figure 2.2b). The indenter was then pressed into the thigh region using a constant loading rate until a physiological resistance was felt. Each person was first tested in the seated position in order to determine what this maximum applied force should be. The resistance was felt in the seated position when the tissue was compressed against the femur and would no longer deform. In other words, additional applied force would have lifted the entire leg. This force was between 60 and 100 N, depending on the individual. Then this was used as the maximum applied in the quadruped and prone positions [221]. The load was then removed. This procedure was followed for each region, making sure that the indenter was perpendicular to the body region during each test. A five minute rest period for tissue recovery was provided before a second trial was conducted. Two trials

were completed for each region of the thigh in each position. An assessment of the repeatability of this protocol is included in Appendix A.

Model Fitting

The force and deflection data were converted into stress and stretch data respectively. Stress values were calculated by dividing the force perpendicular to the indenter face by the area of the indenting face. Stretch values perpendicular to the axis of the thigh were calculated using the undeformed thickness of the soft tissue in each thigh region (described below) and the deflection values collected during the indentations (Eq 2.1).

$$\lambda_1 = \frac{\delta_o - \delta_d}{\delta_o} \quad \text{(Eq. 2.1)}$$

Here, δ_o is the undeformed tissue thickness and δ_d the deflection of the tissue. To determine the undeformed tissue thickness for each individual thigh region, the ratio of the total thickness of the thigh (i.e., anterior to posterior, AP, distance) to the thigh circumference was obtained for each region (Figure 2.3). This ratio was approximately equal to 0.33, as determined through the use of existing data sets that included a 3D scan and anatomical measures of the thigh regions [10], [221]. The ratio of the total thickness to the circumference of the thigh was scaled to each individual's thigh circumference to determine the total thicknesses for each test location. The portion of the soft tissue thickness in the thigh posterior to the femur has been reported to be 0.55 of the total thickness of the thigh [222]. Thus, the undeformed thickness of the tissue was given by Eq. 2.2 where C is the thigh circumference, and the undeformed thickness is δ_o.

$$\delta_o = C * 0.55 * 0.33 \quad \text{(Eq. 2.2)}$$

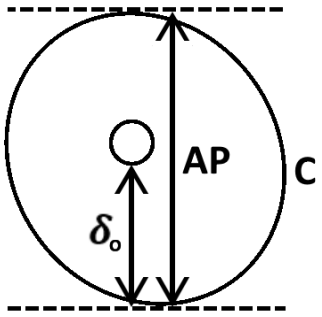

Figure 2.3 Cross-section of the thigh with measurements used to determine the undeformed tissue thickness. The thigh circumference is denoted by 'C', the total thickness of the thigh is denoted by 'AP', and the undeformed thickness is computed as δ_o

The stresses and stretches of every thigh region of each participant in these positions were then modeled using an incompressible first order Ogden material [18], [192], [203], [223]. The strain energy function of this model is represented by Eq. 2.3.

$$W(\lambda) = \frac{\mu}{\alpha}(\lambda_1^\alpha + \lambda_2^\alpha + \lambda_3^\alpha - 3) \quad \text{(Eq. 2.3)}$$

The stretches in the three principal directions were given by λ_1, λ_2, and λ_3 respectively, with λ_1 being the stretch in the direction perpendicular to the femur (i.e., loading direction); μ was a material parameter with the dimension of stress and α was a dimensionless material parameter [18], [192], [203], [223]. The stress in any direction was defined as the derivative of the strain energy function with respect to the stretch in that direction multiplied by the stretch in that direction itself. Stress in the perpendicular direction was defined by Eq. 2.4.

$$\sigma_1 = \lambda_1 \frac{\partial W(\lambda_1, \lambda_2, \lambda_3)}{\partial \lambda_1} = \lambda_1 \left[\mu \lambda_1^{\alpha-1} + \frac{\mu}{\alpha}\left(\frac{d\lambda_2^\alpha}{d\lambda_1^\alpha} + \frac{d\lambda_3^\alpha}{d\lambda_1^\alpha} \right) \right] \quad \text{(Eq. 2.4)}$$

With the condition of incompressibility, the volume of the thigh region must be preserved, i.e., $\lambda_1\lambda_2\lambda_3 = 1$, at all times. Incompressibility can be applied due to the large fluid content of tissue

such as fat and muscle, and near incompressible behavior has previously been observed in human soft tissue [224]. The only forces acting in each transverse direction were the internal tissue forces, meaning that the stretches were the same in each transverse direction ($\lambda_2 = \lambda_3$). Considering these two conditions together, $\lambda_2 = \lambda_3 = \lambda_1^{-1/2}$. This makes λ_1 the only independent variable, which we replaced with the symbol λ. In the uniaxial loading of the indentation tests, the relationship between stress and stretch is described by Eq. 2.5.

$$\sigma = \mu(\lambda^{\alpha} - \lambda^{-\frac{\alpha}{2}}) \quad \text{(Eq. 2.5)}$$

In this case, σ is the stress perpendicular to the axis of the femur, and λ is the stretch perpendicular to the axis of the femur. The μ and α values for the material model were optimized using a Levenberg-Marquardt least squares algorithm to best describe the stress and stretch data collected for each body position and thigh region for each participant.

A two-way, repeated measures ANOVA [225] was used to determine the significance of the μ and α parameters within each sex. A post-hoc Tukey test was used to make all pairwise comparisons for the μ and α parameters between regions and positions. Differences between sexes for μ and α were detected with t tests [226]. A Wilcoxon Signed-Rank Test was used to determine within-individual differences in the μ and α parameters in the three body positions for each region.

Results

Ten males (average age 22.4 ± 2.2 years, average height 179.7 ± 10.8 cm, average weight 77.4 ± 6.4 kg) and ten females (average age 21 ± 1.3 years, average height 164.9 ± 6.0 cm, average weight 66.5 ± 12.6 kg) participated in this study.

Force and Deflection Data

Average force-deflection curves of all participants for each position and region were obtained and are presented in Figure 2.4. The average force-deflection curves included both indentation trials from each participant's thigh. The average load while seated is 50 N (noted by a horizontal line on Figure 2.4) [109], [159], [227]. Upon initial analysis of these data sets, the proximal thigh region while seated was much stiffer than any other region in any position. Since our data indicated a much higher stiffness for the proximal thigh in the seated position as compared to the other positions and regions, the authors investigated further and found that the support structure for the laboratory seat system had caused an additional tension near this thigh region (Figure 2.5, left). The participants sat on a support bar located at the rear of the buttocks which caused a dropping of the buttocks and additional tissue tensions as this region was stretched between the rear bar and front thigh support. The authors were able to successfully recruit half of the original cohort (five males and five females) to return for a follow-up test in a modified seated position that removed this load. This new positioning protocol had the participants sitting on the edge of the testing chair (Figure 2.5, right) so the buttocks load was on the back edge of the buttocks, not the thigh. All three leg regions were tested again. In this positioning protocol, the middle and distal thigh region data yielded the same results as those of the first protocol, however the force and deflection data from the proximal thigh region had a reduction in stiffness. With the modified protocol, the data from the proximal thigh in the seated position still indicated that it was stiffer than the middle and distal regions while seated, but it was no longer the stiffest region across all positions. Therefore, data reported for the proximal thigh in the seated position are from the modified protocol (n=10) while the other two regions include all participant data (n=20). The other two positions (quadruped and prone) included data from all 20 participants.

In the **prone position (red curves in Figure 2.4)**, the proximal thigh showed the most deflection, and the distal thigh showed the least deflection. At 50 N of force, there was an average deflection of 31.9 ± 6.5 mm in the proximal thigh, 28.1 ± 4.0 mm of deflection in the middle thigh, and 21.3 ± 4.5 mm of deflection in the distal thigh. The prone position consistently produced less deflection than the seated and quadruped positions, regardless of the amount of load (Figure 2.4).

In the **seated position (black curves in Figure 2.4)**, all three thigh regions displayed similar force-deflection behaviors. At 50 N of force, there was an average of 39.6 ± 8.4 mm of deflection in the proximal thigh, 39.4 ± 6.7 mm of deflection in the middle thigh, and 40.7 ± 9.0 mm of deflection in the distal thigh. The seated position consistently produced more deflection than the prone position and less deflection than the quadruped position for the same force (Figure 2.4).

In the **quadruped position (blue curves in Figure 2.4),** all three regions displayed similar force-deflection behavior. At 50 N of force, there was an average of 44.4 ± 6.9 mm of deflection in the proximal thigh, 44.5 ± 6.8 mm of deflection in middle thigh, and 45.8 ± 4.9 mm of deflection at 50 N for the distal thigh in the quadruped position (Figure 2.4). The quadruped position consistently produced the most deflection of all the positions with the same force. *The deflection values in the seated position were consistently closer to those in the quadruped position than those of the prone position for all regions.*

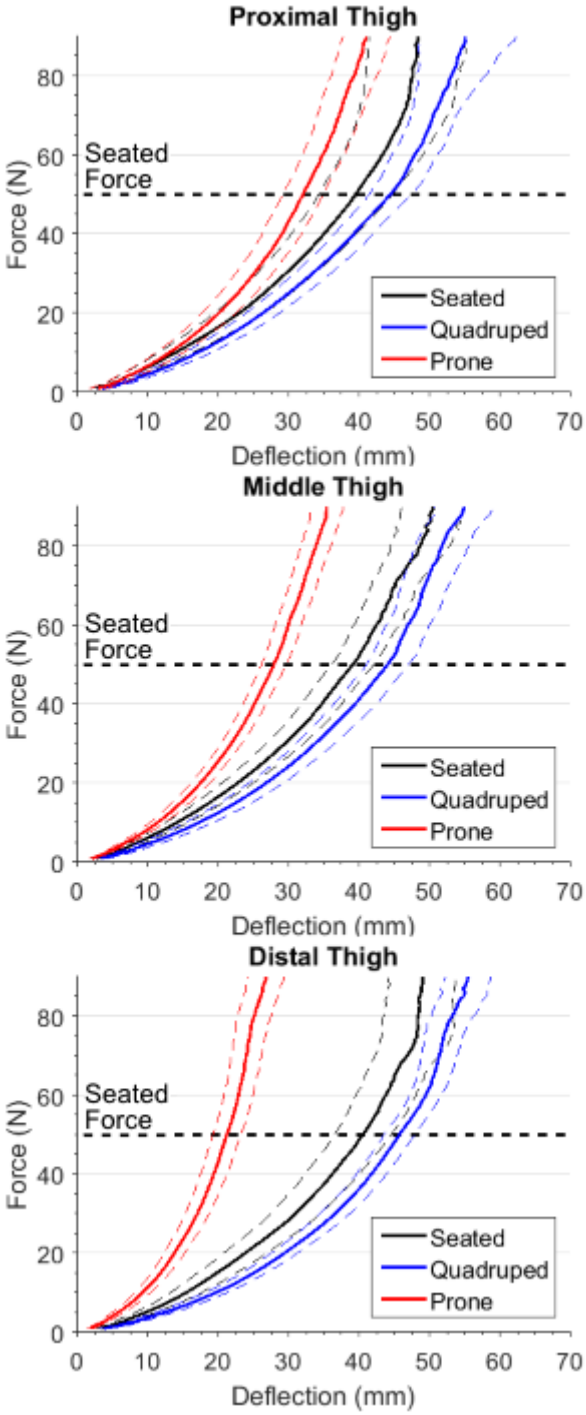

Figure 2.4 Average force-deflection results separated by thigh region. The data for the seated position is represented by black lines, the quadruped position by blue lines, and the prone position by red lines in the proximal thigh region (left), middle thigh region (middle), and distal thigh region (right). Dashed lines are 95% confidence intervals on the mean value of deflection

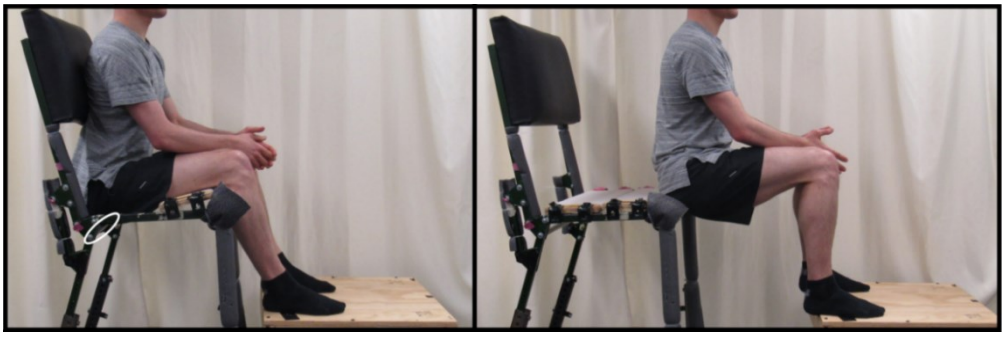

Figure 2.5 The original seated position (left) removed the posterior segment of the seat pan to allow access to the proximal thigh. The participants sat on a support bar located in the white ellipse, which caused a dropping of the buttocks and additional tissue tensions as this region was stretched between the rear bar and front thigh support. The amended seated position (right) included the participant sitting on the edge of testing chair with a straight back

Ogden Material Parameters

The Ogden model has been shown to successfully describe nonlinear materials using only two parameters [10], [191], [198]. All optimized Ogden material parameters for each thigh region in each position are reported for both males and females in Figures 2.6 and 2.7.

Comparisons of Body Positions

The average μ and α values for each position within each thigh region were compared to one another for both males and females. Overall, the μ values were the lowest in the prone position and the α values were the highest in the prone position (Figures 2.6 and 2.7, respectively). In the proximal thigh region overall, the average μ value for the prone position was lower than the average μ for the seated ($p = .022$) and quadruped ($p = .003$) positions. The difference between μ in the prone and quadruped positions were significant for both the groups of males and females, however the difference was not significant between prone and seated positions. In both the middle and distal thigh regions, the average μ value for the prone position was lower than the average μ value for the seated and quadruped positions. These differences were significant for males and

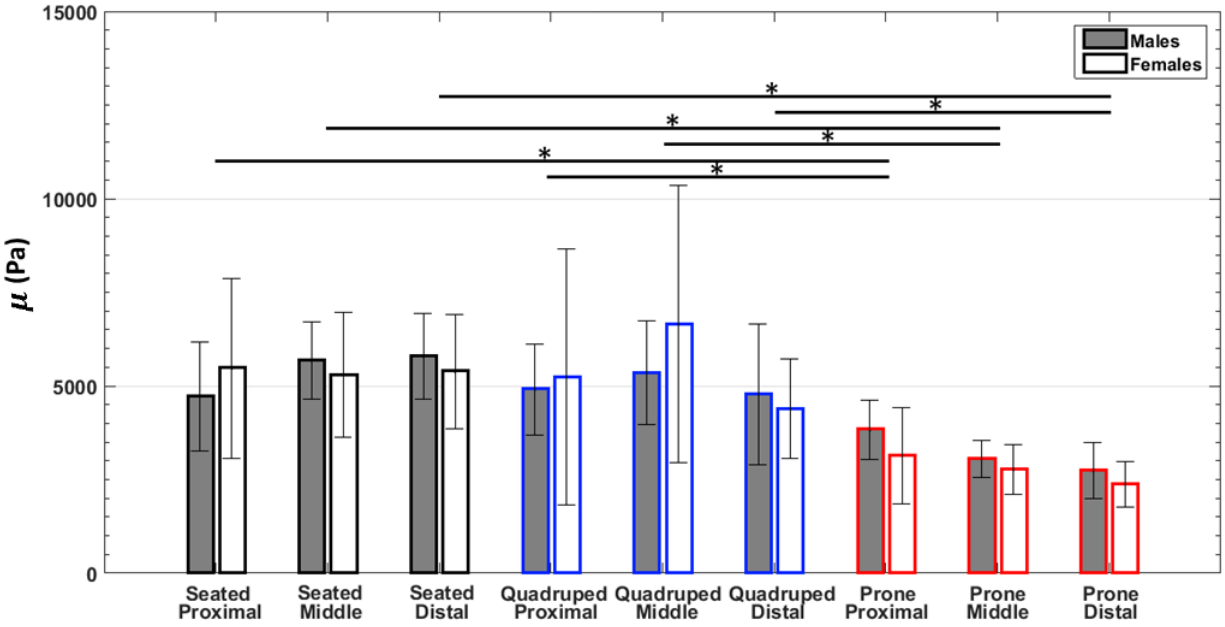

Figure 2.6 μ values for each thigh in each position, separated by sex. The μ values for the thigh regions in the prone position are smaller than those of the seated and quadruped positions, as indicated by the asterisks. Seated parameters are represented with black outlines, quadruped with blue outlines, and prone with red

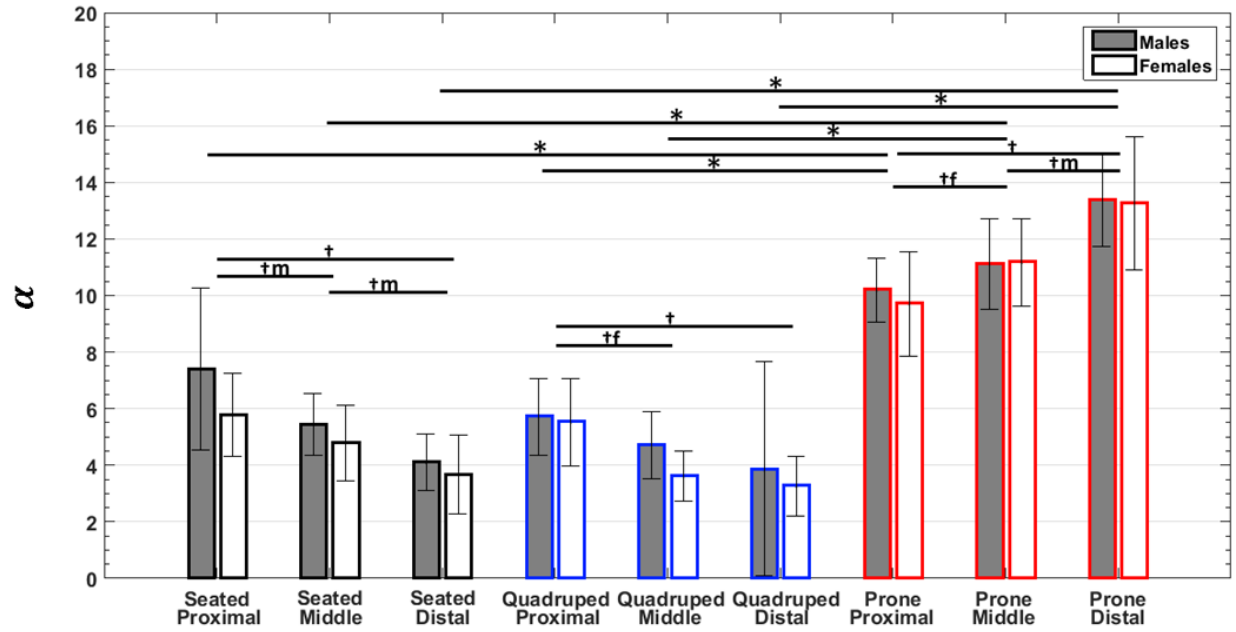

Figure 2.7 α values for each thigh in each position, separated by sex. The α values for the thigh regions in the prone position are larger than those of the seated and quadruped positions, as indicated by the asterisks. Daggers indicate differences between thigh regions within a position for both sexes (†), males only (†m), and females only (†f). Seated parameters are represented with black outlines, quadruped with blue outlines, and prone with red

females, with $p < .0001$ for all comparisons. There were no significant differences between the μ values of the seated and quadruped positions in any thigh region for males or females (Figure 2.6).

For all regions, the average α values of the prone position were higher than the average α values in the seated and quadruped positions. These differences were significant for both the groups of males and females, with $p < .0001$ for all comparisons. In the proximal thigh for males only, the α value while in the seated position was significantly larger than the α value in the quadruped position ($p = .0412$) (Figure 2.7).

From these data, we can see that there are no significant differences between the μ and α values for seated and quadruped positions in any thigh region. However, the μ values for the thigh regions in the prone position were significantly smaller than those in the seated or quadruped position. Also, the α values for the thigh in the prone position were significantly greater than those for either the seated or quadruped position. These data indicate the values obtained in the prone position differed significantly from those in both the seated and quadruped positions, but the seated and quadruped positions were not significantly different.

Comparisons of Thigh Regions within a Given Position

Comparisons of the average μ and α values for each thigh region were conducted to detect differences between the thigh regions in each of the three positions. Males and females were evaluated separately.

There were no overall differences between thigh regions for the μ parameter within any of the three positions (Figure 2.6).

However, there were overall differences between the α parameter values of the thigh regions within each of the three positions. Overall, the α values of the more distal regions of the

thigh were smaller than those of the more proximal regions in the seated and quadruped positions. But the α values in the more distal regions of the thigh were higher than the proximal thigh regions while prone.

Figure 2.7 presents the relationships between regions. Specifically, in the seated position, the α value of the of the proximal thigh was greater than that of the middle thigh in males ($p = .0076$) and the distal thigh in both males and females ($p < .0001$ for both). The middle thigh in the seated position had a greater α value than the distal thigh ($p = .0086$) for males. In the quadruped position, the proximal thigh had a greater α value than the middle thigh in females ($p = .0024$) and the distal thigh in males and females ($p < .0001$ for both). In the prone position, the α value of the proximal thigh was smaller than that of the middle thigh in females only ($p = .0315$) and the distal thigh for both males and females ($p < .0001$ for both). The α value of the middle thigh was also smaller than that of the distal thigh in the prone position for both males ($p = .0009$) and females ($p = .0024$).

Comparisons of Thigh Regions Between Males and Females

Comparisons were made between males and females for each thigh region and each position. The μ values did not show any consistent trends between sexes, nor were there any significant differences identified. The α values of the males were larger than the females (Figure 2.7) for the majority of comparisons and one statistically significant difference was noted; males had higher α values in the middle thigh while in the quadruped position ($p = .0205$).

Within-Individual Differences Between Body Positions

Within-individual differences between the Ogden parameters in each body position were analyzed for each thigh region using a Wilcoxon Signed-Rank Test. Using the Signed-Rank Test, significant differences were found between the μ values of the proximal thigh regions in the quadruped versus prone position ($p = .0006$). Significant differences were also found between the μ values of the middle thigh regions in the seated versus prone position ($p = .0001$) and quadruped versus prone position ($p < .0001$). Lastly, significant differences were found between the μ values of the distal thigh regions in the seated and quadruped position ($p = .0251$), seated and prone position ($p < .0001$), and the quadruped and prone position ($p < .0001$).

Significant within-individual differences were also found between the α parameters in each region. In the proximal thigh regions, the α values were significantly different between the seated position and prone position ($p = .0059$) and the quadruped position versus the prone position ($p < .0001$). α values in the middle thigh regions were significantly different in the seated position and quadruped position ($p = .0025$), the seated position and prone position ($p < .0001$), and the quadruped position and the prone position ($p < .0001$). In the distal thigh regions, α values were significantly different in the seated position versus the prone position ($p < .0001$) and in the quadruped position versus the prone position ($p < .0001$).

Discussion

The goals of this research were to determine and compare the thigh and buttock soft tissue properties in the seated, quadruped, and prone positions. Determining the most realistic material parameters for the seated position is crucial to improve mechanical models of seated individuals.

In situations where collecting data from individuals in the seated position is not possible, identifying the best analog to the seated position is also critical.

Mechanical models have been used to understand internal tissue stresses of seated individuals, particularly wheelchair users, and to identify the risk of PI formation [189]. The accuracy of these simulations have depended on the material properties used in these models. Thus, having *in vivo,* human-based, material properties that reflect the body region and the position being modeled is imperative to yielding the most realistic simulations of internal tissue stresses and strains going forward.

Our force and deflection data are unique in many ways: 1) they identify differences across three positions, 2) they represent multiple regions along the thighs and buttocks, 3) they are *in vivo,* and 4) they represent continuous force and deflection measures which are extremely important for the non-linear nature of soft tissues. These datasets show a clear trend indicating that the thigh soft tissue is stiffer in the prone position than it is in either the seated or quadruped positions. For example, using data from the prone position at the distal region of the thigh underestimates the deflection in that region by approximately 20-25 mm while seated, decreasing the deflection by more than half. Because of this, it is imperative that body position be taken into account when selecting the material parameters for soft tissue in any model.

We chose to use an Ogden model to represent the soft tissue for its relatively small number of parameters and accuracy of describing tissues [191]. In the Ogden model, the values of the material parameters of μ *and* α provide insight into the non-linearity of the stress-stretch curves. A higher α is indicative of a quicker change from a soft to a stiff material as stretch increases. So, the differences identified through the Ogden model relate to material stiffnesses directly. All regions of the thigh had smaller μ values and larger α values in the prone position relative to the

seated position. Following these differences, our data indicated that soft tissues in the thighs and buttocks in the prone position were stiffer for large deformations relative to the soft tissue while seated. Conversely, there were no significant group-level differences between the μ and α values in the seated and quadruped positions, meaning that the shapes of the quadruped stress-stretch curves are closer analogs to the seated curves. Males typically had slightly higher α values than females, with only one significant difference, in the middle thigh while quadruped. This consistent trend may be due to males having larger amounts of muscle versus adipose tissue relative to females [228].

Because they demonstrated similar between-region trends in μ and α, further comparisons can be drawn between the seated and quadruped positions. For both the seated and the quadruped positions, the μ values of the proximal, middle, and distal thigh regions showed no overall difference with respect to one another. But the α values decreased when moving from the proximal to distal regions. This finding matched that of previous work conducted to obtain material properties of the seated thigh [221]. The opposite trend emerged in the prone position, where the α values of the thigh tissue increased when moving distally in the thigh.

The Wilcoxon Signed-Rank Test determined that there were some within-individual differences between the Ogden parameters in the seated position versus the quadruped position (specifically between the μ values in the distal thigh regions and α values in the middle thigh regions). However, there were no consistent differences between the two positions in either of the parameters. Further, because there were no significant group-level differences in either parameter between the two positions, the data suggested that differences in parameters between the seated and quadruped positions were small relative to variations of the parameters within the positions. On the other hand, there were consistent group-level and within-individual differences between

the parameters in the prone position when compared to either the seated or quadruped positions. As such, the prone position should be considered to produce tissue material properties distinct from the seated and quadruped.

The position should determine data used for material properties. Both material parameters across thigh regions were different for the seated and prone positions. Meanwhile, the quadruped position matched for both material parameters across thigh regions of the seated position more closely than the prone position. Because of the similarity between the material properties in the seated and quadruped positions, parameters determined from the quadruped position can be used in finite element models that predict internal stresses in seated individuals, whereas the data from the prone position should not be used. This finding is important as we begin collecting *in vivo* data sets on the buttocks and thighs of wheelchair users.

Limitations of this study were the estimation of the initial tissue thickness in each of the three test regions and assumptions used in the tissue modeling: small, but equal forces in the transverse directions and incompressibility. Measurements of the thigh circumferences of each participant were obtained in each region and used with ratios derived from literature to estimate initial tissue thicknesses. Future work in this area will investigate the use of a portable ultrasound machine to obtain a direct measurement of the tissue thickness [229]. The assumption of incompressibility used in the material model may have caused the values of the Ogden parameters to be underestimated if the internal stresses in the buttock and thigh tissues *surrounding* the testing regions were large (and resisted lateral expansion of the tissue being tested). However, because the lateral forces were assumed to be small, and there were no other external forces applied to the tissues surrounding the testing region, the effects of incompressibility on the reported parameters was likely small.

Another limitation of this study was the population from which the force-deflection data were collected. All participants in this study were healthy, able-bodied individuals. Data from the elderly and wheelchair user groups, who have been deemed at high risk of developing PIs, are also necessary. Work has been conducted to describe the effects of aging and wheelchair use on muscle structure and function, yet there is a lack of research to describe changes in the tissue properties due to the change in structure [80], [86], [230]. Accordingly, obtaining data sets from the thighs and buttocks of wheelchair users and elderly individuals will be the next step in our research.

Conclusions

A common issue for performing research focused on individuals with disabilities has been the lack of equipment adaptation to suit each individual. Having consulted with individuals with disabilities and rehabilitation specialists, we determined that the quadruped position was an acceptable position for this type of test. In this position, it is possible to compare able-bodied individuals and those with disabilities, breaking down a significant barrier to evaluating the stresses in wheelchair sitting.

This research shows that the properties of the soft tissue in the thigh in the prone position do not represent the properties in the same regions when seated or in the quadruped position. Therefore, it is not appropriate to use data collected from the soft tissue in the thighs and buttocks while lying down to represent the seated thighs and buttocks. Instead, it is possible to use the quadruped position as an analog for the seated position if the seated position is not a possibility for testing. Using tissue properties obtained while individuals are in either the seated or quadruped position will provide modeling tools with more accurate inputs and ultimately increase their ability to assess PI risk while seated by making internal stress predictions more realistic. Our research

will yield better models, providing improved data to engineers and clinicians, with the eventual impact of a decrease in the prevalence of PIs in high-risk groups, such as wheelchair users and the elderly.

CHAPTER 3: TISSUE MATTERS: *IN-VIVO* TISSUE PROPERTIES OF PERSONS WITH SPINAL CORD INJURIES TO INFORM CLINICAL MODELS FOR PRESSURE INJURY PREVENTION

The contents of this chapter were originally published in the Journal of Biomechanics.

J. Scott, B. Sheridan, R. Andrus, N. Monday, A. Selby, and T. R. Bush, "Tissue matters: *In-vivo* tissue properties of persons with spinal cord injuries to inform clinical models for pressure ulcer prevention," *J. Biomechanics*, vol. 120 (7), 2021, doi: 10.1016/j.jbiomech.2021.110389.

Introduction

Individuals with spinal cord injuries (SCIs) commonly have secondary medical complications that result in subsequent hospitalizations post-injury. PIs have been reported as the second most common complication and are expensive to treat [6], [54], [231]. The prevalence of PIs in patients with SCIs has been estimated to be between 30% and 47%, with approximately 15% of SCI patients developing a PI within the first year post-injury [7], [54], [60], [232]. PI treatment costs between $20,000 and $30,000 on average, with some PIs costing $70,000 to treat [233]. Because of these costs, the annual expense for treatment in the United States has been estimated at 1.6 billion dollars [90]. This expense has prompted efforts to better understand PI formation and develop clinical models to help in PI risk assessment.

Internal tissue stresses in the buttocks and thighs have repeatedly been noted as a cause of PI development [26], [106], [121], [214]. Internal stress concentrations exist in the soft tissues, especially in those with a SCI; this is due to the large external loads that occur over extended time periods while seated [16], [62], [82], [147], [196], [234]. Almost half of the PIs affecting the SCI population are located in the buttock and thigh regions [6]. As such, numerous models of the

buttocks and thighs have been developed to help assess the risk of PI formation [21], [69], [148], [159], [163], [196], [235].

Finite element models are used to obtain a better understanding of the internal stresses seen in soft tissues and to inform device design. These models have relied on body geometry, external load, and material properties of the soft tissues to make internal stress evaluations in seated individuals. However, persistent limitations exist in the material properties used in these models. The majority of finite element models used material properties determined from animal models, such as rats or pigs [192], [196]. The limited research with humans has typically been conducted with able-bodied (AB) participants lying down [23], [208], [219]. Material properties from such studies are appropriate for models of people lying down. However, wheelchair users are seated. The tension and thickness of muscle tissue in the buttocks change while seated versus lying down and affect the tissue's material properties [210], [211], [236]. Recent work found that material properties and tension affect pressure distributions experienced by a human limb analog [237]. Currently, there are only three studies with humans that included data from the soft tissue of the buttocks or thighs while seated. Two of them described the buttocks and thighs of AB individuals [221], [236], while the third collected force and deflection data from the buttocks of wheelchair users in two load states [238]. The material properties of the tissues of wheelchair users have been explored in some studies [239]. However, models designed to evaluate internal stresses and strains in wheelchair users have yet to integrate *in-vivo* material properties, such as indentation moduli, from persons with disabilities.

Muscle progressively atrophies and intramuscular fat increases in the buttocks and thighs of individuals with SCIs [79], [80], [240]. Thus, material properties from this population, which affect the tissues' responses to external load, are hypothesized to differ from those of AB

individuals. Differences in material properties manifest as increased interface pressure, increased internal stress, and decreased perfusion in tissue under seated load [82], [83], [241]. This is reinforced by findings from several existing studies, which have shown that the higher levels of muscle atrophy and fat infiltration in individuals with SCIs are correlated with higher PI risk [78], [242]. As such, there is a need for *in-vivo* material properties of the buttock and thigh soft tissues from individuals who use wheelchairs, such as patients with SCIs. Material properties representative of individuals with SCIs will lead to improved human body models, which lead to improved PI risk assessment and better device designs.

There are numerous challenges in obtaining material properties for soft tissues, particularly in the buttocks and thighs of seated individuals with SCIs. Doing so requires access to the buttock and thigh regions while seated. Access to those regions can be accomplished by using a specialized chair with removable supports. Using such a chair is likely to be difficult for individuals with SCIs, requiring balance while the supports are removed. Furthermore, transferring out of the individuals' wheelchairs and into a lab-type chair adds another challenge. As an alternative to the seated position, the quadruped position is commonly used in the physical therapy of individuals with SCIs and produces similar joint angles to a seated posture. We previously showed that the material properties obtained in the quadruped position were similar to those in a seated position [236].

The aims of this research were to determine the material properties of soft tissue in the buttocks and thighs of individuals with SCIs while in the quadruped position and to compare these material properties to those of AB people. Realistic material properties in human body models will lead to advancements in the understanding of PI formation, further improvements in existing device designs, such as pressure relieving cushions [21], [175], [198], [201], and be the basis for the development of new devices.

Methods

Participants

Eleven individuals who were wheelchair users with a spinal cord injury and twenty AB individuals volunteered to participate in this study. All testing was approved by the Biomedical and Health Institutional Review Board at Michigan State University, and consent was obtained from all participants. Participants were excluded from the study if they did not feel they would be able to maintain a supported quadruped position for half an hour, if they were pregnant, had active wounds on the leg, osteoporosis, or occult bone disease. Participants with spinal cord injuries were required to have been using a wheelchair for at least six months.

Quadruped Position

AB participants wore athletic clothing and were placed in a quadruped (crawling) position that provided support at the torso and knees [236]. The heights of the supports were adjusted such that the individuals' hips and knees were bent at ninety degrees. The thighs of the participants were blocked with a support to ensure that their thighs did not move during testing, as seen in Figure 3.1.

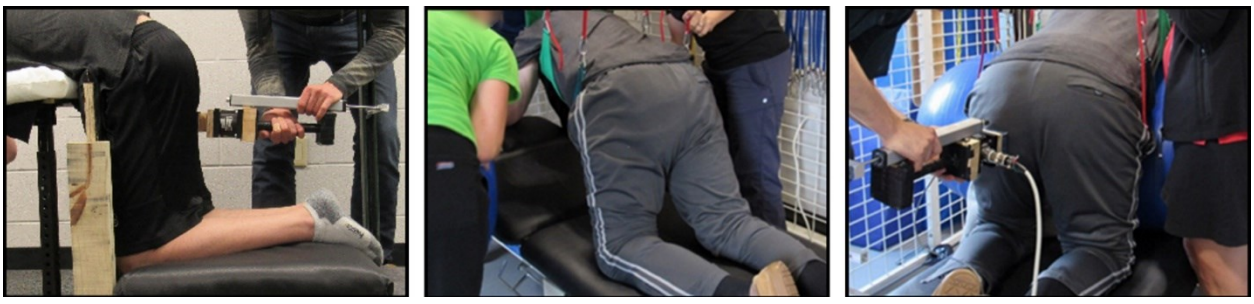

Figure 3.1 Positioning protocol for users in the AB (left) and SCI (middle and right) groups. Participants with SCIs were helped onto a table and into the quadruped position by their therapists while the harnesses were secured (middle); and then supported in the testing position with an exercise ball beneath the torso and sand bags in front of the knees (right)

Individuals in the SCI group wore clothes that they regularly wore to physical therapy, and testing occurred prior to their physical therapy sessions at their rehabilitation clinic. With their therapists' help, they transferred onto a therapy table in the universal exercise unit. Individuals were first positioned prone on the table with harness straps beneath their thorax and pelvis. The harnesses were attached to the universal exercise unit and tightened as the table was lowered, moving the participant into a quadruped position with the hips and knees flexed at ninety degrees. A peanut-shaped exercise ball was used to assist in supporting the torso; and sandbags were positioned in front of the thighs and ball to stop their thighs from moving during the testing session, seen in Figure 3.1.

Three body regions were evaluated: the proximal thigh/buttocks (proximal thigh), middle thigh, and distal thigh regions. These regions were identified based on a percentage length of the femur. The length of the femur was considered as the distance from the greater trochanter to the lateral epicondyle, and the three regions were defined by their locations relative to the two bony landmarks. The respective distances of the proximal, middle, and distal thigh regions distal from the greater trochanter were 10, 50, and 90 percent of the length of the femur. For the region called "proximal thigh", a 10% distance along the femur yielded a placement of the indenter surface (which was 5 cm by 5cm) that encompassed tissues over the ischial tuberosity as well as tissues just distal to the ischial tuberosity. This is a region in which PIs commonly develop. The distal thigh was just proximal to the popliteal fossa of the knee, a place where PIs have been also reported [70], [71], [73], [74], [243]. The middle thigh was between these two locations. Circumference measurements were recorded at each of the three testing locations on each participant's thighs and buttocks.

Tissue Testing Protocol & Material Parameter Estimation

A custom-made indenting tool previously reported was used to collect continuous force and deflection data for this study (Figure 3.2a) [236]. Force and deflection data were collected in each of the three testing regions during two indentations with a maximum applied load of between 30 and 40 kPa (Figure 3.2b). These force values were in the same ranges as those used during the testing of able-bodied participants in Chapter 2. These force and deflection data were converted into stress and stretch data using the geometry of the indenting tool and the circumference measurements of the participants' thighs [10], [221], [236]. Stress and stretch data were mapped to an incompressible first-order Ogden material model. A complete characterization of these methods has been included in the supplemental material.

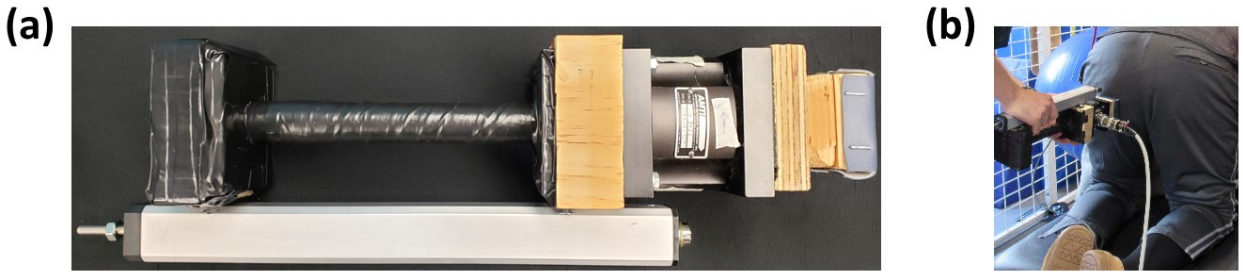

Figure 3.2 a) Indenting tool with the six-axis load cell embedded beneath the indenting surface and linear potentiometer used to obtain distance data, and b) Indenting tool as used during testing with the participant

Statistical Analysis

Two statistical analyses were conducted on the material parameters, μ and α. A repeated measures ANOVA was used to differentiate between the values of parameters in the three regions (proximal, middle, and distal thigh regions). An ANOVA was used to differentiate between the values of the parameters in each group (SCI versus AB). Post-hoc Tukey tests were used to detect

significant differences in the values of μ and α. Effect sizes were computed using Cohen's d method.

Results

Demographic Data

Nine males with spinal cord injuries (age 44.0 ± 5.2 years, height 180.6 ± 1.7 cm, mass 77.6 ± 2.9 kg, time in chair 9.8 ± 5.1 years), and two females with spinal cord injuries (age 45.5 ± 7.5 years, height 165.1 ±2.5 cm, mass 73.0 ± 22.2 kg, time in chair 3.25 ± 2.75 years) were recruited for this study. Additionally, ten AB males (age 22.4 ± 2.2 years, height 179.7 ± 3.4 cm, mass 77.4 ± 2.0 kg) and ten AB females (age 21 ± 1.3 years, height 164.9 ± 1.9 cm, mass 66.5 ± 4.0 kg) volunteered. The two groups will be referred to as the SCI and AB groups.

Force and Deflection Data

Force and deflection curves are shown for each region in Figure 3.3. For each region, the average force and deflection data from AB individuals were plotted, including 95% confidence intervals. Deflections at 50 N of applied force (20 kPa of applied pressure) were compared across groups because it has been reported as a typical load on the buttocks and thighs while seated [227], [244]. Seven of the eleven in the SCI group had more deflection in their proximal thigh than the average AB individual at 50 N of force (denoted by the thick line in Figure 3.3), and two had less. In the middle thigh, seven in the SCI group had more deflection, and one had less. In the distal thigh, two members of the SCI group had more deflection and seven had less. Upon statistical analysis of these data, the SCI group had significantly more deflection at 50 N in both the proximal and middle thighs (8.5mm, $p = .0222$ and 7.2 mm, $p = .0162$, respectively). Although the deflection

in the distal thighs of the SCI group was 4 mm less than the deflection in the distal thighs relative to AB group, the difference was not significant (p = .6173).

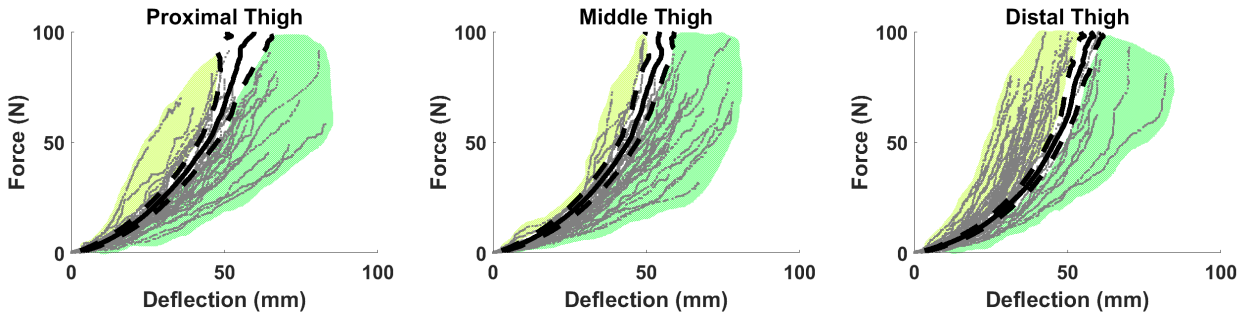

Figure 3.3 Force and deflection data from the proximal thigh (top), middle thigh (middle), and distal thigh (bottom) regions of the SCI group. The solid black line is the average AB data, and the dashed black lines represent the confidence intervals of the AB group. The data shaded in light green (left of the average) has less deflection than the average AB, and the data shaded in darker green has more deflection

To ensure that the inclusion of both sexes did not change the results, statistical analyses were run twice. No significant differences were found between the deflection data of AB males and females. For the SCI group, one analysis included only males (the SCI group only had two females), and one included both sexes. As there were no differences in the results, the latter are reported here.

Ogden Material Parameters

To describe the material properties, the stress-stretch curves were mathematically fit using the Ogden model (Eq. 3.5 in the Supplementary Material). Values for the material parameters μ and α were calculated for each region for males and females in the SCI group and are located in Tables 3.1 and 3.2, respectively. The parameters μ and α describe the shapes of the material

response curves for each region. The material parameters for each region in each group are presented with standard errors in Figure 3.4. The values of μ and α were compared between groups to detect differences. The proximal, middle, and distal thigh regions of both the SCI and AB groups were compared to find between-region differences within each group.

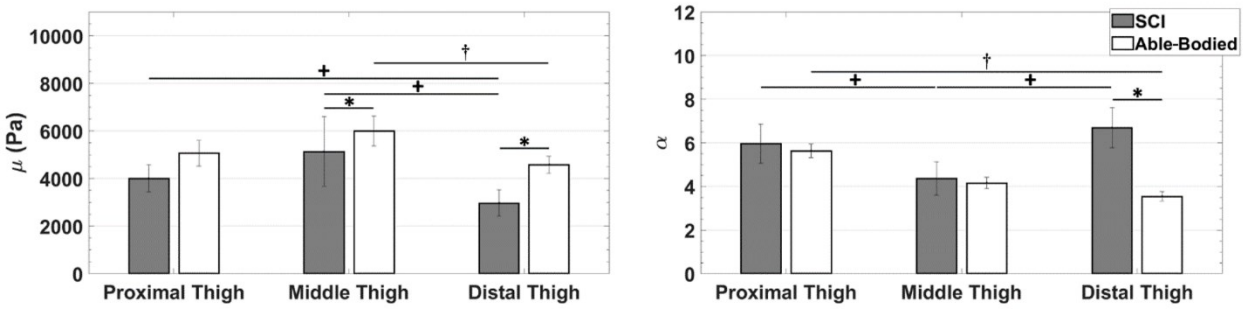

Figure 3.4 Average μ values (left) and α values (right). Data from the SCI group are grey, and the able-bodied group are white. Significant differences between groups are indicated by asterisks (*). Between-region (i.e., proximal, middle, distal) differences within the SCI group are indicated by plus signs (+). Between-region differences in the able-bodied group are indicated by daggers (†)

There were no significant differences between the μ values of AB males and females in any region. The α values for the AB males were larger than AB females ($p = .0205$) for the middle thigh region only. Thus AB males and females were considered together. Although there were only two females in the SCI group, there were no significant between-sex differences in the deflection or either of the parameters of that group. Therefore, males and females were also considered together in the SCI group.

The μ values for the wheelchair users were significantly smaller than those of the AB individuals in the middle thigh ($p = .0075$) and distal thigh ($p = .0349$) regions. The μ values for the SCI group's proximal thighs were smaller than those of the AB group; and although they did not achieve significance ($p = .1831$), a medium effect size of 0.50 was computed. For comparisons of α between the SCI and AB groups, a significant difference was found for the distal thighs ($p <$

.0001). Additionally, a medium effect size of 0.40 was found for the middle thigh region and a small effect size (.25) was identified for α in the proximal thigh region.

Between-region differences within each group were detected by comparing the proximal, middle, and distal thigh regions. In the SCI group, both the proximal thigh ($p = .0094$) and the middle thigh ($p = .0175$) regions had larger μ values than the distal thigh region. The α values for the proximal ($p = .0091$) and distal ($p < .0001$) thigh regions of SCI group were greater than the middle thigh regions. There was no significant difference between the α values of the proximal and distal thigh regions in the SCI group.

Table 3.1 Material parameters for each region for males in the SCI and AB groups with standard errors

		Proximal Thigh	Middle Thigh	Distal Thigh
μ (kPa)	**SCI**	3.90 ± .54	4.54 ± .66	3.51 ± .52
	AB	4.91 ± .38	5.35 ± .44	4.78 ± .59
α	**SCI**	5.89 ± .78	4.42 ± .69	6.37 ± .85
	AB	5.72 ± .43	4.72 ± .38	3.84 ± .27

Table 3.2 Material parameters for each region for females in the SCI and AB groups with standard errors

		Proximal Thigh	Middle Thigh	Distal Thigh
μ (kPa)	**SCI**	3.95 ± .22	2.91 ± .32	2.31 ± 1.32
	AB	5.24 ± 1.14	6.65 ± 1.17	4.39 ± .42
α	**SCI**	6.13 ± 1.12	4.98 ± 1.27	6.40 ± 1.64
	AB	5.53 ± .52	3.61 ± .28	3.26 ± .34

The μ values for the middle thigh regions of AB individuals were larger than those of the distal thigh regions ($p = .0107$). The α values in the proximal thigh regions of the AB group were significantly greater than the values in the distal thigh ($p < .0001$), and the α values of the middle thigh regions were larger than the values in the distal thigh, but that difference was not significant ($p = .4051$).

Discussion

The motivation of this research was to determine the material properties of the soft tissue in the buttocks and thighs of individuals who had a SCI and compare them to those of AB individuals. Distinguishing between the material properties of individuals with SCIs and AB individuals is vital to understanding PI risk and formation. Additionally, developing human body models that are informed by *in-vivo* material properties of the population being studied will lead to improved engineering devices and designs, such as new wheelchairs and cushions.

The research presented shows clear differences between the tissue properties of AB individuals and people with SCIs. Published research concluded that there are optimal material properties for seat cushions to best distribute seated pressures [165]. These optimal cushion characteristics are dependent on the properties of the soft tissue of the occupant. Material property differences between AB people and those with SCIs may help explain why wheelchair users experience higher peak tissue stresses than AB individuals while seated on the same foam cushion [82]. Human body models used to identify internal stresses and strains have implemented tissue properties from AB individuals and animals [18], [180], [196]. Although these models provide initial findings that can be applied to those who use wheelchairs, these models will improve when material properties obtained from the population being studied are implemented. Using material

properties derived from individuals with SCIs will lead to more realistic internal tissue stress predictions and even personalized modeling. Internal stresses and strains have been linked to the development of PIs; therefore, it is imperative that they be quantified using realistic soft tissue properties so improved PI mitigation techniques can be developed.

The dataset reported here is the first continuous force-deflection dataset for undeformed buttock and thigh tissue in individuals with SCIs and the only one to compare them to AB individuals. One published study collected an unloaded condition and two points of force-deflection data from buttock tissues in wheelchair users directly on top of the ischial tuberosity while experiencing a seated load [238]. Differences in the testing protocol and location of testing between the previous study and the one presented here likely contributed to differences measured tissue responses between both studies. Here, continuous force and deflection data were obtained in the quadruped position, which is similar to the seated position. These data will support tissue property selection, particularly for design and modeling applications [236]. These force and deflection data show an increase in deflection of the proximal and middle thigh regions for participants in the SCI group relative to AB participants. In the distal thigh region, the SCI group experienced less deflection than AB individuals. The same trends seen in the force and deflection data were also reflected in the Ogden material parameters used to describe the tissue.

Values of μ and α obtained from a first order Ogden material model described the stiffness and non-linearity of the materials' responses to external load. Increasing either parameter increases the stiffness of the tissue model, whereby an increase in μ increases the slope of the stress-stretch, and an increase in α increases the non-linearity of the curve. The μ parameter is a multiplicative term in the strain energy function of the model, while the α parameter is an exponential term. Thus,

the α parameter largely affects the large-stretch behavior of the model; and load bearing regions of the buttocks and thighs experience large compressive stretches while seated.

For the SCI group, the μ and α values of the proximal thigh were between those of the middle and distal thigh regions. The middle thigh regions had the largest μ and the smallest α values. The distal thigh had the smallest μ value and the largest α values. The SCI group tended to have smaller μ values, indicating the softer tissue. This finding is supported by previous work showing an increase in intramuscular fat and decrease in muscle in the buttocks and thighs, which would lead to softer tissue responses [78], [80], [245]. In the middle and distal thigh regions, the decreases in μ values were significant for the SCI group. Additionally, the between-group comparison of the μ parameter had a medium effect size in the proximal thigh. Such an effect size suggests that a larger sample of participants would likely result in a significant difference between the SCI and AB groups. Moreover, parameters indicated that the middle thighs were the softest in the SCI group, while the distal thighs were softest in the AB group. Thus, there were differences in trends within the thighs of the SCI and AB groups.

Overall, the proximal and middle thigh regions of those who had SCIs were softer than the same regions as AB individuals, while the distal thigh regions were stiffer. The Ogden model used to describe the tissues of AB group consistently had larger μ values than the models of the SCI group across all regions, indicating softer tissues in SCI group. In the distal thigh, the α values of the models of the SCI group were larger than those of AB group, indicating the stiffer tissue. In the proximal and middle thigh regions, the smaller μ values and similar α values in SCI group relative to the AB group indicated softer tissues. Due to these variations in stiffness, it is critical to consider wheelchair users and AB individuals separately in design and modeling applications. Further, future studies may consider the varying degrees of SCIs, such as the level of the injuries

and whether they are complete or incomplete. Doing so will provide a more complete description of the material properties individuals with SCIs because it is known that complete SCI leads to more intramuscular fat than incomplete SCI, ultimately leading to higher risk of PI development [78], [241].

Limitations of this work included the ratio of males and females in the SCI group. The clinic we tested has a comparable number of males and females over the course of a year, however more men volunteered for our study than women. Additionally, to convert the force-deflection data sets to stress and stretch, MRI or ultrasound measurements would have been ideal. Circumference measurements of the thighs, and ratios to relate the thigh circumferences to the posterior compartment thicknesses, were used instead of imaging or direct measurements of the anterior-posterior thicknesses of the thighs. Either of these methods would have provided a more direct measurement of initial tissue thickness and will be utilized in future work. Future work will identify approaches that can that identify other options for in-clinic measures. Lastly, the location of the proximal thigh region was used to represent the regions around the ischial tuberosities, as they are prone to PI development. The indentation testing for the proximal thigh region occurred with the center of the indenter just distal to the ischial tuberosities, while the proximal half of the indenter overlapped the ischial region. The tissue over the ischia region has a different underlying anatomical structure than the middle and distal thigh regions. Thus, variation within a given group due to region of testing could be attributed to anatomical differences. This anatomical difference was not addressed as part of this study, but is likely to be relevant for modeling.

Supplementary Material

Tissue Testing Protocol

A custom-made indenting tool previously reported was used to collect continuous force and deflection data for this study [236]. A five centimeter by five centimeter square indenting surface was mounted on a six-axis load cell (Figure 3.2a). A linear potentiometer was attached to the indenting tool to record deflections during tissue indentation. Before each indentation, the tool was positioned flush with the skin without deforming the tissue. At this point was a zero force value and the largest distance between the tool and a fixed reference pole [236]. This was defined as the undeformed thigh position for each region (Figure 3.2b). This was unique for each region of each individual and depended on body geometry. Distance measurements during indentation recorded by the tool were accurate within 2 mm, and force measurements were accurate to within 2 N. The tool was then pressed into the thigh using a constantly increasing load until the soft tissue no longer compressed, at approximately 40 kPa of pressure (Figure 3.2b). The load was then slowly removed. Deflection was calculated by subtracting the reference measurement from the distance measurements. During each indentation, the indenting tool moved perpendicular to the long axis of the thigh and was positioned at the height of each test region (e.g. the proximal, middle, and distal thigh). Two trials were completed for each region; a five minute rest period for tissue recovery was provided after testing before a second trial was conducted.

Material Parameter Estimation

The experimental data were mapped to the Ogden material model and model parameters obtained. To map to the model, force and deflection data collected during the indentation tests were transformed into stress and stretch data. The force data were converted into stress by dividing

the magnitude of the force by the area of the indenting tool's face. The deflection data were converted to stretch using each individual's thigh geometry. The undeformed tissue thickness for every thigh region was determined through the use of previously published data and anthropometric measurements from each individual [10], [221]. Based on published literature, the ratio of the total anterior-posterior thickness of the thigh with respect to the thigh circumference was identified as 0.33 [10]. The portion of soft tissue thickness in the thigh posterior to the femur has been reported to be 0.55 of the entire anterior-posterior thickness of the thigh [221], [222]. Thus, the undeformed tissue length was computed by multiplying these two ratios with each individual's thigh circumference. The final equation to determine the undeformed thickness of the thigh tissue was Eq. 3.1.

$$\delta_o = c_t \frac{t_{AP}}{c_t} \frac{t_p}{t_{AP}} = c_t \times 0.33 \times 0.55 \quad \text{(Eq. 3.1)}$$

In Eq. 1, c_t was the measured thigh region circumference, t_{AP} was the anterior-posterior thickness, and t_P was the thickness of the thigh tissue posterior to the femur. The undeformed thickness of each region and the deflection data were used to calculate stretch perpendicular to the long axis of the thigh using Eq. 3.2.

$$stretch = \lambda_1 = \frac{\delta_o - \delta_d}{\delta_o} \quad \text{(Eq. 3.2)}$$

In Eq. 3.2, δ_o was the undeformed thickness of the tissue thickness, and δ_d was the deflection.

The stress and stretch data were used to fit parameters in an incompressible first order Ogden material. The strain energy function of this material was given by Eq. 3.3.

$$W(\lambda) = \frac{\mu}{\alpha}(\lambda_1^\alpha + \lambda_2^\alpha + \lambda_3^\alpha - 3) \quad \text{(Eq. 3.3)}$$

λ_1, λ_2, and λ_3 were the principal stretches. λ_1 specifically was the stretch in the direction perpendicular to the femur. μ was a linear stiffness parameter with the units of Pascals, while α was a unit-less nonlinearity parameter. The stress in any direction was defined as the product of the stretch itself and the derivative of the strain energy function with respect to the stretch in that direction. The stress perpendicular to the long axis of the femur was defined by Eq. 3.4.

$$\sigma_1 = \lambda_1 \frac{\partial W(\lambda_1, \lambda_2, \lambda_3)}{\partial \lambda_1} = \lambda_1 \left[\mu \lambda_1^{\alpha-1} + \frac{\mu}{\alpha} \left(\frac{\partial \lambda_2^{\alpha}}{\partial \lambda_1} + \frac{\partial \lambda_3^{\alpha}}{\partial \lambda_1} \right) \right] \quad \text{(Eq. 3.4)}$$

Incompressibility was enforced by conserving the volume of the buttock and thigh tissue, with $\lambda_1\lambda_2\lambda_3 = 1$ at all times. Only internal forces, which were assumed to be the same in both directions due to the isotropic nature of the Ogden model, acted in the transverse directions; thus the stretches in the transverse directions were equal ($\lambda_2 = \lambda_3 = \lambda_1^{-1/2}$). The relationship between the stress and stretch during the uniaxial compression was described using Eq. 3.5.

$$\sigma = \mu \left(\lambda_1^{\alpha} - \lambda_1^{-\frac{\alpha}{2}} \right) \quad \text{(Eq. 3.5)}$$

Stress and stretch perpendicular to the femur were represented by σ and λ_1, respectively. The values of μ and α were calculated to best fit the stress and stretch data of each thigh region in each individual.

CHAPTER 4: SHIFTING LOADS AND PERFUSION RESPONSES AS A RESULT OF CHAIR ARTICULATION IN THE CONTEXT OF PRESSURE INJURIES

Introduction

Pressure injuries (PIs) disproportionately affect wheelchair users, such as those with spinal cord injuries (SCIs). Prevalence rates are as high as 47% in some care facilities [7], [17]. PIs can take months to heal and incur an average cost of $35,000 per incident, with some PIs costing over $120,000 [8], [13], [14], [16]. Recurrence rates up to 53% indicate that PIs can become chronic, debilitating conditions that disengage people from their daily lives [246]. Further, the prevalence of PIs, cost of treatment, and recurrences result in annual costs estimated near $27 billion in the United States alone [15].

PIs are localized soft tissue injuries, usually around bony prominences [24]. However the mechanisms that cause PI formation have yet to be confirmed [24], [25]. One thought is that interface pressures on soft tissue occludes the blood perfusion to the affected area and deprives tissue of nutrients, resulting in necrosis [119], [213]. This theory was supported by studies reporting decreased blood perfusion in tissue experiencing normal and shear pressure [101], [120]. Another potential mechanism is that tissue dies due to direct mechanical compression [26]. Animal studies have shown that tissues experienced necrosis within two hours with sufficient compressive pressure [104]–[107]. Regardless of the mechanism, sustained pressures have been linked to PI development. Thus, it is imperative to identify new approaches of decreasing pressures on high-risk areas to reduce PI incidence.

Sustained pressure is especially salient for individuals with SCIs, as many use wheelchairs and have limited sensation, making it difficult for them to determine when body regions experience such pressures. Those with SCIs have numerous regions of the body susceptible to PI formation, including the heels, greater trochanters, ischial tuberosities, sacrum, coccyx, and scapulae [17],

[30]–[33], [51]. In particular, the soft tissue in the buttocks (beneath the ischial tuberosities, or ITs, and around the coccyx) and lower back (behind the sacrum) are high-risk areas, in part due to lack of a thick layer of soft tissue overlaying the bony prominences [16], [51], [182]. One PI prevention strategy is seated repositioning, either with back recline or whole-body tilt to change pressure patterns [2], [161], [247]. Whole-body tilt as implemented in current chairs is a simultaneous back and seat pan rotation where the angle between the back and seat pan remains constant at approximately 90°, resulting with the wheelchair user facing upwards. The effects of back recline on risk factors associated with PIs are mixed [108], [248]. And although whole-body tilt has shown promise for reducing factors related to PI incidence, maximum benefits in terms of pressure reduction are achieved at large tilt angles, which are the least popular because they disengage people from tasks of daily living [247], [249]. A robust study on the effects of both back recline and isolated seat pan tilt on seated pressure and blood perfusion has yet to be published. Understanding how these individual movements affect pressure and perfusion is essential to identifying seated positions that can reduce PI risk.

There are limited investigations into how changes in interface pressures on the buttocks due to wheelchair repositioning affect blood perfusion [69], [100], [247]. Some studies have probed the effects of normal pressure, shear pressure, and skin temperature on perfusion, but these have not replicated seated pressures [3], [100], [101]. Research to address the relationships between pressures and perfusion in various seated positions needs to be expanded for a more comprehensive assessment of PI risk. Therefore, the goals of this research were to evaluate the ability of an articulating chair design with isolated back recline, seat pan tilt, and back articulations to 1) redistribute pressures on the body and 2) change blood perfusion.

Methods

Participant Recruitment

Twenty able-bodied adults, ten male and ten female, gave consent to participate in this study. Approval for this study was granted by the Biomedical and Health Institutional Review Board at Michigan State University.

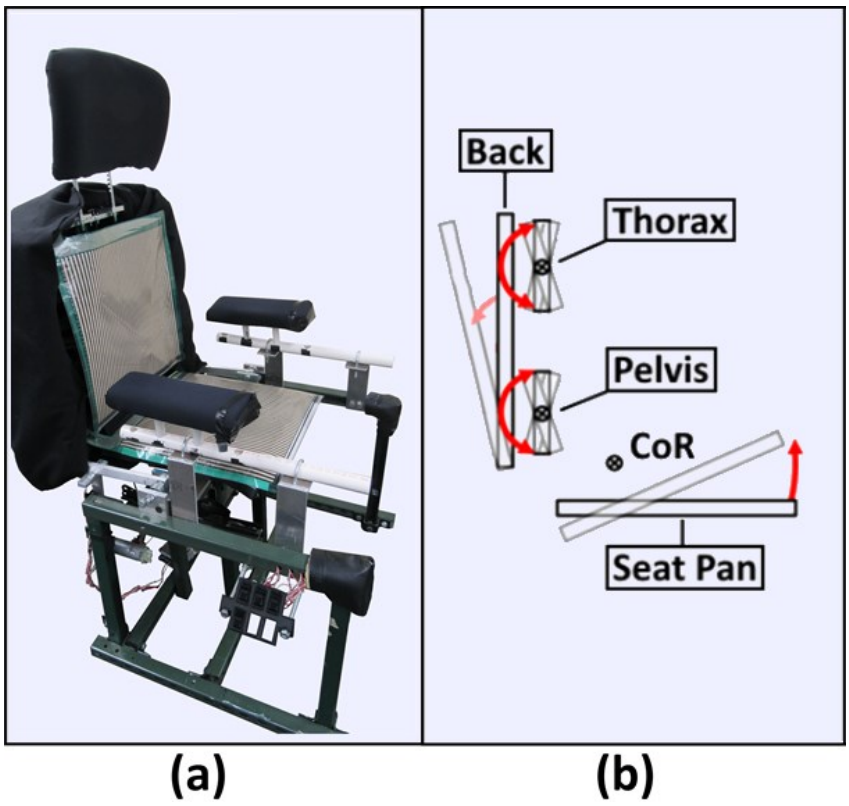

Figure 4.1 a) Pressure mats were also affixed to the chair during portions of testing, b) Schematic of the rotations of the articulating chair, with the back, thorax, pelvis and seat pan identified. The thorax and pelvic supports rotated about their centers, and the back and seat pan rotated about the point labelled CoR

Articulating Chair Design

An articulating chair was designed with an independently rotating (tilting) seat pan, as well as independently rotating pelvic and thoracic supports. The pelvic and thoracic supports were mounted on a reclining back, as seen in Figure 4.1. All three supports were attached to six-axis

load cells (AMTI, Watertown, MA) and covered by a thin layer of foam with a vinyl cover. A "neutral" chair position was defined when the seat back was vertical (0° recline), the seat pan was horizontal (0° tilt), and the pelvic and thoracic supports were parallel to the back (vertical). The back recline was able to move from vertical to 20° rearward of recline [2]. The front of the seat pan was able to tilt up to 30° with respect to horizontal, such that the front edge of the seat pan was higher than the back. The rotation center for the chair back and seat pan (CoR in Figure 4.1b) was located approximately at the hip joint center. Both the pelvic and thoracic supports (which rotated about their centers) were able to rotate 15° in either direction (i.e. upward facing 15° or downward facing 15°). The thoracic support was rotated to face downward 15°, and the pelvic support was rotated to face upward 5°to create a concave surface for a slouched (kyphotic) back articulation. The opposite rotations were used to support an erect (lordotic) articulation [250] (Figure 4.1b).

The articulating chair was used to collect data in two sequential sessions, as described in the following sections. Pressure data were collected in 27 seated positions. Based on the results of the pressure data during pilot testing, a second set of tests were conducted in nine positions to collect perfusion data. These nine positions were those chair configurations that had the largest effects on pressure in the regions of the ITs. Note, chair back articulations had the least effect on the IT pressures; therefore only back recline and seat pan tilt were used during the collection of perfusion data.

Table 4.1 Combinations of chair back recline, seat pan tilt, and back articulation in which pressure measurements were taken. Each back recline was used with each seat pan tilt and back articulation resulting in 27 different chair positions

Back Recline	Seat Pan Tilt	Back Articulation
No recline (0°)	No pan tilt (0°)	Slouched
Half recline (10°)	Half pan tilt (15°)	Neutral
Full recline (20°)	Full pan tilt (30°)	Erect

Back and Seat Pan Pressure Measurements

Pressure measuring mats (Tekscan, Boston, MA) covered the seat pan and the pelvic and thoracic supports of the articulating chair (Figure 4.1a). Each mat was an array of 42 by 48 sensors. The pressure mats were secured to the seat pan and back supports to maintain consistent alignment. To quantify interface forces, the seat pan, pelvic, and thoracic supports were mounted on load cells located in the centers of their cross sections. All load cells were calibrated before the participant sat in the chair.

Each participant was instructed to sit with their buttocks in contact with the pelvic support while the chair was in a neutral position (i.e. no back recline, no seat pan tilt, neutral back articulation). The chair was then articulated into each of 27 positions (Table 4.1) with a randomization strategy. A measurement of the pressure on the buttocks and back was obtained while in each position with simultaneous recordings from the load cells.

Pressure Data Analysis

The total force measured by the pressure mats (in Newtons) on the seat pan and back supports were compared to the perpendicular forces measured by the load cells (also in Newtons) beneath the supports [251], [252]. Uniform scaling factors (the force measured by the load cell(s) divided by the force measured by the pressure mat) were applied to the pressure measurements (in kPa) on each pressure mat to ensure the sums of the forces measured by pressure sensors equaled the total force obtained by the load cells, described by Eq. 4.1.

$$Pressure_{adjusted} = \frac{Force_{load\ cell(s)}}{Force_{pressure\ mat}} \times Pressure_{raw} \qquad \text{(Eq. 4.1)}$$

The total back pressure mat force was compared to the sum of the pelvic and thoracic load cell forces, and the total seat pan pressure mat force was compared to the seat pan load cell force. The value of each sensor with a nonzero measurement of pressure ($P_{i,j}$) was then reported as the average value of nine sensors (the sensor itself and all eight adjacent sensors). This process is described by Eq. 4.2.

$$P_{i,j} = \frac{\sum_{m=i-1}^{i+1} \sum_{n=j-1}^{j+1} P_{m,n}}{9} \quad \text{(Eq. 4.2)}$$

where the indices 'i' and 'j' were the row (1-42) and column (1-48) of the individual pressure sensor. The indices 'm' and 'n' were defined as the ranges from 'i-1' to 'i+1' and 'j-1' to 'j+1', as indicated in Eq. 4.2.

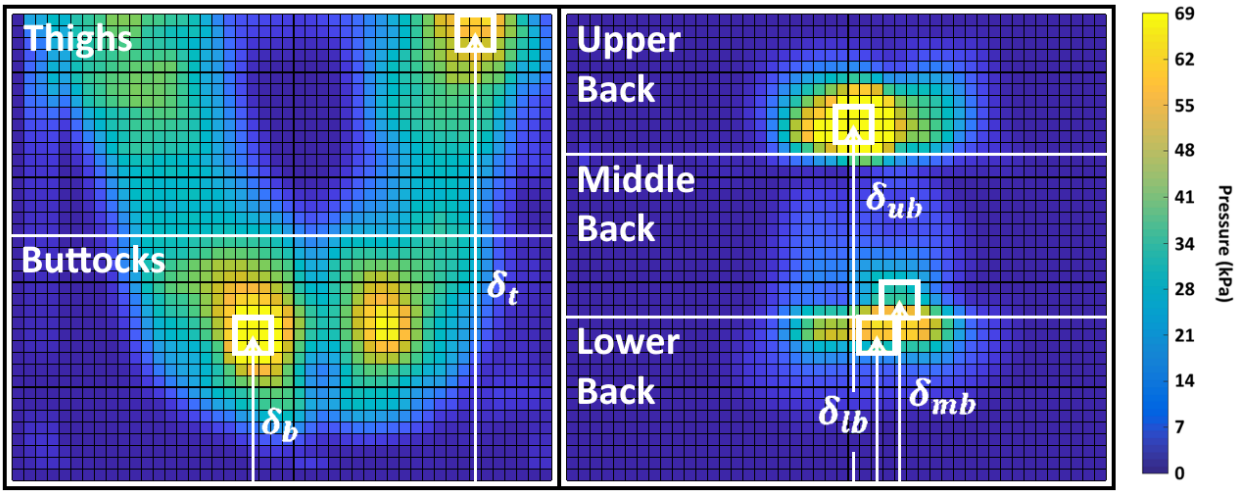

Figure 4.2 Segmentation of the seat pan (left) and back (right) pressure mat readings into regions. The seat pan was split up into the buttocks and thigh regions. The back was split up into the upper, middle, and lower back regions. δ, the location of the maximum pressure, was measured in mm from the posterior edge of the pressure mat in the buttocks and thighs and from the inferior edge of the pressure mat for the upper, middle, and lower back regions

Regions of interest were determined by segmentation of the back and seat pan pressure mats. The back regions were determined by the segmentation of the back pressure mat into thirds from

superior to inferior (upper, middle, and lower). The seat pan pressure mat was segmented into posterior and anterior halves, labeled the buttocks and thighs (Figure 4.2). The locations and magnitudes of the sensors recording the maximum pressures within each body region were recorded (i.e., the row of the measurement from the pressure mat). These rows were used to determine the superior-inferior location of the maximum pressures on the back and the anterior-posterior location of the maximum pressures on the seat pan. The locations of the maximum pressures were recorded as the distances from the posterior edge of the seat pan in millimeters for the buttocks and thighs ($\delta_b and\ \delta_t$, respectively, larger values indicated more anterior); and locations of the maximum pressures in the back regions were recorded as distances from the inferior edge of the back (δ_{ub} is the upper back location, δ_{mb} is the mid back location, δ_{lb} is the lower back location, and larger values indicated more superior), as seen in Figure 4.2.

Perfusion Measurements

An initial analysis of pressure data indicated that back recline and seat pan tilt had much larger effects on the magnitude and locations of pressure concentrations in the buttocks than back articulation. Therefore, perfusion data were collected on the skin over the right IT in the nine combinations of back recline and seat pan tilt indicated in the first two columns of Table 4.1, while the back articulation was maintained in the neutral position.

All participants wore athletic shorts so a perfusion sensor could be attached directly to the skin over the right IT. Participants were instructed on how to identify the IT via palpation; and once identified, a researcher attached a laser Doppler flowmetry sensor (Perimed, Järfälla, Sweden) to the tissue with a double-sided tape ring under and tape over the sensor to ensure good contact throughout the session. Participants sat in the position for two minutes to allow perfusion

to stabilize [164]. Perfusion measurements consisted of recording 30 seconds of data in each of the nine positions during which participants did not move.

Perfusion Data Analysis

The average values of perfusion over each recording period were calculated. Perfusion data were then normalized *for each individual* by dividing the average measurement in each position by the maximum average measurement recorded for that individual, meaning the values reported spanned between zero and one. Such normalization has previously been conducted to ensure that comparisons between chair positions were not affected by inter-person differences in perfusion magnitude [247].

Statistics

A repeated measures ANOVA, followed by a Tukey test, was conducted to determine the effects of the back recline, seat pan tilt, and back articulation on the magnitudes and locations of the maximum pressures in the three back regions, buttocks, and thighs. A second analysis was conducted to determine the effects of the seat pan tilt and back recline on the blood perfusion in the tissue over the IT.

Results

Participants

Ten males (average age 22.2 ± 3.0 years, average height 178.8 ± 4.2 cm, average mass 78.6 ± 11.6 kg), and ten females (average age 22.7 ± 3.6 years, average height 165.5 ± 5.4 cm, average mass 58.9 ± 9.3 kg) participated in this study.

Seated pressures and perfusion were analyzed within each sex. There were no differences in trends of pressure or perfusion between sexes with respect to recline or seat pan tilt. There were also no differences in pressure trends in response to changes in back articulation. Thus, the seated loading data and perfusion for both sexes were analyzed together and are presented in the results.

Recline

The effects of back recline on the magnitudes and locations of the maximum pressures in each region are reported in Figures 4.3 and 4.4, respectively. Reclining the chair back increased the maximum pressure in the buttocks ($p < .0001$) and lower back ($p < .0001$) regions, while it decreased the maximum pressures in the upper back ($p < .0001$) and thigh ($p < .0001$) regions. Reclining the back also caused a significant posterior shift of the maximum pressures in the buttocks ($p < .0001$) and inferior movement of maximum pressure in the middle back ($p < .0001$).

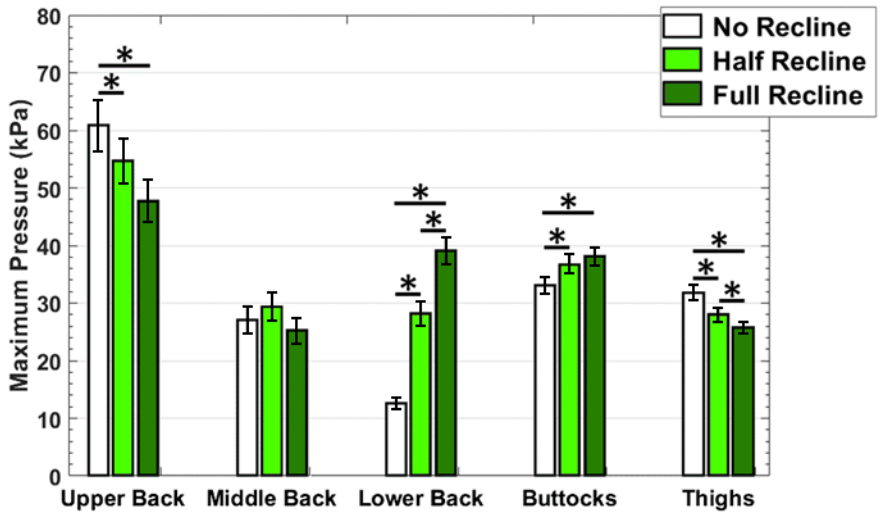

Figure 4.3 The effects of back recline on the magnitudes of the maximum pressures within each region. Columns are grouped by regions. Statistical differences between recline angles are indicated by asterisks (*). Increases in back recline angle consistently resulted in significant decreases in maximum pressures in the upper back and thighs and increases in maximum pressure in the lower back and buttocks

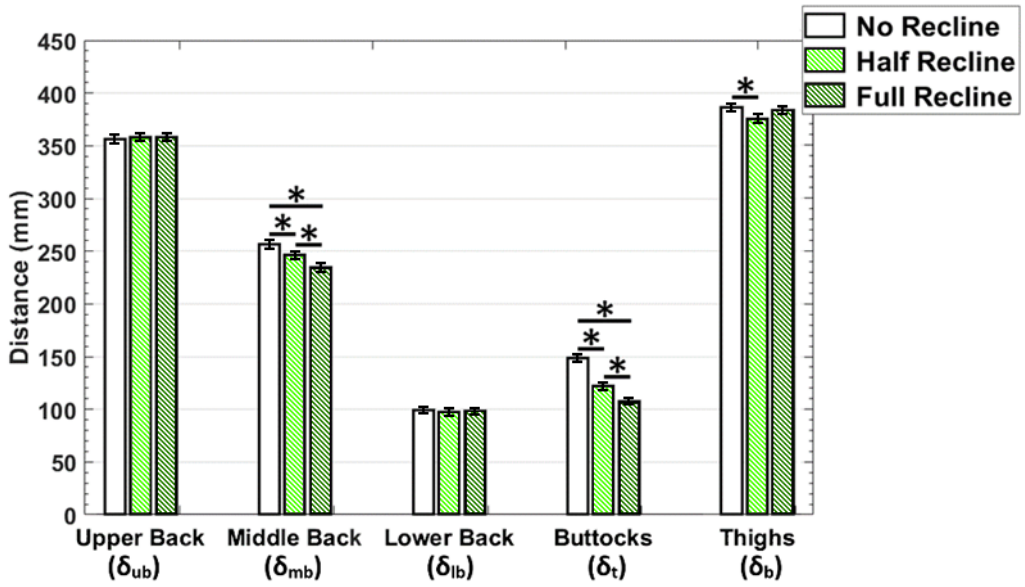

Figure 4.4 The effects of back recline on the locations of the maximum pressures within each region. Statistical differences between recline angles are indicated by asterisks (*). Increases in back recline angle resulted in the maximum pressure shifting inferiorly for the middle back and posterior shifts in the buttocks

Seat Pan Tilt

The effects of seat pan tilt on the magnitudes and locations of the maximum pressures in each region are reported in Figures 4.5 and 4.6, respectively. Increasing seat pan tilt decreased the maximum pressures in the buttocks ($p < .0001$) and lower back ($p < .0001$) regions and increased the maximum pressures in the thighs ($p < .0001$) and in the upper ($p < .0001$) and middle ($p < .0001$) back regions. The maximum pressures in the middle ($p < .0001$) and lower ($p = .0005$) back regions shifted superiorly when the seat pan was tilted. The maximum pressures in the buttocks shifted anteriorly with increasing seat pan tilt ($p < .0001$).

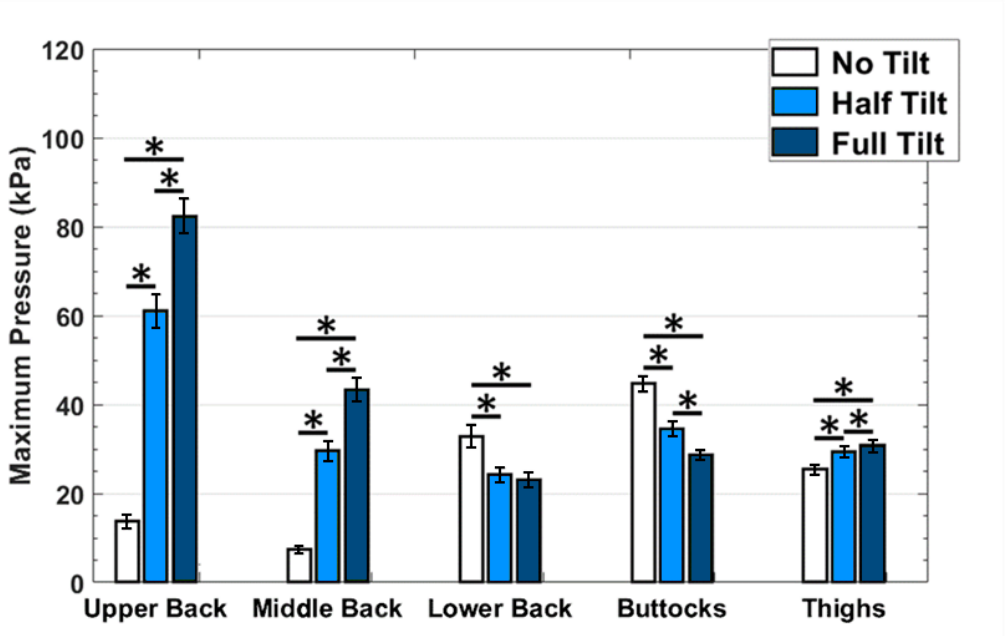

Figure 4.5 The effects of seat pan tilt on the magnitudes of the maximum pressures within each region. Statistical differences between seat pan tilts are indicated by asterisks (*). Increases in seat pan tilt corresponded to increased maximum pressure in the upper back, middle back, and thigh regions and decreased maximum pressure in the lower back and buttocks regions

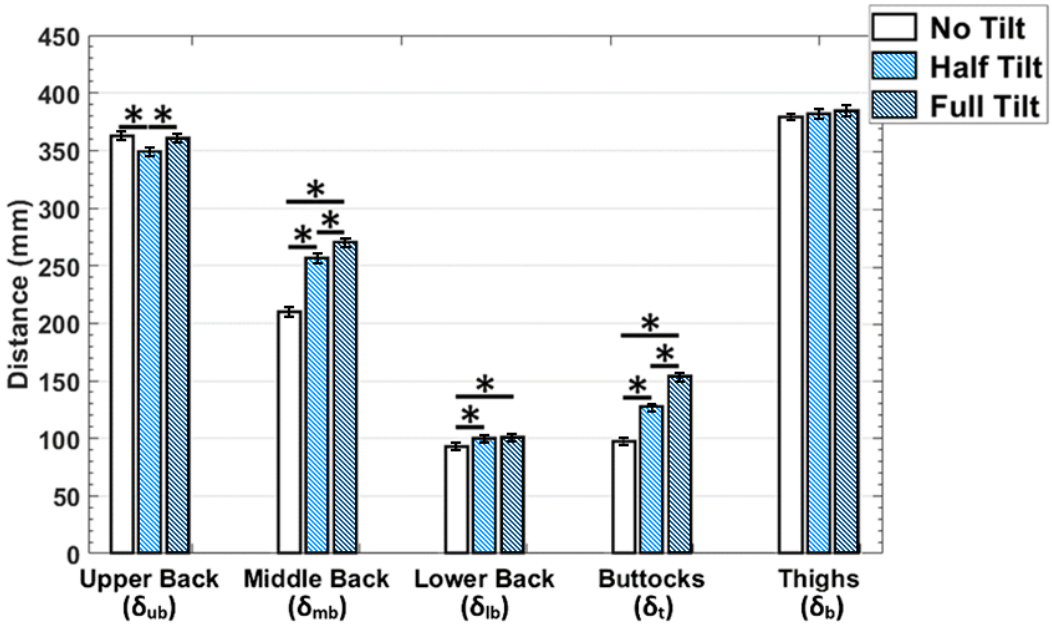

Figure 4.6 The effects of seat pan tilt on the locations of the maximum pressures within each region. Statistical differences between seat pan tilts are indicated by asterisks (*). Increasing seat pan tilt corresponded to superior shift of maximum pressures in the middle and lower back regions and the anterior shift of maximum pressures in the buttocks region

Articulation of the thorax and pelvic supports – slouched, neutral, erect

The effects of thorax and pelvic support articulations on the magnitudes and locations of the maximum pressures are reported in Figures 4.7 and 4.8, respectively. When changing articulation from slouched to erect, the maximum pressures in the upper back increased ($p < .0001$), while the maximum pressures in the middle ($p < .0001$) and lower ($p = .0106$) back regions decreased. Changing articulation from slouched to erect shifted the maximum pressures inferiorly in the upper ($p < .0001$) and middle ($p = .0012$) back regions and superiorly in the lower back region ($p < .0001$).

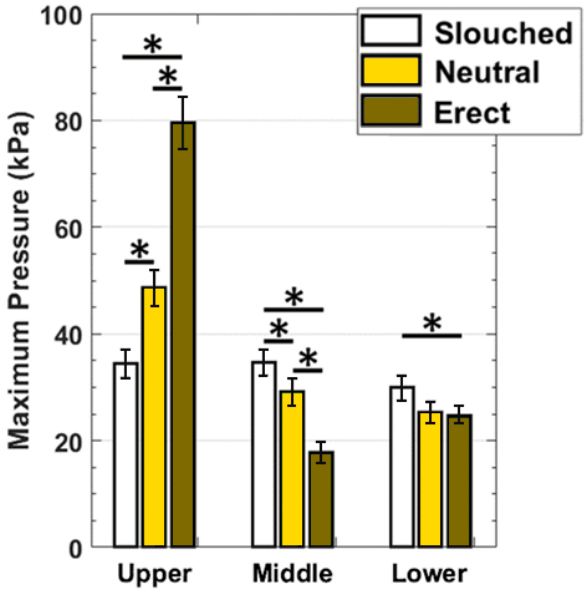

Figure 4.7 The effects of back articulation on the magnitudes of the maximum pressures within each back region. Statistical differences between back articulations are indicated by asterisks (*). When changing articulation from slouched to erect, the maximum pressures in the upper back region increased, while the maximum pressures in the middle and lower back regions decreased

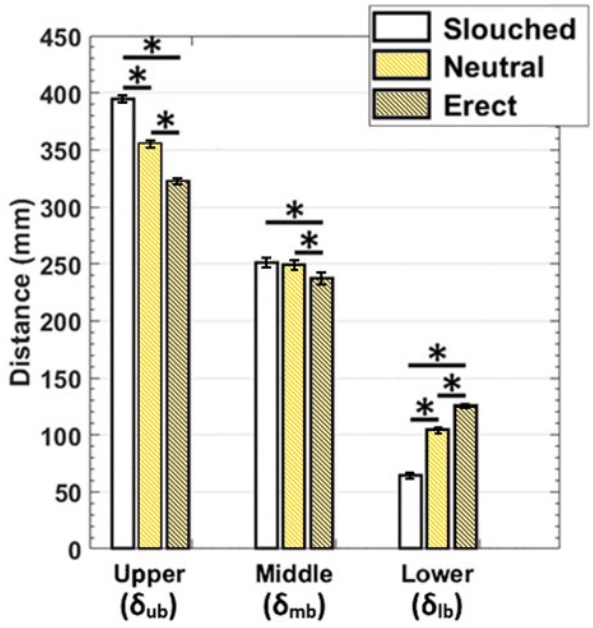

Figure 4.8 The effects of back articulation on the locations of the maximum pressures within each back region. Statistical differences between back articulations are indicated by asterisks (*). When changing articulation from slouched to erect, the maximum pressures in the upper and middle back regions shifted inferiorly, while the maximum pressures in the lower back regions shifted superiorly

Effects of Chair Articulation on Perfusion

The average perfusion values at each back recline and seat pan tilt angle are shown in Figure 4.9. Perfusion values were observed to have stabilized in each position before/during each measurement (slope of -.01±.14 perfusion units/second over the duration of each recording period). Participants had less perfusion in positions with larger back recline angles than in positions with no recline ($p = .0450$). Increasing seat pan tilt increased blood perfusion in the buttocks regardless of back recline angle ($p = .0006$). Participants had greater perfusion in positions with the half tilt angle relative to positions with no tilt ($p = .0265$) and greater perfusion in positions with full tilt than positions with half tilt ($p = .0158$).

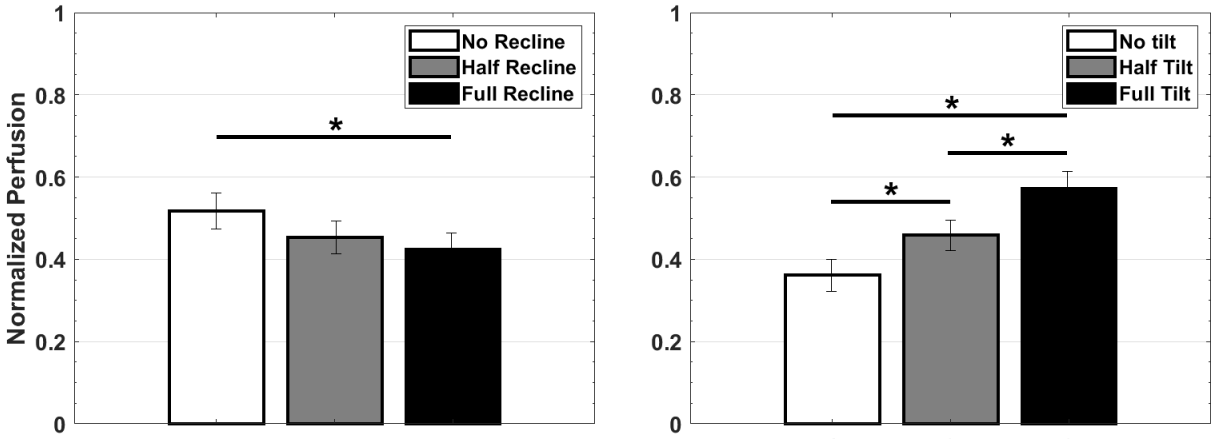

Figure 4.9 Average buttock perfusion values for each back recline (left) and seat pan tilt angle (right). Statistical differences between back recline or seat pan tilt angles are indicated by asterisks (*). Perfusion decreased in the full back recline positions relative to the no back recline positions and increased with seat pan tilt, regardless of the back recline angle

Discussion

The primary goal of this research was to investigate the effects of chair articulation on interface pressure and perfusion while seated. This goal was met by determining the relationships between isolated chair articulations, seated pressures, and perfusion measurements. Of particular interest were the buttocks and lower back regions due to the prevalence of PIs in those areas. Our data suggested that implementing only back recline, which is a commonly recommended approach for wheelchair users to reduce pressure on the ITs, may not be effective at relieving the pressure concentrations in those high-risk regions. On the contrary, our data indicated that the opposite occurred, and back recline increased pressure on the ITs. However, tilting the seat pan independently of the back significantly decreased the maximum pressure in the buttocks and caused a shift in pressure concentrations to different body regions. Furthermore, an increase in blood perfusion was consistently seen with seat pan tilt, further supporting the use of an isolated seat pan tilt for PI risk reduction. These findings indicated that with the correct combination of chair articulations, we can affect changes in parameters that are linked to PI formation.

Trends in these data showed that back recline and slouching increased the maximum pressures on the buttocks and lower backs, thus increasing the risk of PI formation. This is problematic because back recline is the most common pressure relief movement for wheelchair users [2]. Moreover, both recline and slouching moved the locations of the maximum pressures towards bony landmarks around which PIs form (sacrum, ITs, and coccyx), further increasing risk in those areas [30], [51].

The data from the seat pan tilt articulation and erect back articulation showed the opposite trends, indicating potential protective effects in the buttocks and lower back. These movements led to reduced pressures and, in the case of seat pan tilt, increased perfusion. Seat pan tilt shifted pressure from the buttocks onto the thighs and shifted the maximum pressure locations anteriorly in the buttocks region, away from the ITs and coccyx. In the back, the erect articulation decreased the maximum pressure in the lower back and shifted its location superiorly, offloading the bottom area of the lower back near the sacrum. These movements reduced risk factors associated with PI formation in the buttocks and lower back, both of which are PI prone areas.

This research study provides new insights into how seated articulations affect key PI risk factors. Previous research indicated that tissues can survive large loads, as long as they are applied intermittently [106], [253]. Thus, the work presented here indicates that one potential strategy to reduce PI risk would be a new wheelchair design that cyclically loads and unloads different regions of the body while seated. Not only would such a regimen intermittently unload regions of the body, our research indicates that it restores perfusion to areas that may experience decreased perfusion while seated, such as the ischium. Further research is needed to confirm these effects in wheelchair users, but these initial findings in able-bodied individuals are promising.

Conclusions

This work conducted tests on able-bodied individuals in an articulating chair to investigate the effects of seated repositioning on interface pressure over the entire body and blood perfusion in the buttocks. Results indicated that 1) tilting the seat pan while seated reduced the pressure on the buttocks and lower back, 2) reclining the back reduced pressure on the upper back and thighs, and 3) reductions in pressure in the buttocks coincided with increased perfusion under the ITs. Based on these results, a seated repositioning regimen to cyclically reduce pressure on body regions and promote blood flow can be used, thus leading to a reduction of reduce pressure injury risk. Future work will investigate whether pressure and perfusion trends seen in able-bodied individuals are also the same in wheelchair users.

CHAPTER 5: KEY COMPONENTS RELATED TO PRESSURE INJURY FORMATION: UNDERSTANDING PRESSURE DISTRIBUTION AND BLOOD PERFUSION RESPONSES IN WHEELCHAIR USERS

Introduction

PIs have been shown to cause significant challenges for wheelchair users, including prevalence rates as high as 47%, hospital stays of up to 22 weeks and increased risk of infection [7], [14], [16], [254]. Furthermore, studies showed that recurrence rates were as high as 53% [246]. Treatment costs of PIs have also been reported to be significant with expenses of $120,000 per incident [8]. These factors contributed to the reported annual costs of $27 billion for PI treatment in the United States [15]. The problem of PIs for wheelchair users is not trivial.

The regions that have the largest incidence of PI formation were predominately found around bony landmarks that experience large loads while seated [16]. Specifically, the ischial tuberosities, coccyx, sacrum, and shoulder blades have been reported as having the highest incident of PI formation [16], [17], [21], [32]. Wheelchair users have been reported to spend 10-12 hours a day in their chair with limited movement; studies have shown that the seated position produced larger tissue stresses in their buttocks than able-bodied people [2], [82], [255], [256]. Reduced capillary blood flow, or blood perfusion, combined with the increased internal tissue stresses for extended time in the seated position has been shown to result in tissue necrosis and PI formation [17], [27], [101]. Thus, loading and blood perfusion have been frequently been used by researchers as metrics for the risk assessment of PI development [28], [91], [120].

Several strategies have been utilized by clinicians and wheelchair users in an attempt to reduce the incidence of PI formation. These strategies have included specialized cushions, whole-body-lifts executed by the patient (e.g., using their arms to lift their buttocks off the seat pan) and seated repositioning [21], [257] [146]. Studies reported that cushions were able to reduce, but not

eliminate, the occurrence of PIs [21], [147], [148]. Also, the literature reported that whole-body-lifts required more mobility than some wheelchair users possess [164]. The most commonly used repositioning strategies in wheelchairs were back recline and whole body tilt, yet limited evidence has been published to support their ability to reduce pressures in high-risk regions [2], [108], [125], [248]. A recent study found that whole body tilt and back recline could improve perfusion in the buttocks, however, this was true only if the tilt and recline angles were large [161]. Tilted positions also were shown to have some negative outcomes, such as increased pressure on the sacrum and disengaged patients from tasks of daily living [68], [249]. Thus, a need exists for PI prevention strategies that are accessible to all wheelchair users and have evidence to support their usage.

Seated repositioning has been one strategy for PI prevention, but existing research on repositioning is limited both by the populations tested and the modalities of recorded data. Two published studies were located that included individuals with SCIs and evaluated the effects of isolated seat pan tilt and whole-body tilt on seated interface pressure. One study investigated isolated seat pan tilt, but it did not include any other movements of the chair, and interface pressure data were only collected on the seat pan [258]. The second study investigated pressure changes in the buttocks and back due to whole body tilt, but isolated back recline or seat pan tilt were not investigated [68]. Neither of these studies included isolated back recline, which is the most commonly used position for pressure relief in wheelchair users [2]. Existing work noted that peak loads on the buttocks of individuals with SCIs were greater than those of able-bodied individuals, deepening the need for an improved understanding of interface pressure data from wheelchair users using common repositioning strategies [21], [108], [160]. Pressure changes on tissue have been shown to affect perfusion in the tissue [100], [101], [119], [259]. While one study investigated how perfusion in the buttocks changes with seated repositioning and pressure changes, it focused

on able-bodied individuals [161]. Since pressures in wheelchair users are larger than able-bodied individuals, there is a need to understand perfusion responses in the buttocks of that population as well.

The research reported here was designed to address some of these gaps. Thus, the goals of this study were to evaluate the effects of back recline, seat pan tilt, and back articulation on the interface pressures and buttock perfusion across a sample of wheelchair users.

Methods

Participant Recruitment

Ten adult male wheelchair users volunteered to participate in this study. Exclusion criteria included active wounds on the buttocks or thighs, vascular diseases, or an inability to transfer into or change position in the laboratory chair. Approval for this study was granted by the Biomedical and Health Institutional Review Board at Michigan State University.

Articulating Chair Positions

A custom designed articulating chair was used to collect data for this study, shown in Figure 5.1. The articulating chair had independently rotating seat pan, pelvic, and thoracic supports; and the pelvic and thoracic supports were mounted on a reclining back. Both the seat pan and back rotated about a point approximately at the hip joint center of a seated individual (labeled 'CoR' in Figure 5.1). The seat pan, pelvic, and thoracic supports were each mounted to a six-axis load cell (AMTI, Watertown, MA) located in the middle of their cross sections and covered with a thin foam layer and vinyl. Angles of back recline, seat pan tilt, and rotation of the pelvic and thoracic supports are reported in Table 5.1. The angle of the back was measured relative to the

vertical axis (up to 20° of recline), the seat pan relative to the horizontal axis (up to 30° of rearward tilt) (Figure 5.1). The rotation of the thoracic support face was downward 15° for the slouched back articulation, while the rotation of the pelvic support face was 5° upward with respect to the overall recline [250]. The opposite rotations were used for the erect back articulation. For the neutral back articulation, both supports were parallel to one another. Controls were positioned on the arm of the chair to adjust the motors that drove articulations. 27 combinations of back recline, seat pan tilt, and back articulation were included in the study, with a "neutral" position being no back recline, no seat pan tilt, and a neutral back articulation.

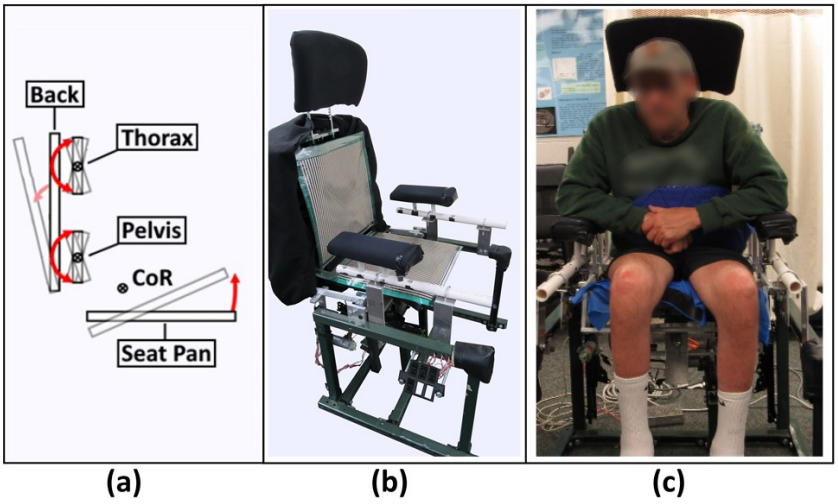

Figure 5.1 a) Schematic of the rotations of the articulating chair, with the centers of rotation for the back and seat pan (CoR), pelvic support, and thoracic support identified. b) Pressure mat placement on the articulating chair during testing. c) Wheelchair user sitting in the articulating chair during testing

Based on the results of pilot work, it was found that back recline and seat pan tilt caused the largest changes in pressure (both magnitude and locations) under the buttocks and thus also affected perfusion the most. Therefore, a subset of positions with three back recline angles and three seat pan tilt angles (9 in total) were repeated with the addition of a perfusion probe under the right ischial tuberosity.

Table 5.1 Combinations of chair back recline, seat pan tilt, and back articulation in which pressure measurements were taken. Each back recline was tested with each seat pan tilt and back articulation

Back Recline	Seat Pan Tilt	Back Articulation
No recline (0°)	No pan tilt (0°)	Slouched
Half recline (10°)	Half pan tilt (15°)	Neutral
Full recline (20°)	Full pan tilt (30°)	Erect

Interface Pressure Data Collection & Analysis

Pressure and force data were collected in all 27 chair positions. Two pressure mats (Tekscan, Boston, MA), consisting of 42 rows of 48 sensors, covered the seat pan, pelvic, and thoracic supports (Figure 5.1b). One mat covered the seat pan, and the other covered the pelvic and thoracic supports. Consistent alignment throughout the testing was maintained by securing the pressure mats to their respective supports. The load cells mounted beneath each support were calibrated before participants transferred into the chair and were used to collected forces on each support.

Participants transferred into the chair while it was in a neutral position, and each participant sat with their buttocks contacting the back of the chair along the pelvic support. The chair was then articulated, using a randomization strategy to select the back recline angle, seat pan tilt angle, and back articulation until data were collected in all positions.

The forces measured from the load cells were used to calibrate the pressure data. The total forces measured by each pressure mat were related to the forces perpendicular to the face of each support measured by each load cell [251], [252]. The magnitudes of each pressure sensor measurement on the seat pan were multiplied by the ratio of the perpendicular force measured by the load cell under that support divided by the total force measured by the pressure mat on the seat pan. The magnitudes of every pressure sensor measurement on the back were multiplied by the ratio of the sum of the perpendicular forces measured by the load cells behind the pelvic and

thoracic supports divided by the total force measured by the pressure mat on the back. This process is described by Eq. 5.1:

$$P_{m,n} = \frac{F_{load\ cell(s)}}{\sum_{x=1}^{42}\sum_{y=1}^{48} P_{x,y}A_{x,y}} \times P_{x,y} \quad \text{(Eq. 5.1)}$$

where $P_{x,y}$and $A_{x,y}$ were used to represent the pressure magnitude (in kPa) and area (in mm^2) of each sensor in the mat, $F_{load\ cell(s)}$as the perpendicular force (in N) measured by either the load cell under the seat pan or the sum of the load cells behind the pelvic and thoracic supports, and $P_{m,n}$ represented the pressure adjusted so that the total force matched that of the load cell.

After adjustment, the final pressure value for each sensor was determined to be the average value of the sensor itself and the eight surrounding sensors. This process is summarized by Eq. 5.2:

$$P_{i,j} = \frac{\sum_{m=i-1}^{i+1}\sum_{n=j-1}^{j+1} P_{m,n}}{9} \quad \text{(Eq. 5.2)}$$

where $P_{i,j}$ represented the final averaged pressure value for the sensor in the ith row (1-42) and jth column (1-48).

Regional Analysis of Pressures

Each pressure mat was split into regions based upon the rows of sensors. The pressure mat on the seat pan was split into anterior and posterior halves, termed the thighs and buttocks. The pressure mat on the back was split into thirds from inferior to superior, termed the lower back, middle back, and upper back (Figure 5.2). The locations of the ischial tuberosities and sacrum were in the buttocks and lower back regions, respectively. Both magnitudes and locations of the

largest pressure values in each region were recorded. Locations on the seat pan (δ_b for the buttocks and δ_t for the thighs) were measured as distances in millimeters from the posterior edge of the seat pan, and locations on the back (δ_{lb} for the lower back, δ_{mb} for the middle back, and δ_{ub} for the upper back) were measured as distances from the inferior edge of the pelvic support.

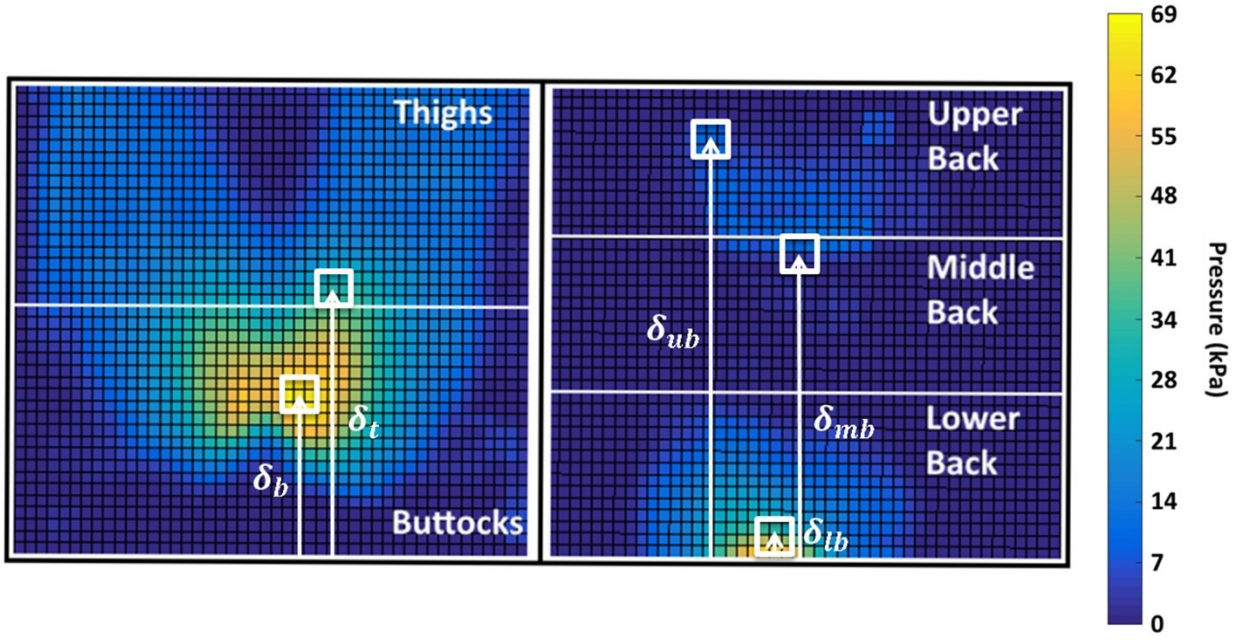

Figure 5.2 Break down of the seat pan (left) and back (right) pressure mat readings. The seat pan was split up into the buttocks and thigh regions with the zero reference point being at the most posterior location of the mat. The back was split into the upper, middle, and lower back region with the zero reference being at the most inferior point of the mat (near sacrum)

Perfusion Measurements & Analysis

The right ischial tuberosity was located via palpation, and a laser Doppler flowmetry sensor (Perimed, Järfälla, Sweden) was attached to the soft tissue over the right ischial tuberosity with double-sided tape beneath the sensor and medical tape over top of the sensor. Participants then sat in the articulating chair in a neutral position. With the participant seated and a neutral back articulation, the chair was then moved into one of the 9 combinations involving back recline and seat pan tilt. The participants sat in that position for two minutes before perfusion measurements

were obtained [164]. Thirty seconds of blood perfusion data were collected; and if the participant moved or encountered a spasm during a recording, the recording for that position was started over after the movement or spasm finished. The reported measurement for each position was the average value of the perfusion recording over the thirty seconds. Lastly, the perfusion measurements were normalized *within individuals* by dividing them by their largest perfusion measurement across all positions. This permitted comparisons of the changes caused by posture changes across individuals [247].

Statistics

A repeated measures ANOVA was used to determine the effects of back recline, seat pan tilt, and back articulation on magnitudes and locations of the maximum pressure data across all positions. A second repeated measures ANOVA was used to determine the effects of back recline and seat pan tilt on perfusion measurements in the buttocks. Differences in the magnitudes and locations of the maximum pressures and perfusion data due to the articulations were detected with post-hoc Tukey tests.

Results

Participants

Ten male wheelchair users (average age 37.1±7.89 years, average time using a chair 21.8±12.85 years, average height 174.8±13.21 cm, average mass 76.4±16.53 kg) participated in this study. Participants reported spending an average of 11.50±2.51 hours per day in their chair and had a range of conditions and injuries that resulted in wheelchair usage. These included spinal cord injuries, cerebral palsy, and spina bifida.

Articulation Effects on Pressure

Recline

Back recline affected the magnitudes and/or locations of the maximum pressures in the upper back, lower back, buttocks, and thighs, shown in Figures 5.3 and 5.4. The maximum pressures in the buttocks and lower back regions increased with back recline ($p < .0001$ for both regions), while the maximum pressures in the upper back ($p < .0001$) and thighs ($p = .0003$) decreased. The locations of the maximum pressures shifted posteriorly in the buttocks ($p = .0002$) and thigh regions ($p = .0136$) with back recline.

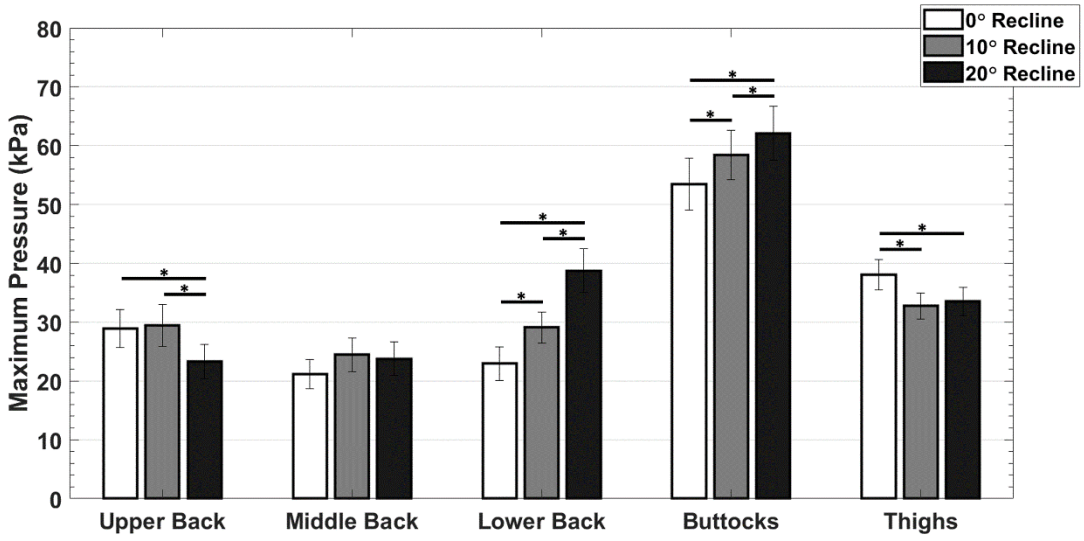

Figure 5.3 The effects of back recline on the *magnitudes* of the maximum pressures within each region. Increasing the back recline angle increased maximum pressures in the buttocks and lower back and decreased maximum pressures in the upper back and thighs. Differences between recline angles are indicated by asterisks (*)

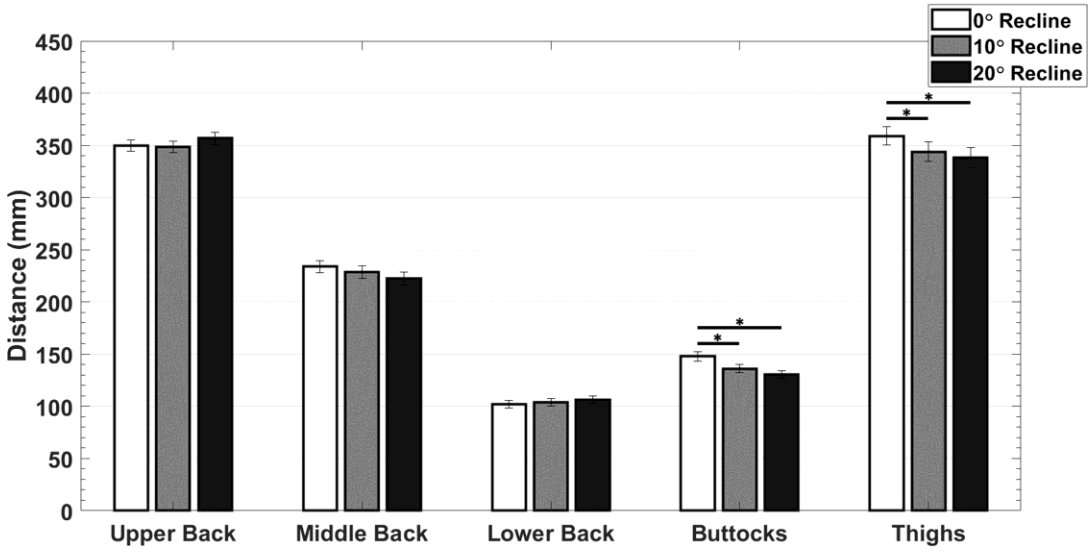

Figure 5.4 The effects of back recline on the *locations* of the maximum pressures within each region. Increasing the back recline angle caused a posterior shift in the maximum pressure regions of the buttocks and thighs. Differences between recline angles are indicated by asterisks (*)

Seat Pan Tilt

Seat pan tilt affected the magnitudes and/or locations of the maximum pressures in the upper back, middle back, buttocks, and thighs, shown in Figures 5.5 and 5.6. The maximum pressures in the buttocks decreased ($p < .0001$) and maximum pressures in the middle ($p < .0001$) and upper ($p < .0001$) back regions increased with seat pan tilt. The locations of the maximum pressures in the middle ($p < .0001$) and lower ($p < .0001$) back regions shifted superiorly and locations shifted anteriorly in the thigh ($p < .0001$) regions with seat pan tilt.

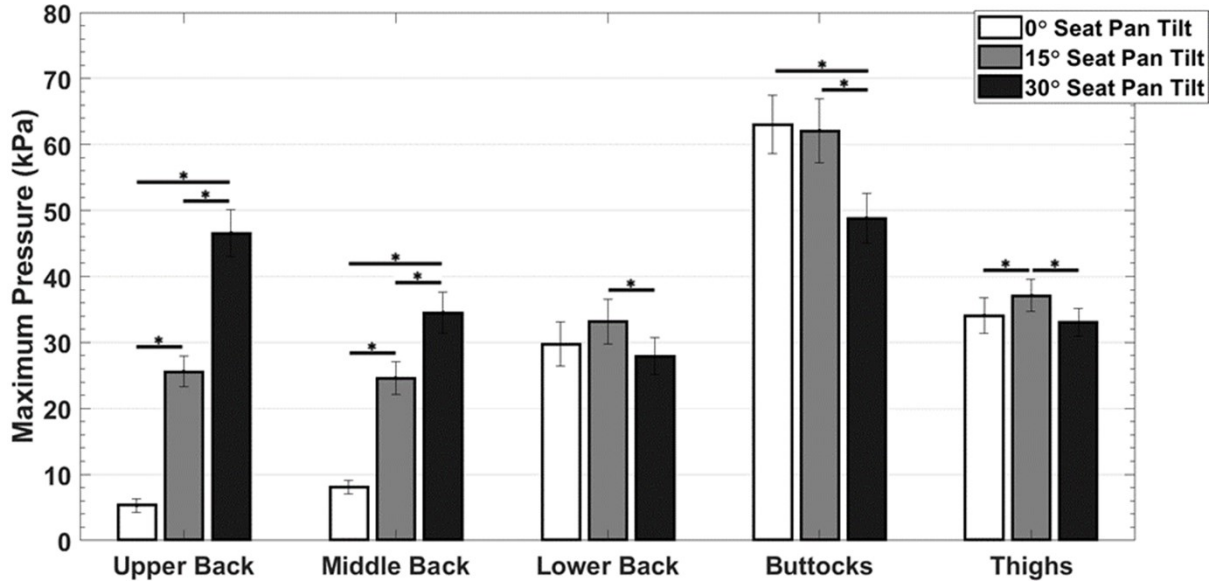

Figure 5.5 The effects of seat pan tilt on the *magnitudes* of the maximum pressures within each region. Increasing the seat pan tilt angle increased the maximum pressures in the upper and middle back and decreased maximum pressures in the buttocks. Differences between seat pan tilts are indicated by asterisks (*)

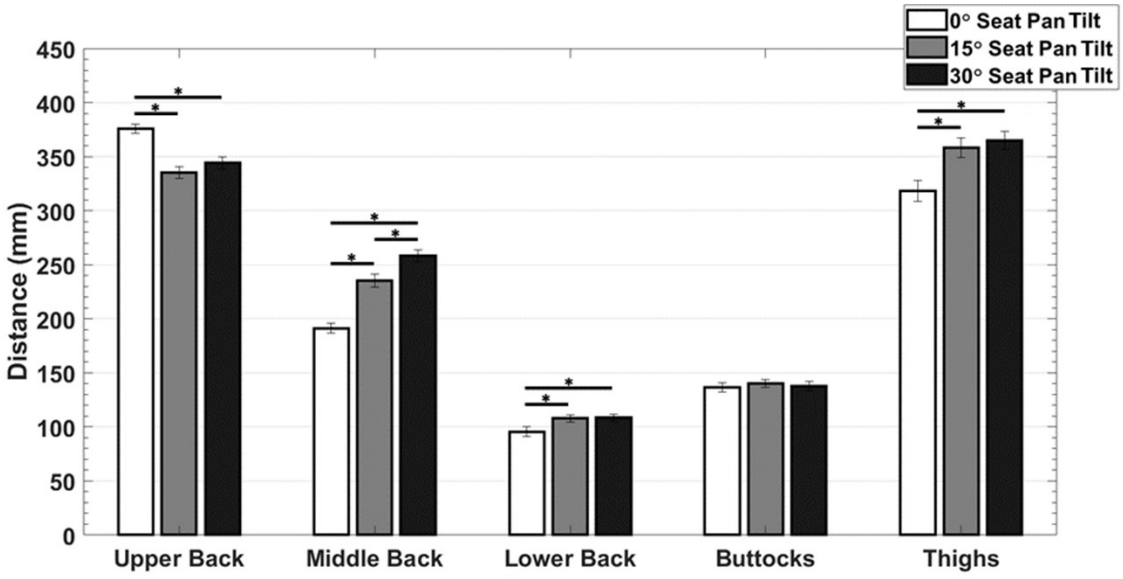

Figure 5.6 The effects of seat pan tilt on the *locations* of the maximum pressures within each region. Increasing seat pan tilt angle caused a superior shift in the maximum pressure regions of the middle and lower back and an anterior shift in the maximum pressure regions in the thighs. Differences between seat pan tilts are indicated by asterisks (*)

Back Articulation

Back articulation affected the magnitudes and/or locations of the maximum pressures in upper, middle, and lower back regions, shown in Figures 5.7 and 5.8. No significant effects due to back articulation were detected in the magnitudes or locations of the maximum pressures in the buttocks and thighs. The maximum pressures increased in the upper back ($p < .0001$) and decreased in the middle back ($p < .0001$) regions when changing back articulation from slouched to erect. The locations of the maximum pressures shifted inferiorly in the upper back ($p < .0001$) and superiorly in the lower back ($p < .0001$) when changing back articulation from slouched to erect.

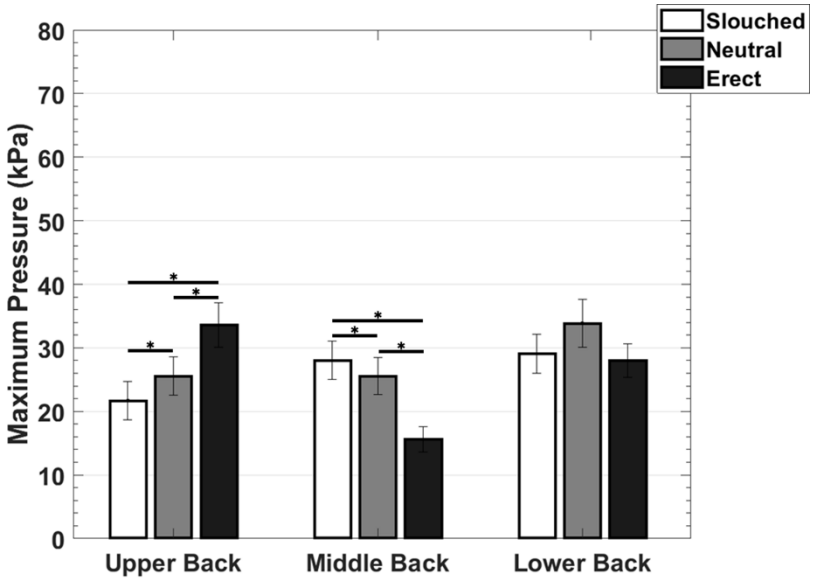

Figure 5.7 The effects of back articulation on the *magnitudes* of the maximum pressures within each region. Articulating the back from slouched to erect increased maximum pressures in the upper back and decreased maximum pressures in middle back. Differences between back articulations are indicated by asterisks (*)

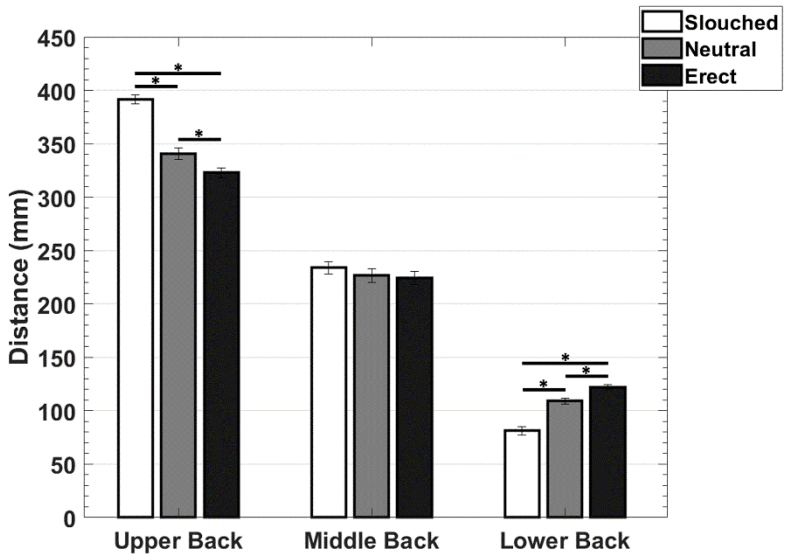

Figure 5.8 The effects of back articulation on the *locations* of the maximum pressures within each region. Articulating the back from slouched to erect caused an inferior shift in the maximum pressure regions in the upper back and a superior shift of the maximum pressure regions in the lower back. Differences between back articulations are indicated by asterisks (*)

Postural Effects on Perfusion

Mixed results were observed with respect to blood perfusion in the wheelchair users. Perfusion values were observed to have stabilized in each position before/during each measurement (slope of .00±.20 perfusion units/second over the duration of each recording period). Participants fell into two groups: 1) those who experienced an increase in blood perfusion in the buttocks in response to seat pan tilt (termed responders), and 2) those who did not experience an increase in perfusion in response to seat pan tilt (termed non-responders). Four participants experienced an increase in perfusion with increasing seat pan tilt ($p = .0013$) and were designated the responder group. The non-responder group included two participants who had no change to their buttocks perfusion with seat pan tilt and four participants who experienced a decrease in buttock perfusion with seat pan tilt ($p < .0001$). The perfusion values for the entire cohort and responder group are reported in Figure 5.9.

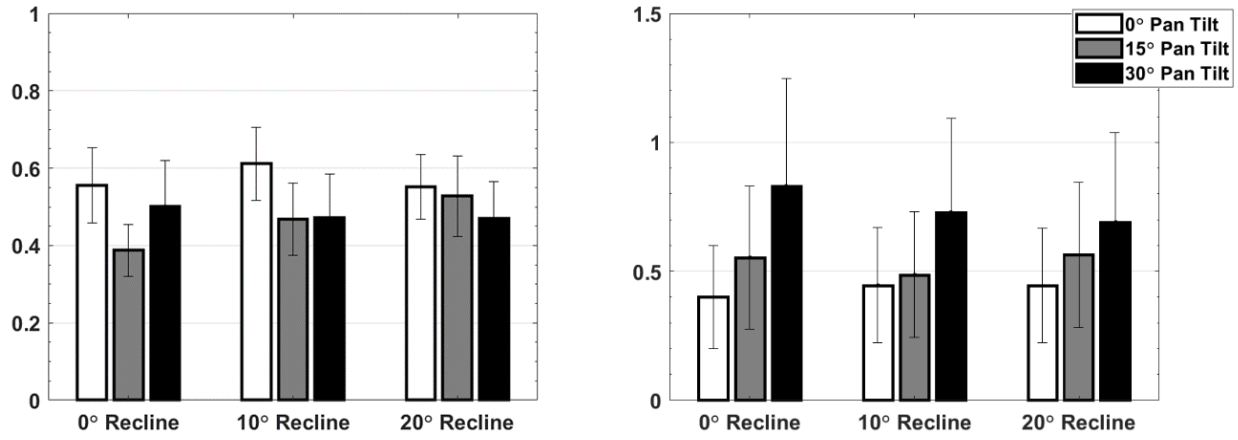

Figure 5.9 Normalized perfusion values for the entire cohort (left) and responders (right) at every back recline and seat pan tilt angle. Seat pan tilt increased perfusion in the responder group (p = .0013)

While both the responder and non-responder groups experienced the smallest maximum pressures in the buttocks in the positions with the maximum seat pan tilt, the magnitudes of the pressures differed between the two groups. The average maximum pressure in the buttocks of the responder group was 22.7 ± 3.6 kPa in positions with a full seat pan tilt. This average pressure was significantly smaller ($p < .0001$) than the average maximum pressure in the buttocks of the non-responder group in the same position (66.3 ± 4.3 kPa). Though there was a significant difference between pressures in the responder and non-responder group, there was not a significant difference between the masses of the responders (81.1 ± 7.6 kg) and non-responders (73.3 ± 6.5 kg) ($p = .50$).

Discussion

This research was conducted to evaluate the effects of chair articulations on interface pressures and buttocks perfusion of wheelchair users while seated. This research filled a knowledge gap, permitting a detailed understanding of how changes in seating position of wheelchair users affect interface pressures and blood perfusion.

Wheelchair users experienced increased pressure in the buttocks and lower back with back recline. In addition, they experienced a posterior movement of pressure concentrations in the buttocks. These two findings combined indicated that back recline produces circumstances that negatively affect factors known to increase PI formation. This is specifically true for body regions where PIs are common, the buttocks and lower back. However, one of the strategies wheelchair users are encouraged to implement frequently is to recline – the common clinical advice being that reclining would reduce pressures in these regions [2]. Based on our findings, the clinical suggestion of recline as a pressure relieving mechanism for the buttocks (ischial tuberosities and coccyx) and lower back (sacrum) should be re-evaluated.

Seat pan tilt decreased pressure on the buttocks, which supports its use for the reduction of PI risk in the buttocks. The superior shift in maximum pressure of the lower back with seat pan tilt further suggests that seat pan tilt may reduce PI risk around the sacrum. However, few wheelchairs offer the ability to change the seat pan tilt as an option; many times tilting is done as a whole-body-tilt, where the seat back and pan tilt together as a single motion. Our research also indicated changes in the back supports which created erect and slouched positions also showed the ability to shift pressure from one body region to another. An erect back articulation was observed to shift pressure concentrations in the lower and upper back towards the middle of the back and away from the bony prominences of the sacrum and scapulae. The presented data show that chair articulations such as seat pan tilt and back articulation are able to affect factors that are known to cause PIs.

Despite the consistent reduction of pressures in the buttocks with seat pan tilt, all participants did not exhibit a consistent change in perfusion. Some participants showed an increase in perfusion, while others showed no change, and some exhibited a decrease with seat pan tilt. This issue needs further exploration. These differences could be related to the anatomy of the individual

(less muscle mass and more adipose tissue), or the fact that the sample had varying types of injuries/diseases, or that there was a minimal layer of foam on our chair as compared to a thicker cushion. Those who did not experience an increase in buttock perfusion had approximately three times as large a pressure concentration in the buttocks as those who had increased perfusion, providing insight into the relationship between pressure and perfusion changes. While seat pan tilt alone did not increase the buttock perfusion of all the participants in our chair, it could be used in conjunction with other pressure reducing tools, such as specialized cushions, to further reduce pressure in the buttocks to a magnitude small enough that all wheelchair users are able to experience an increase in perfusion.

Based on the findings of our research, seated repositioning has promise as a tool to reduce the incidence of PIs by shifting the magnitudes and locations of interface pressure concentrations, and for some individuals, by increasing perfusion. Prior research indicated that tissues were able to survive external pressures for limited lengths of time [213]. Therefore, seat articulations such as the ones evaluated in this study could be used to cyclically load each region of the body, reducing the risk of PIs in any specific region by limiting exposure to pressure [106]. Doing so would be protective of the ischial tuberosities, coccyx, sacrum, and scapulae, all bony landmarks where PIs frequently occur [51]. Thus, a regimen of timed articulations presents one additional strategy in the prevention of PIs in wheelchair users.

Limitations

This work investigated the seated pressures under the buttocks and backs of wheelchair users. Although the cohort of wheelchair users in this study had ten people, there were no females who volunteered to participate. Additionally, we did not have a homogenous group in terms of

their injury or disease which required wheelchair use. Both of these limitations should be addressed in future studies. A limitation of the perfusion measurements was that the positions in which the maximum perfusion measurements were taken were not consistent for all individuals. Ideally, the maximum measurements could have been obtained in a position with the buttocks unloaded for all individuals, but such a position was not feasible with this cohort. In future studies, accessible perfusion data collection protocols will be explored for a position with no load on the buttocks Such a position can be used as a consistent maximum perfusion position with which to normalize all perfusion data. Future work may also consider normalizing loads by the body weight of the participants as an alternative to comparing raw pressure values to describe trends in the load data.

CHAPTER 6: THE EFFECTS OF PANTS AND CUSHION COVER MATERIAL ON SHEAR FORCES EXPERIENCED WHILE SEATED

Introduction

There are over 3 million wheelchair users living in the United States [1]. These wheelchair users are at an elevated risk of developing pressure injuries (PIs), with up to an 80% lifetime risk of experiencing one [61]. Incidence of a PI is highly disruptive, as treatment for PIs almost always involves consistent repositioning to offload the area around the wound, debridement of the wound itself, and dressings that need to be changed, among many other lesser used treatment strategies [260]. Further, treatment of PIs cost about $27 billion in the United States each year [15]. Thus, PIs are serious issues in how widespread, disruptive, and expensive they are.

One of the most consistent factors cited in the development of PIs is the presence of shear loading on the tissue [91], [98], [122], [261]. Shear loading has been implicated in the formation of PIs that start in superficial tissues and spread to deeper tissues [27]. Shear causes internal stress in tissues to which it's applied, as estimated by finite element models, and also a decrease in blood perfusion to the loaded tissues [3], [101], [120], [124], [175]. Both internal stress and reduced blood perfusion contribute to tissue necrosis over time, which can lead to PI formation.

Soft tissues in the buttocks and thighs experience shear loading while seated, which creates a higher risk for PI development [101], [262]. Almost half of all pressure injuries occur in the buttocks and thighs, indicating a need to address the shear loading those regions experience [16]. Despite evidence showing that the buttocks and thighs experience increased shear load while sitting in reclined positions, reclined positions are the most popular positions for wheelchair users, and they are prescribed for pressure relief clinically [2], [108], [249], [263], [264]. The popularity of reclined positions while seated, paired with the prevalence of PIs in the buttocks and thighs,

underscore a need to reduce the shear loading on the buttocks and thighs while seated, especially in reclined positions.

One method by which the shear load on the buttocks and thighs may be reduced is by selecting materials for the cushion covers that have low coefficients of friction. Standard cushion covers use materials such as vinyl, however those materials may have relatively high coefficients of friction, causing increased shear loading on the buttocks and thighs while seated. Another material, such as the nylon used in transfer sheets in hospitals, may provide a lower friction surface that helps lower the shear force and therefore reduce the risk of PIs. By using a material with a lower coefficient of friction for a cushion cover, the maximum amount of friction the cover can sustain is reduced, and that provides a mechanism by which shear on the buttocks and thighs is reduced.

Friction is generated by contact between two surfaces; and thus the interaction between the cushion cover material and that of clothing is an important factor in order to understand shear force. Numerous studies have investigated the effects of moisture and temperature on friction between *skin* and textiles commonly used to make clothes [113], [115], [265]. These studies found that increasing moisture on the skin increased friction, correlating two factors that are thought to contribute to PI risk [91]. However, there is a dearth of literature describing the friction generated between cushion cover materials and materials commonly used to make pants while seated. As such, there is a need to evaluate the frictional properties of cushion covers when paired with clothing to reduce shear loading.

Though there is a lack of information regarding the interactions of the material on the cushion cover and the clothing worn by the wheelchair user, this interaction is critical to the generation of shear force on the buttocks and thigh tissues. Thus, it is necessary to determine the

friction and shear forces on these material pairings. As stated, reducing the coefficient of friction between pants and cushion cover reduces the maximum amount of shear that can be sustained by a pair of materials before sliding occurs, potentially reducing friction on the buttocks and thighs. Additionally, understanding the effects of a commonly used positioning method – back recline – on shear force is also important.

Therefore, the goals of this study included using a tilting seat pan 1) to determine the coefficients of friction between three cushion covers (vinyl, one-layer nylon, and two-layer nylon) and two clothing fabrics commonly worn by able-bodied individuals and wheelchair users (cotton denim and cotton-polyester blend) using a laboratory system (called a sled) to simulate the buttocks, 2) to compare the coefficients of friction found using the sled to coefficients found with human participants, and 3) use a chair with back recline to evaluate the ability of the cushion covers to reduce shear loading on the buttocks and thighs while seated in *reclined positions*.

Methods

Overview

Three specific hypotheses were tested in this work to address the three specific goals. The first hypothesis was that the coefficients of friction when pairing pant materials with seat pan covers would differ and that pairings of pant materials with covers made from nylon would have smaller coefficients of friction than pairings with vinyl covers. This was tested using a mechanical system that consisted of a weighted wooden sled, whose bottom was covered by the pant materials. This experimental work utilized the tilting seat pan surface of the articulating chair designed for the work in chapters 4 and 5.

The second hypothesis was that coefficients of friction could be determined using humans instead of the sled and that the frictional coefficients would be the same with either the sled or the humans, even though humans have deformable soft tissue in their buttocks and thighs. To test this hypothesis, participants sat in the articulating chair while wearing pants made of the same material tested with the sled, and the seat pan was tilted until the participants started to slide. This was done for each of the pant materials and each of the seat pan covers used in the sled testing.

The third hypothesis was that the seat pan covers would affect the shear forces on the buttocks and thighs while seated **in reclined positions**, specifically that the nylon seat pan covers would reduce shear on the buttocks and thighs. To do this, motion capture data and force data were collected as participants sat in the articulating chair, and the chair was reclined. Shear force data were collected at three levels of recline, as determined by motion capture, and compared between the pairings of seat pan cover and pant materials for which the coefficients of friction were previously determined.

Articulating Chair Design

The custom-designed articulating chair designed for chapters 4 and 5 was also used for this research. The articulating chair had independent, motor-driven back recline and seat pan tilt movements. The back was able to recline rearward from vertical to nearly 20 degrees and the seat pan was able to tilt up to 40° such that the anterior edge of the seat pan was higher than the posterior edge. Two reflective markers were attached to the chair back, and four reflective markers were attached to the seat pan to record the orientations of the back and seat pan, respectively (Figure 6.1). The seat pan was mounted on a six-axis load cell (AMTI, Watertown, MA) to collect normal and shear force data on the seat pan during testing.

Determination of Coefficients of Friction via a Sled to Simulate the Buttocks

Static and kinetic coefficients of friction were determined for the pairings of two pant materials (denim and cotton-polyester blend) and three cushion covers (vinyl, one-layer nylon, and two-layer nylon) using a sled that simulated the buttocks (Table 6.1). The sled had a square cross-sectional area of 225 cm^2, was designed to hold 45 N of weight (weight carried by the ischial tuberosities while seated), and had interchangeable fabrics attached to the bottom [5], [266]. The seat pan covers were attached to the seat pan with Velcro. For the one-layer covers, and for the bottom layer of the two-layer nylon cover, the material was attached with Velcro to the lateral and anterior edges of the seat pan. The top layer of nylon for the two-layer nylon cover was attached to the posterior edge of the seat pan to ensure that it could freely slide on top of the bottom layer. Four reflective motion capture markers were attached to the sled to determine its position in space (markers S1-4 in Figure 6.1).

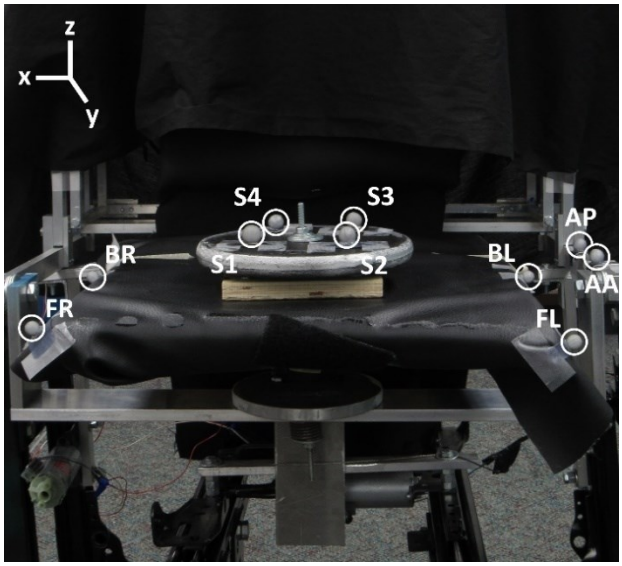

Figure 6.1 Articulating chair setup for the sled testing. The markers on the front right (FR), front left (FL), back left (BL), and back right (BR) were used to determine the orientation of the seat pan ($\widehat{e_1}$). The markers on the sled, S1-4, were used to determine the sled's position. The anterior (AA) and posterior (AP) markers on the chair arm were used to determine the back recline. All positions were given in the coordinate system in the top left of the figure

Table 6.1 Material pairings for the pants materials and seat pan covers

Seat pan cover material	Sled bottom material
Vinyl	Denim (100% cotton)
One-layer nylon	
Two-layer nylon	Cotton (60%)-polyester (40%) blend

Motion capture data were collected at 60 Hz to determine the static and kinetic coefficients of friction of the different material pairings using the position of the sled and the orientation of the seat pan. The position of the sled ($\vec{s}$) was the average position of the four markers on the sled (i.e. $\frac{\sum_{i=1}^{4}[S_{i,x}\ S_{i,y}\ S_{i,z}]}{4}$). The orientation of tilt of the seat pan was determined using two of the markers (Front left (FL) and back left (BL) in Figure 6.1) and Eq. 6.1.

$$\widehat{e_1} = \frac{\overrightarrow{FL} - \overrightarrow{BL}}{\left\|\overrightarrow{FL} - \overrightarrow{BL}\right\|} \quad \text{(Eq. 6.1)}$$

where $\overrightarrow{FL}$ was the position vector of marker FL, $\overrightarrow{BL}$ was the position vector of marker BL, and $\widehat{e_1}$ was the unit vector that represented the orientation of the seat pan. The angle of tilt of the seat pan was determined using vector $\widehat{e_1}$ and Eq. 6.2.

$$\theta_t = \tan^{-1}\left(\frac{\widehat{e_{1,z}}}{\widehat{e_{1,y}}}\right) \quad \text{(Eq. 6.2)}$$

where $\widehat{e_{1,y}}$ was the y-component of the seat pan orientation vector, $\widehat{e_{1,z}}$ was the z-component of the seat pan orientation vector, and θ_t was the angle of tilt of the seat pan. The position of the sled along the seat pan was calculated using the orientation of the seat pan and the positions of the sled and marker BL in space. This is described in Eq. 6.3.

$$\vec{r} = \hat{e_1} \cdot \left(\vec{s} - \overrightarrow{BL}\right) \quad \text{(Eq. 6.3)}$$

where $\vec{r}$ was the position of the sled along the seat pan.

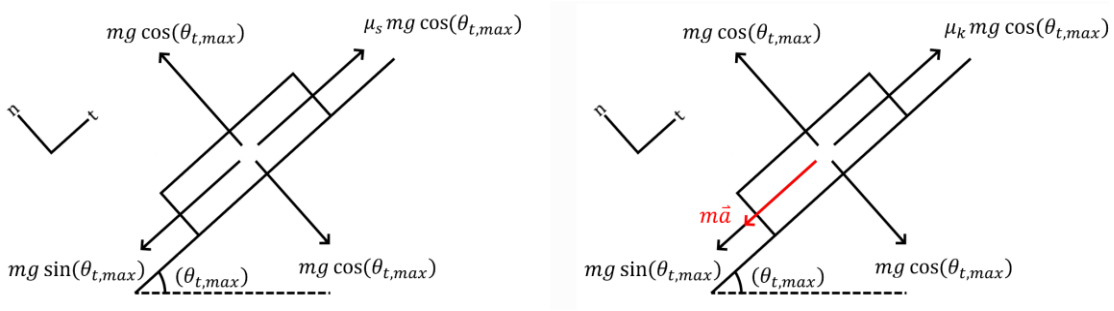

Figure 6.2 Free body diagrams for the sled before (left) and after (right) it starts to slide. The friction before the sled starts to slide is determined by the static coefficient of friction (μ_s), and the friction after it starts to slide is determined by the kinetic coefficient of friction (μ_k)

The sled was placed on the seat pan while it had 0° of tilt. The seat pan was then tilted until the sled started to slide along the seat pan. Just prior to the sled starting to slide along the seat pan, the angle of tilt ($\theta_{t,max}$) was held constant. The only forces acting on the sled were gravity, friction parallel to the seat pan, and the force normal to the seat pan (Figure 6.2). As such, the static coefficient of friction (μ_s) for the material pairing was determined using Eqs. 6.4 through Eq. 6.6.

$$\Sigma F_t = \mu_s mg\ cos\left(\theta_{t,max}\right) - mg\sin\left(\theta_{t,max}\right) = 0 \quad \text{(Eq. 6.4)}$$

$$\mu_s mg\ cos\left(\theta_{t,max}\right) = mg\sin\left(\theta_{t,max}\right) \quad \text{(Eq. 6.5)}$$

$$\mu_s = \tan(\theta_{t,max}) \quad \text{(Eq. 6.6)}$$

All motion of the sled was along the seat pan orientation vector ($\hat{e_1}$). Thus, the acceleration ($\vec{a}$) of the sled along the seat pan was determined by using changes in the position of the sled along the seat pan ($\vec{r}$) to determine mean acceleration between frames. To determine velocity, the change in

position along the seat pan was tracked from frame to frame. Since the frequency of data collection was known (60 Hz), the change in position was divided by time between frames to determine the velocity of the sled during frames when it slid. Changes in velocity between frames were then divided by the time between frames to determine the acceleration of the sled during frames when it slid. The acceleration while the sled was sliding was used to determine the kinetic coefficient of friction (μ_k) for the material paring using Eq. 6.7.

$$\mu_k = \tan(\theta_{t,max}) - \frac{|\vec{a}|}{g\cos(\theta_{t,max})} \quad \text{(Eq. 6.7)}$$

where g was the gravitational constant ($9.81\frac{m}{s^2}$). Ten trials were conducted for each material pairing, and the coefficients of friction were averaged among the trials.

Coefficients of Friction with Human Participants

The coefficients of friction for each material pairing were also computed with data sets collected on human participants. 10 able-bodied individuals (5 male, 5 female) volunteered, and testing protocols were approved by the Biomedical and Health Institutional Review Board at Michigan State University. Consent was obtained from all participants.

As with the simulated buttocks, four reflective markers were attached to the seat pan. Reflective markers were also attached bilaterally on the participants' anterior superior iliac spines, greater trochanters, lateral epicondyles, and lateral malleoli (Figure 6.3). Motion capture data of all the markers were collected. Participants each wore two pairs of pants: denim jeans and cotton-polyester blend sweatpants, and three cushion covers were tested (Table 6.1).

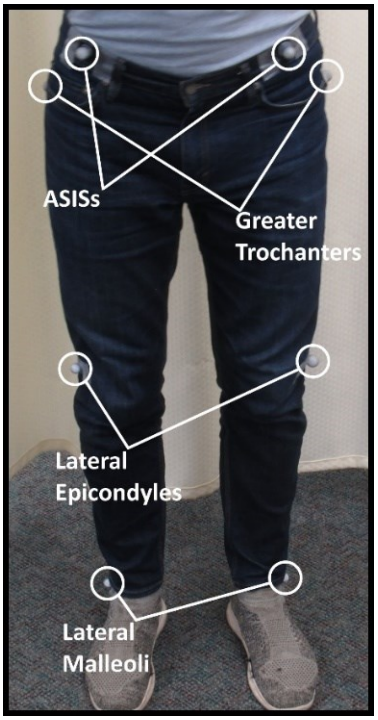

Figure 6.3 Reflective marker placements on the lower body of a participants: anterior superior iliac spines (ASISs), greater trochanters, lateral epicondyles, and lateral malleoli

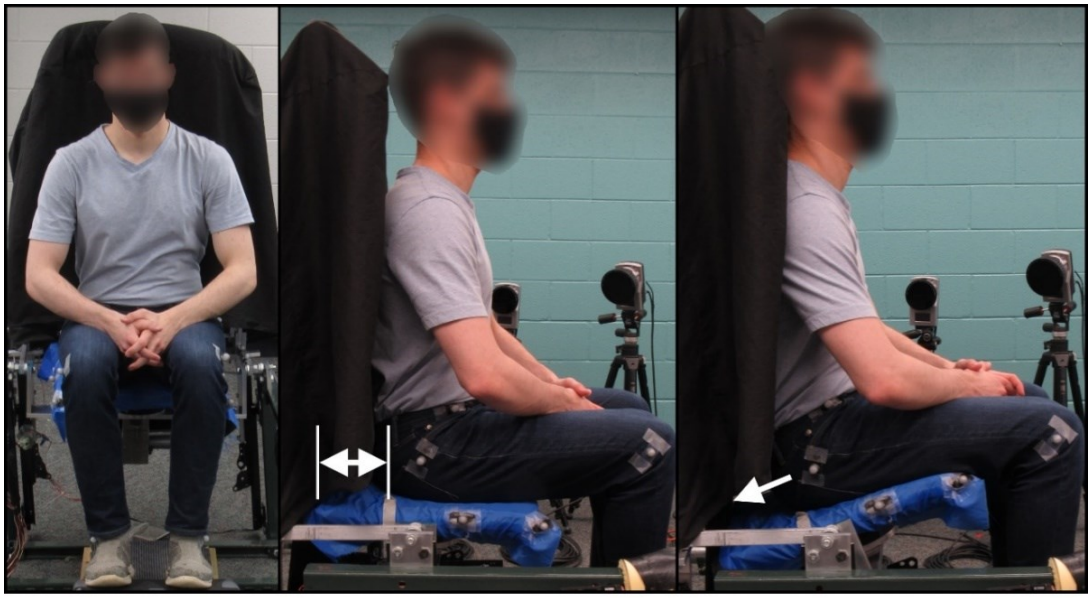

Figure 6.4 (a) Front view of a participant sitting on a flat seat pan, (b) side view of a participant sitting on a flat seat pan, with the arrow indicating the space between the participant and the chair back, (c) participant sitting on a tilted seat pan just before starting to slide

Participants initially sat down on the seat pan with 0° of seat pan tilt, with the back of their buttocks 15 cm from the posterior edge of the seat pan, hands placed in their lap, and were instructed to not contact the back of the chair with any part of their back (Figure 6.4a and Figure 6.4b). A footrest was adjusted at the participants' feet so that their initial knee flexion was 90° and thighs were fulling resting on the seat pan. The seat pan was then tilted until the participant started to slide or until the participant's upper back made contact with the back of the chair, whichever came first (Figure 6.4c). After the participant started to slide or contacted the back of the chair, the seat pan tilt was held constant. The orientation and angle of the seat pan tilt were calculated using Eqs. 6.1 and 6.2. The average position of the lateral epicondyles was recorded relative to the seat pan, similarly to position of the sled in the previous section. The average position of the markers on the lateral epicondyles was used to determine when participants slid along the seat pan because the markers on the anterior superior iliac spines and greater trochanters were sometimes obscured by the participants' hands This is described in Eq. 6.8.

$$\vec{q} = \widehat{e_1} \cdot \left(\vec{k} - \overrightarrow{BL}\right) \qquad \text{(Eq. 6.8)}$$

where $\vec{k}$ was the average position vector of the markers attached to the lateral epicondyles, and $\vec{q}$ was the average position of lateral epicondyles along the seat pan. The acceleration of the knees along the seat was found using the same process that was used to obtain the acceleration of the sled, and the static and kinetic coefficients of friction were calculated using Eqs. 6.6 and 6.7, respectively. Three trials were conducted for each participant wearing each pair of pants on each cushion cover, and coefficients of friction were averaged across trials. In trials where the vinyl seat pan cover was used, participants did not slide along the pan. A seat pan tile of over 30 degrees was required to start sliding and by the time the pan reached that angle, participants were unable to

keep their upper backs from touching the back of the chair without leaning significantly forward, which would have affected results. Thus, coefficients of friction were not found for the material pairings including the vinyl cover with human participants.

Evaluating the Effects of Seat Pan Cover on the Shear Forces While Seated

When back recline happens, shear force on the buttocks and thighs of wheelchair users increases. To identify the effects of seat pan cover materials during back recline, a third set of tests was run.

Motion capture data of the participant and chair, and shear force data on the seat pan, were collected while participants sat in the articulating chair at multiple recline angles for all the material pairings listed in Table 6.1. Participants sat on the articulating chair with the backs of their buttocks contacting the pelvic support, their hands in their laps, and their feet resting on the footrest. The back was reclined to 17° past vertical and then moved back to the 0° recline (vertical) position while the seat pan remained horizontal. Participants then stood up out of the chair to prepare for the next trial. Three separate trials were conducted for each material pairing (for a total of 18 trials per participant), and motion capture and shear force data were collected during each trial.

Motion capture and shear force data (collected at 60 Hz and 120 Hz, respectively) were used to determine the recline angle of the back and shear force on the seat pan, respectively. Markers AA and AP (Figure 6.1) were used to determine the angle of back recline. The shear forces in the anterior-posterior direction of the seat pan were recorded when the angle of back recline was 5°, 10°, and 15° for each trial. A description of the procedure used to verify the accuracy of the shear force measurements on the seat pan is included in Appendix B.

Statistics

A two-way repeated measures ANOVA was used to determine the effects of recline angle and material pairing on the shear forces on the seat pan. Tukey tests were then used to identify significant differences between the shear forces in different recline angles and material pairings.

Results

Coefficients of Friction with the Simulated Buttocks

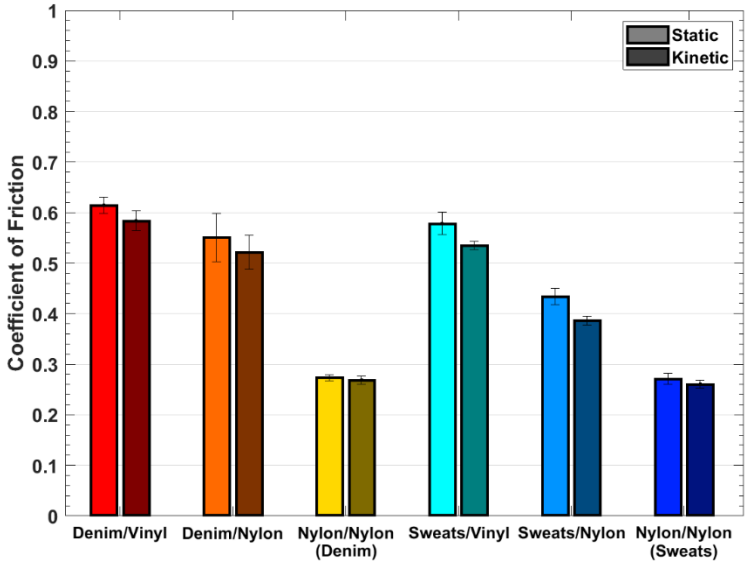

Figure 6.5 Coefficients of friction for each of the material pairings, found using the sled to simulate the buttocks. Brighter bars represent static coefficients of friction, while darker bars are kinetic coefficients of friction

The coefficients of friction as found from the weighted sled are reported in Figure 6.5 and Appendix C. The static and kinetic coefficients of friction were largest for the vinyl cover, regardless of pants material it was paired with; and the coefficients of friction were smallest for the two-layer nylon cover for both pant materials. Though the coefficients of friction for the pant materials on one layer of nylon were consistently smaller than the coefficients of friction of the

pants on the vinyl cover, the reduction in the coefficient of friction was dependent on the type of fabric used in the pants. The reduction in both static and kinetic coefficients of friction when switching the cover from vinyl to the one-layer nylon cover was 10% for the denim pants material and 26% for the cotton-polyester blend. The kinetic coefficients were smaller than the static coefficients of friction by a range of 2-9%, with the smallest change occurring in the denim on two-layer nylon cover and the largest change occurring in the cotton-polyester blend on one-layer nylon cover.

In summary, the vinyl seat pan cover had the largest coefficients of friction, and the two-layer nylon cover had the smallest for both pant materials. The cotton-polyester blend pant material had smaller coefficients than the denim pant material on the vinyl and one-layer nylon seat pan covers. However, the two pant materials had similar coefficients of friction when interacting with the two-layer nylon seat pan cover.

Coefficients of Friction with Human Participants

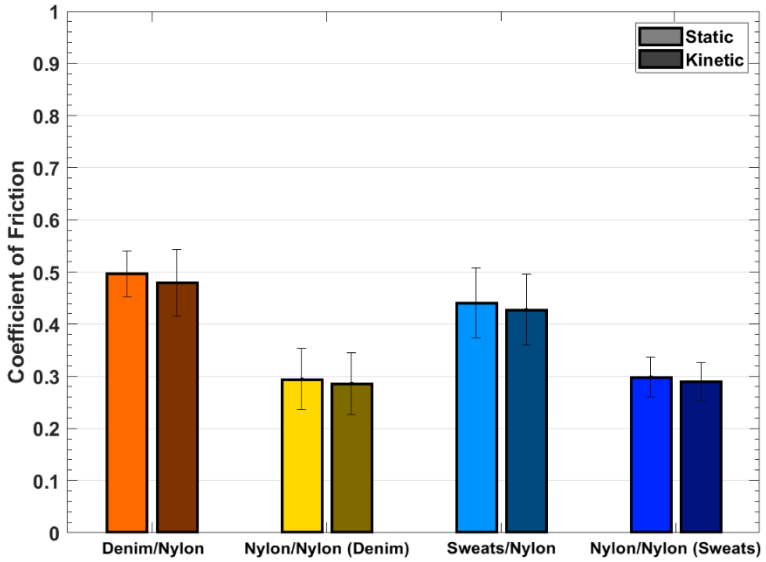

Figure 6.6 Coefficients of friction for each of the material pairings, found using human participants. Brighter bars represent static coefficients of friction, while darker bars are kinetic coefficients of friction

Five able-bodied males (average age 22.4 ± 3.1 years, average height = 181.4 ± 5.0 cm, average weight = 754.7 ± 85.9 N) and five able-bodied females (average age 23.0 ± 6.2 years, average height = 162.6 ± 10.5 cm, average weight = 607.9 ± 39.3 N) participated in this study. The coefficients of friction as found from the human participants are reported in Figure 6.6. and Appendix C. As stated in the methods, coefficients of friction were not found with human participants when a vinyl seat pan cover was involved because the angle of tilt needed start the participant sliding was too great, so participants' backs contacted the back of the chair.

For both pairs of pants, the coefficients of friction were smaller on the two-layer nylon cover than on the one-layer nylon cover. The kinetic coefficients of friction determined from the human trials were between 2.5-3.5% smaller than the static coefficients of friction.

Effects of Seat Pan Cover on Shear Forces

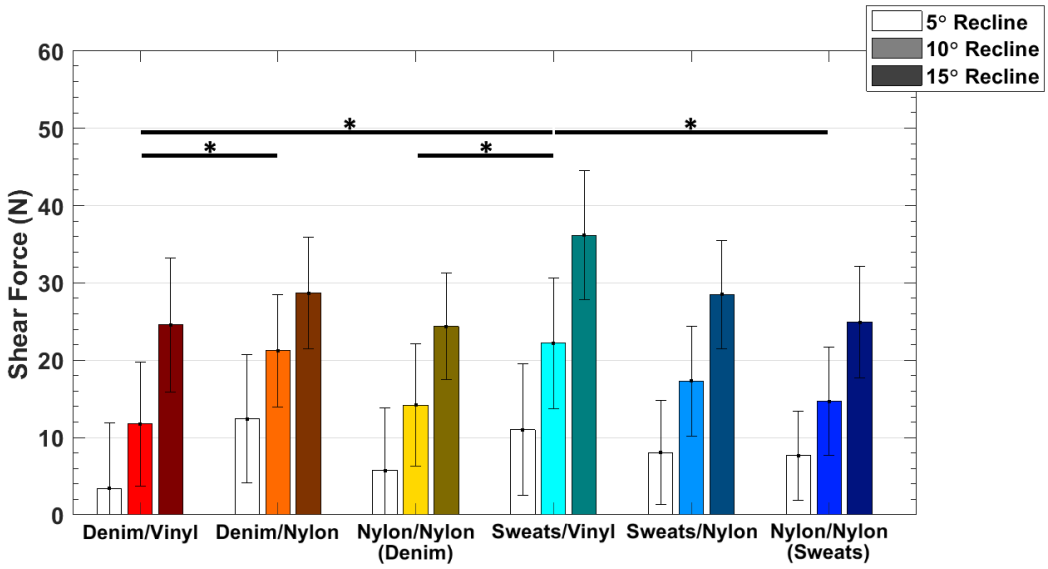

Figure 6.7 Shear forces on the seat pan of each material pairing at each angle of recline. All shear forces are in the anterior direction of the seat pan. Recline increased shear force on the seat pan, regardless of the material pairing. Asterisks (*) indicate significant differences in shear forces on each pair

The shear forces on the seat pan with all three covers and both pants materials at three recline angles are reported in Figure 6.7. Interaction effects between the recline angle and material pairing were investigated, but there were no significant findings. All shear forces reported are in the anterior direction of the seat pan (+y in Figure 6.1). The data indicated that increasing back recline, **regardless of seat pan cover**, increased the shear force on the seat pan ($p < .0001$). Though there were no significant differences between the shear forces on any of covers across pant materials, the two-layer nylon cover reduced shear force on the buttocks and thighs by about 20% relative to the vinyl cover. The results also showed that there were several material pairings that reduced shear force relative to others. Denim on vinyl had less shear force than denim on one-layer nylon ($p = .0370$) and cotton-polyester blend on vinyl ($p = .0071$). Denim on two-layer nylon ($p = .0258$) and cotton-polyester blend on two-layer nylon ($p = .0487$) also had less shear force than cotton-polyester blend on vinyl.

Discussion

This work was carried out to determine frictional properties of pairings of seat pan covers and pant materials. Additionally, this work investigated the effects different seat pan covers had on shear force as recline was varied. The methods used to determine frictional properties, the frictional properties themselves, and the shear force results have implications that span experimental, computational, and clinical biomechanics, in particular as they relate to PI prevention.

Coefficients of friction of the material pairs were found using a sled and tilted surface. This method was previously used to determine coefficients of friction between material samples of rocks, whose shape remains relatively constant during testing [266], [267]. However, this was the

first published work that applied the method to the human body, specifically the buttocks and thighs covered by pants materials. The results indicated that the nylon covers had smaller coefficients of friction than the vinyl cover. This is significant because the shear forces that the nylon covers can support are smaller than those that of the vinyl cover, providing one mechanism by which shear may be reduced on the buttocks and thighs of wheelchair users. This was determined using a seated position with a tilting seat pan. Understanding the effects a material surface has on shear force generation can help in reducing internal tissue shear as well as maintaining positioning of seated occupants.

The coefficients of friction of the material pairs were found using the tilted surface method with a rigid mechanical system (sled) used to simulate the buttocks and again with human participants. The results of this study showed the same trends and similar numerical coefficients of friction with the rigid sled and the deformable human. The coefficients of friction for the denim and cotton-polyester blend pants on the one- and two-layer nylon cushions were close to one another (within 10%) between the simulated buttocks and human participants. It also means that using simulated buttocks may be an adequate substitution for human participants when determining coefficients of friction. Experiments with simulated buttocks are more repeatable than using human participants, as evidenced by the smaller standard deviations of the coefficients of friction found using the sled. Because simulated buttocks remove human variation, they provide a method to consistently determine coefficients of friction that may be useful for clinical settings (by using cushion covers with small coefficients of friction).

One finding from this work that directly impacts current clinical care and best practices is that back recline increased shear force on the buttocks and thighs regardless of material pairing. This finding can be taken in conjunction with previous work that shows that normal forces on the

buttocks, specifically over the ischial tuberosities, increase with back recline as well. Together, this research does not support the current practice of using back recline as a prevention method for PIs in the buttocks**.** Instead, back recline increases normal and shear pressure on the buttocks, which have been shown to increase tissue stress and decrease perfusion, thereby increasing the risk of PI formation.

From a PI prevention perspective, it was essential to identify material pairings that could reduce shear force on the buttocks and thighs while seated. In this study, the three material pairings with the smallest amount of shear on the buttocks were denim on vinyl, denim on two-layer nylon, and cotton-polyester blend on two-layer nylon. The denim and cotton-polyester blend on two-layer nylon were both material pairings with low coefficients of friction as found with the simulated buttocks and human participants, and they indicated that the two-layer nylon cover may have the potential to yield small shear forces on the buttocks and thighs while seated. The two-layer nylon cover decreased the shear force on the buttocks and thighs by about 20% relative to the vinyl cover for the denim and cotton-polyester blend pants. The lack of a statistically significant difference was due to large standard deviations of the shear force measurements. Nevertheless, that decrease in shear force could reduce tissue stresses in the buttocks and thighs, increase perfusion in the skin in those regions, and help protect tissues in those regions from PI formation.

To implement a shear reducing cover of any kind in a wheelchair, precautions must be taken to ensure that chair occupants do not slide into an unintended position or even out of their chair. Most manual and powered wheelchairs have foot plates mounted in front of the seat pan that provide some protection against the chair occupant sliding forward, and lateral pads and support straps can be implemented as well. The combination of shear reducing covers and wheelchair supports can reduce the risk of PIs and unintended repositioning at the same time.

This work furthers the understanding of shear forces on the buttocks and thighs while seated, thereby aiding in the task of reducing PI incidence. The results from the tilted surface method of determining coefficients of friction suggested that it can be used to consistently determine coefficients of friction and yields results similar to humans with deformable tissues. Shear force measurements from human participants sitting in reclined positions showed that recline increases shear on the buttocks and thighs and that the two-layer nylon cover may be able to reduce shear. Further testing will be needed to determine the coefficients of friction for other commonly worn fabrics (such as polyester) on seat pan covers and other types of material with which the two-layer cushion works well. However, these results show that the two-layer nylon cover is a promising avenue for shear force reduction, reducing PI risk in seated individuals.

A limitation to this work is that the coefficients of friction were not found for pant materials *on the vinyl cover using human participant*s. This was because participants contacted the back of the chair at the large tilt angles needed to overcome static friction with the vinyl cover. The participants touching the back of the chair instead of sliding indicated that the tilting surface method of determining coefficients of friction may not be used for humans and materials with high coefficients of friction. While the coefficients of friction are not limited for methods using a sled on a tilting surface, experiments that use human participants need to limit the magnitude of the coefficients of friction tested. Additionally, because one of the seat pan covers tested consisted of two layers of nylon attached on different sides of the seat pan, the potential existed for wrinkling or creasing. This attachment approach was used to accommodate for the load cell mounted beneath the seat pan, which would not permit a complete wrapping around the seat pan of the fabric. However, if a two-layer cover is implemented on an actual wheelchair cushion, the top layer of the cover could enclose the entire cushion and bottom layer of the cover. Doing so would create

tension in the top layer and simulate a conveyor belt, where the occupant could slide on the cushion cover without the potential of the cover wrinkling.

CONCLUSIONS

The overall objective of this work was to use novel methods to generate a description of the soft tissues of wheelchair users that may be used in finite element models and to develop wheelchair technology to address limitations in the practices used to prevent PIs. Additionally, this work investigated pant and seat pan cover material pairings to reduce shear forces on the buttocks while seated, an area where there is a dearth of research. The components of this research address several assumptions used in engineering applications, especially in designs meant for persons with disabilities.

Accurate representations of soft tissues are integral to designs of engineering models and devices with which people interact. Though people spend much of their day in a seated position, and many wheelchair users develop PIs, the protocols used to obtain material properties from the buttocks and thighs of humans have mostly been limited to able-bodied people while lying down. Therefore, it was imperative to determine if the differences between the hip and knee joint angles in the seated position versus the lying position affected the reported material properties of the buttocks and thighs. Further, creating an *accessible* protocol to determine the material properties of the soft tissues in the buttocks and thighs in a seated or seated-like position was a challenge that was overcome. Successfully completing this component of the research allowed for comparisons of material properties between able-bodied individuals and wheelchair users. Several challenges arose during the path to completion of this work.

The first challenge was to determine whether hip and knee joint angles affected the material properties in the buttocks and thighs. This was done by creating a protocol to collect and analyze force and deformation data from the buttocks and thighs of able-bodied individuals in the seated, quadruped, and prone positions. The seated and quadruped positions produced similar buttock and

thigh tissue responses, while the prone position elicited stiffer tissue responses, indicating that the buttock and thighs tissues were affected by hip and knee joint flexions. This meant that it would be appropriate to use the tissue response in the quadruped position, but not the prone position, to represent the seated position.

Confirming that the seated and quadruped positions produced similar material responses from the buttocks and thighs was critical to being able to obtain and calculate material properties from those tissues in wheelchair users. There were numerous obstacles to evaluating wheelchair users. They included issues related to balance and support while transferring into and then sitting in a laboratory test chair. These challenges were addressed by conducting tests in the quadruped position. Thus, the protocol to collect force and deformation data from people in the quadruped position was adapted to test people with SCIs in a rehabilitation clinic. The tissue responses were obtained and compared to those of able-bodied people. People with SCIs had softer tissue responses in the buttocks and more proximal regions of the thighs, while their distal thigh regions were stiffer than those of able-bodied people. These findings had implications for both experimental and computational biomechanics. First, the differences in tissue stiffness throughout the buttocks and thighs of people with SCIs relative to able-bodied individuals showed that it is vital to differentiate between groups as differences are significant. Secondly, the differences in stiffnesses themselves were considered in conjunction with the effects of body position on tissue responses in the buttocks and thighs. Together, these studies indicated that the buttocks and proximal thigh tissues of wheelchair users in a seated position were softer than those of able-bodied people lying down. Since the soft tissues in the buttocks and thighs are prone to PI development, it is important to accurately represent them in all engineering applications that evaluate PI risk and

prevent PI occurrence. The comparisons made and the data sets yielded by these new methods will benefit wheelchair users through device designs and human body models.

Equipment designed for the purpose of PI prevention has yet to eliminate these injuries, and PIs continue to be a significant problem for wheelchair users. Most commercial wheelchairs, if able to reposition the occupant, are limited to back recline and whole-body tilt. The evidence to support the use of back recline and whole-body tilt for PI prevention was limited, and spending time in those positions affects the tasks occupants can conduct. As such, it was important to determine whether those repositioning strategies actually reduced PI risk, and if not, to develop new strategies to do so. Therefore, an accessible articulating chair was built to collect interface pressure data and perfusion data from the skin over the ischial tuberosities of seated individuals. The chair was first tested on able-bodied individuals and had independently rotating seat pan, pelvic, and thoracic supports, of which the pelvic and thoracic supports were mounted on an independently reclining back. Interface pressure data were segmented into body regions and regional averages found over key areas in the thighs, buttocks, lower back, middle back, and upper back. Segmentation allowed for specific characterizations of the effects of seated repositioning. After analysis, it was found that back recline *increased* pressure on the buttocks and lower back, two regions where PIs are common. Back recline also decreased perfusion in the skin over the ischial tuberosities. However, seat pan tilt decreased pressure on the buttocks and lower back and increased perfusion in the skin over the ischial tuberosities. Back articulation shifted pressure concentrations between back regions. The results of this study suggest that using back recline as a method to reduce pressure on the buttocks, though popular, may actually have the opposite effect. Instead, new repositioning strategies, such as seat pan tilt or changes in back articulation, may be

effective ways to protect the buttocks and lower back. Studying these movements required a custom, laboratory chair because these features are not available via any commercial chair.

As with the studies on the factors that affect material properties of the buttocks and thighs, it was necessary to determine whether the results of seated repositioning were the same for wheelchair users as they were for able-bodied individuals. Similarly to able-bodied individuals, back recline increased pressure on the buttocks and lower back, and back articulation was able to shift pressure concentrations between back regions. Seat pan tilt decreased pressure on the buttocks, with mixed results on the lower back. Seat pan tilt only increased perfusion in wheelchair users whose maximum buttocks pressures were similar to those of able-bodied individuals. Wheelchair users who had larger maximum buttocks pressure did not experience an increase in perfusion. These results indicated that the use of specialized cushions, or other pressure distributing strategies, may be necessary with seat pan tilt to increase perfusion in wheelchair users with high buttocks pressures. Though the effects of the chair articulations on the interface pressures of wheelchair users were similar to able-bodied individuals, the differences in the perfusion trends between the two groups were not predictable based on the able-bodied data alone. The data collected from the wheelchair users, while they still suggest that seat pan tilt and back articulation are viable strategies for PI prevention, illustrate the need to include people with disabilities.

Lastly, a study was conducted on the shear forces experienced while seated on various seat pan covers. Though shear loads on soft tissue have been repeatedly implicated in the formation of PIs, and there has been research on how to reduce shear on individuals while lying down, there is relatively little research on how to reduce shear on seated individuals. Recent attempts to create a shear reducing seat pan cover had limited success.

This work aimed to further understand how seat pan covers may be used to reduce shear forces while seated. To do this, the coefficients of friction of vinyl, one-layer nylon, and two-layer nylon seat pan covers were determined experimentally when paired with materials commonly used to make pants. The shear forces experienced while reclining in the articulating chair were then quantified for each of the three seat pan covers. It was found that the coefficients of friction between the one- and two-layer nylon covers were consistently smaller than those of the vinyl seat pan cover, regardless of the pant material with which they were paired. Further, the two-layer nylon seat pan cover showed trends towards reducing shear forces on the buttocks and thighs while seated. Regardless of seat pan cover, shear force on the buttocks and thighs increased at higher back recline angles, indicating that again, recline may not be a viable seated repositioning strategy to reduce PI risk. The methods used to 1) determine the coefficients of friction between two materials using the simulated buttocks and 2) measure the shear force on the buttocks at multiple back recline angles can be used to evaluate other material pairings that may reduce shear forces on the buttocks and thighs while seated. The results of this research yielded useful material pairings for clinicians and input parameters for modelers investigating the effects of shear force on soft tissue.

This research has implications for clinical, experimental, and computational biomechanics. This work included novel methods and experimental approaches, with associated computations to obtain these findings. This research yielded first-of-its-kind continuous, *in-vivo* material response data from people with SCIs. The articulating chair that was developed included chair articulations not available in commercial chairs and also evaluated common seated repositioning strategies, with the resulting data suggesting that the current methods for PI prevention need re-evaluation. Finally, the experiments to determine the coefficients of friction for material pairings that

commonly occur between pants and seat pan covers showed that seat pan covers can significantly affect the coefficients of friction and that simulated buttocks can be representative of human participants.

Overall, this work contributes significantly to our understanding of components related to human in-vivo material properties, device design and frictional properties – all which play significant roles in the formation of PIs.

APPENDICES

APPENDIX A: REPEATABILITY OF TISSUE INDENTATION PROTOCOL

Repeatability of the indentation protocol was investigated by considering multiple trials per individual. Since there were two trials per testing region per body position for each individual, the force and deflection data from the first trial were compared to the second. A sample of force and deflection data from all three regions in all three positions for one participant are provided in Figure A.1. The data indicate that the protocol has very good repeatability.

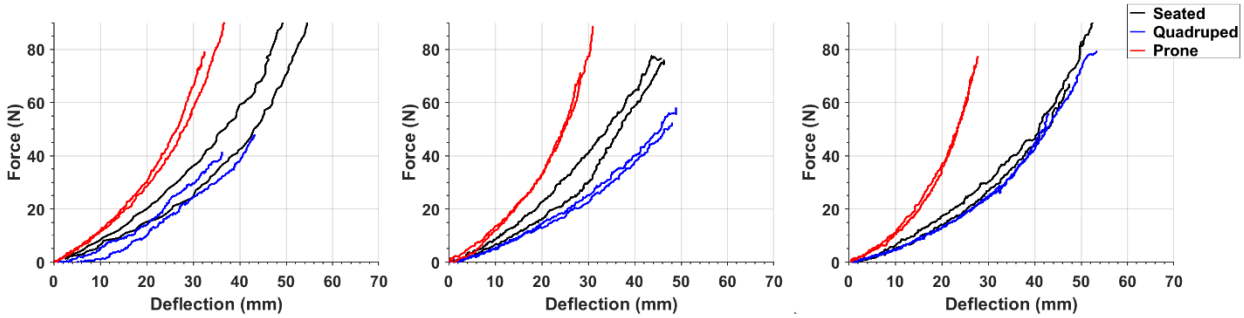

Figure A.1 Force and deflection data from repeated indentation protocols on the proximal (left), middle (middle), and distal (right) thigh regions in all three body positions for one participant. Data from each region in each position are consistent, showing very good repeatability

APPENDIX B: CONFIRMATION OF SYSTEM ACCURACY WITH VINYL COVER ON THE SEAT PAN

The load cells used in this research have been shown to accurately measure normal and shear forces on a rigid surface attached to the load cell itself. However, it was important to ensure that shear forces measured on a deformable surface with a cover were accurate because wheelchair cushions are deformable and have covers; and thus testing for this research occurred on a thin deformable foam layer whose thickness was approximately 1 cm. To do this, shear force measurements were obtained for the sled on the foam layer with the vinyl cover for seat pan tilt angles up to 30°. The vinyl cover was chosen because it could support the shear forces on the sled at large tilt angles.

The same markers used in the protocol to determine the coefficients of friction using the sled were attached to the articulating chair to determine the seat pan's orientation and tilt angle, and force data were collected by the load cell beneath the seat pan. The sled was placed on the seat pan while it was covered by the vinyl cushion cover and had a tilt angle of 0° to record the weight of the sled. The seat pan was then tilted to 30° while the sled was on the seat pan. Force and motion capture data were collected at 60 Hz throughout the tilting movement. This was done with the sled weighing 45 Newtons because that was weight of the sled during the trials to determine the coefficients of friction, and 110 Newtons because that weight represented the average contact pressure of a seated person over the area of the sled bottom [5].

Theoretical and normal shear forces on the seat pan were calculated for the sled at seat pan tilt angles using the free body diagram from Figure 6.2. The normal force of the sled on the tilted seat pan was $N_{sled} = W_{sled}\cos(\theta_t)$, where N_{sled} was the normal force on the sled, and W_{sled} was

the weight of the sled on the flat seat pan. The shear force of the sled on the tilted seat pan was $N_{sled} = W_{sled}\sin(\theta_t)$.

Experimental motion and force data collected on the seat pan were compared to the theoretical calculations. The angle of the seat pan tilt was determined using $\widehat{e_1}$, and the normal and shear forces on the seat pan were plotted against the angle of seat pan tilt in Figure 6.8. The largest difference between the experimentally measured and theoretical values of shear force were approximately 1.5 Newtons for the 45 Newton sled and 3.5 Newtons for the 110 Newton sled, which were both within the sensitivity of the load cell beneath the seat pan.

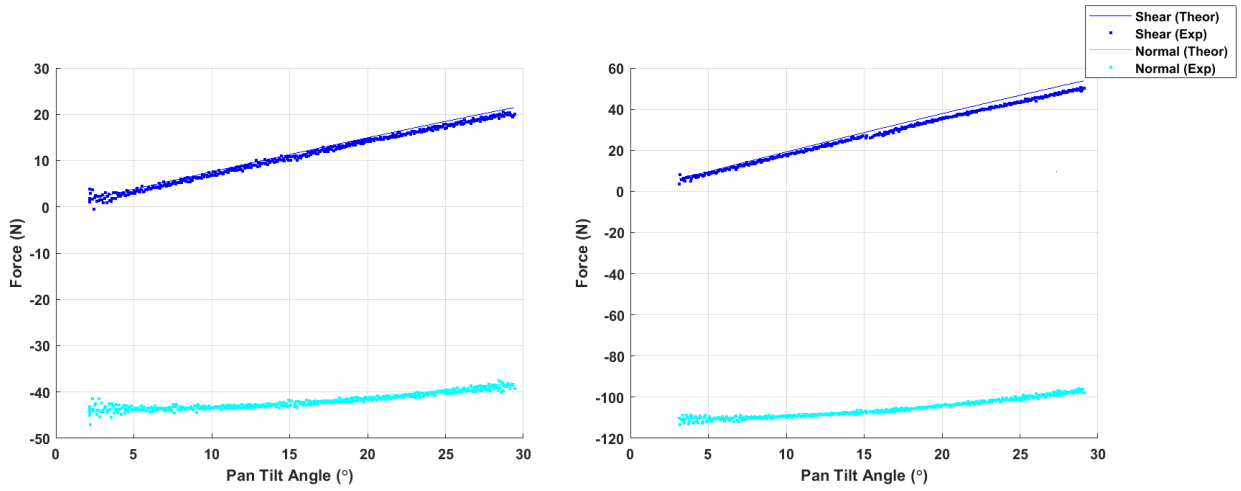

Figure B.1 Experimental and theoretical normal shear forces on the seat pan at tilt angles up to 30° for the 45 Newton sled (left) and 110 Newton sled (right)

APPENDIX C: COEFFICIENTS OF FRICTION CALCULATED USING THE SLED AND HUMAN PARTICIPANTS

Table C.1 Static coefficients of friction for each pair of materials during the sled trials

		Cover Material		
		Vinyl	**One-Layer Nylon**	**Two-Layer Nylon**
Pants Material	**Denim (100% cotton)**	0.61 ± .016	0.55 ± .048	0.27 ± .006
	Cotton (60%)-polyester (40%) blend	0.58 ± .022	0.43 ± .016	0.27 ± .011

Table C.2 Kinetic coefficients of friction for each pair of materials during the sled trials

		Cover Material		
		Vinyl	**One-Layer Nylon**	**Two-Layer Nylon**
Pants Material	**Denim (100% cotton)**	0.58 ± .020	0.52 ± .034	0.27 ± .008
	Cotton (60%)-polyester (40%) blend	0.53 ± .008	0.39 ± .009	0.26 ± .008

Table C.3 Static coefficients of friction for each pair of materials during the human trials

		Cover Material		
		Vinyl	**One-Layer Nylon**	**Two-Layer Nylon**
Pants Material	**Denim (100% cotton)**	--	0.50 ± .044	0.29 ± .059
	Cotton (60%)-polyester (40%) blend	--	0.44 ± .067	0.30 ± .038

Table C.4 Kinetic coefficients of friction for each pair of materials during the human trials

		Cover Material		
		Vinyl	**One-Layer Nylon**	**Two-Layer Nylon**
Pants Material	**Denim (100% cotton)**	--	0.48 ± .064	0.29 ± .059
	Cotton (60%)-polyester (40%) blend	--	0.43 ± .068	0.29 ± .037

REFERENCES

REFERENCES

[1] M. W. Brault, “Americans With Disabilities: 2010,” 2012.

[2] D. Ding *et al.*, “Usage of tilt-in-space, recline, and elevation seating functions in natural environment of wheelchair users,” *Journal of Rehabilitation Research and Development*, vol. 45, no. 7. pp. 973–984, 2008, doi: 10.1682/JRRD.2007.11.0178.

[3] C. Lachenbruch, Y. T. Tzen, D. Brienza, P. E. Karg, and P. A. Lachenbruch, “Relative Contributions of Interface Presssure, Shear Stress, and Temperature on Ischmic-induced, Skin-reactive Hyperemia in Healthy Volunteers: A Repeated Measures Laboratory Study,” *Ostomy Wound Manag.*, vol. 61, no. 2, pp. 16–25, 2015.

[4] S. Shirogane, S. Toyama, A. Takashima, and T. Tanaka, “The relationship between torso inclination and the shearing force of the buttocks while seated in a wheelchair: Preliminary research in non-disabled individuals,” *Assist. Technol.*, pp. 1–7, 2018, doi: 10.1080/10400435.2018.1547333.

[5] P. V. B. Mendes, L. C. C. Gradim, N. S. Silva, A. L. C. Allegretti, D. C. D. M. Carrijo, and D. M. C. da Cruz, “Pressure distribution analysis in three wheelchairs cushions of subjects with spinal cord injury,” *Disabil. Rehabil. Assist. Technol.*, vol. 14, no. 6, pp. 555–560, 2019, doi: 10.1080/17483107.2018.1463399.

[6] J. Vidal and M. Sarrias, “An analysis of the diverse factors concerned with the development of pressure sores in spinal cord injured patients,” *Paraplegia*, vol. 29, no. 4, pp. 261–267, 1991, doi: 10.1038/sc.1991.37.

[7] L. J. Cowan *et al.*, “Pressure Ulcer Prevalence by Level of Paralysis in Patients With Spinal Cord Injury in Long-term Care,” *Adv. Ski. Wound Care*, vol. 32, no. 3, pp. 122–130, 2019, doi: 10.1097/01.ASW.0000553109.70752.bf.

[8] H. Brem *et al.*, “High cost of stage IV pressure ulcers,” *Am. J. Surg.*, vol. 200, no. 4, pp. 473–477, 2010, doi: 10.1016/j.amjsurg.2009.12.021.

[9] C. VanGilder, C. Lachenbruch, C. Algrim-Boyle, and S. Meyer, “The international pressure ulcer PrevalenceTMSurvey: 2006-2015: A 10-year pressure injury prevalence and demographic trend analysis by care setting,” *J. Wound, Ostomy Cont. Nurs.*, vol. 44, no. 1, pp. 20–28, 2017, doi: 10.1097/WON.0000000000000292.

[10] S. Chen, J. Scott, T. R. Bush, and S. Roccabianca, “Inverse finite element characterization of the human thigh soft tissue in the seated position,” *Biomech. Model. Mechanobiol.*, no. 0123456789, 2019, doi: 10.1007/s10237-019-01212-7.

[11] E. Jaul and R. Calderon-Margalit, “Systemic factors and mortality in elderly patients with pressure ulcers,” *Int. Wound J.*, vol. 12, no. 3, pp. 254–259, 2015, doi: 10.1111/iwj.12086.

[12] A. Yadav and R. Kaushal, “Bedsore is a curse in disguise: capturing the zeitgeist,” *Int.*

Surg. J., vol. 7, no. 4, p. 1229, 2020, doi: 10.18203/2349-2902.isj20201402.

[13] B. Chan, S. Cadarette, W. Wodchis, J. Wong, N. Mittmann, and M. Krahn, "Cost-of-illness studies in chronic ulcers: a systematic review," *J. Wound Care*, vol. 26, no. sup4, pp. S4–S14, 2017, doi: 10.12968/jowc.2017.26.Sup4.S4.

[14] S. Brewer *et al.*, "Effect of an arginine-containing nutritional supplement on pressure ulcer healing in community spinal patients," *J. Wound Care*, vol. 19, no. 7, pp. 311–316, 2010, doi: 10.12968/jowc.2010.19.7.48905.

[15] W. V. Padula and B. A. Delarmente, "The national cost of hospital-acquired pressure injuries in the United States," *Int. Wound J.*, vol. 16, no. 3, pp. 634–640, 2019, doi: 10.1111/iwj.13071.

[16] S. D. Horn *et al.*, "Description of The National Pressure Ulcer Long-Term Care Study," *J. Am. Geriatr. Soc.*, vol. 50, no. 11, pp. 1816–1825, 2002, doi: 10.1046/j.1532-5415.2002.50510.x.

[17] J. H. M. Verschueren, M. W. M. Post, S. De Groot, L. H. V. Van Der Woude, F. W. A. Van Asbeck, and M. Rol, "Occurrence and predictors of pressure ulcers during primary in-patient spinal cord injury rehabilitation," *Spinal Cord*, vol. 49, no. 1, pp. 106–112, 2011, doi: 10.1038/sc.2010.66.

[18] R. M. A. Al-Dirini, M. P. Reed, J. Hu, and D. Thewlis, "Development and Validation of a High Anatomical Fidelity FE Model for the Buttock and Thigh of a Seated Individual," *Ann. Biomed. Eng.*, vol. 44, no. 9, pp. 1–12, 2016, doi: 10.1007/s10439-016-1560-3.

[19] A. Macron *et al.*, "Is a simplified Finite Element model of the gluteus region able to capture the mechanical response of the internal soft tissues under compression?," *Clin. Biomech.*, vol. 71, no. October 2019, pp. 92–100, 2020, doi: 10.1016/j.clinbiomech.2019.10.005.

[20] C. W. J. Oomens, M. Broek, B. Hemmes, and D. L. Bader, "How does lateral tilting affect the internal strains in the sacral region of bed ridden patients? - A contribution to pressure ulcer prevention," *Clin. Biomech.*, vol. 35, pp. 7–13, 2016, doi: 10.1016/j.clinbiomech.2016.03.009.

[21] D. Brienza *et al.*, "A randomized clinical trial on preventing pressure ulcers with wheelchair seat cushions," *J. Am. Geriatr. Soc.*, vol. 58, no. 12, pp. 2308–2314, 2010, doi: 10.1111/j.1532-5415.2010.03168.x.

[22] C. Then, T. J. Vogl, and G. Silber, "Method for characterizing viscoelasticity of human gluteal tissue," *J. Biomech.*, vol. 45, no. 7, pp. 1252–1258, 2012, doi: 10.1016/j.jbiomech.2012.01.037.

[23] J.-S. Affagard, P. Feissel, and S. F. Bensamoun, "Identification of hyperelastic properties of passive thigh muscle under compression with an inverse method from a displacement field measurement," *J. Biomech.*, vol. 48, pp. 4081–4086, 2015, doi: 10.1016/j.jbiomech.2015.10.007.

[24] L. E. Edsberg, J. M. Black, M. Goldberg, L. McNichol, L. Moore, and M. Sieggreen, "Revised National Pressure Ulcer Advisory Panel Pressure Injury Staging System," *J. Wound, Ostomy Cont. Nurs.*, vol. 43, no. 6, pp. 585–597, 2016, doi: 10.1097/WON.0000000000000281.

[25] J. Black *et al.*, "From the NPUAP National Pressure Ulcer Advisory Panel ' s Updated Pressure Ulcer Staging System From the NPUAP," no. May, pp. 269–274, 2007.

[26] J. Peart, "The Aetiology of Deep Tissue Injury: A Literature Review," *Br. J. Nurs.*, vol. 25, no. 15, pp. 840–843, 2016.

[27] C. V. Bouten, C. W. Oomens, F. P. Baaijens, and D. L. Bader, "The etiology of pressure ulcers: Skin deep or muscle bound?," *Arch. Phys. Med. Rehabil.*, vol. 84, no. 4, pp. 616–619, 2003, doi: 10.1053/apmr.2003.50038.

[28] M. Zhang, A. R. Turner-Smith, and V. C. Roberts, "The Reaction of Skin and Soft Tissue to Shear Forces Applied Externally to the Skin Surface," *Proc. Inst. Mech. Eng. Part H J. Eng. Med.*, vol. 208, no. 4, pp. 217–222, 1994, doi: 10.1243/PIME_PROC_1994_208_291_02.

[29] J. A. Witkowski and L. C. Parish, "Histopathology of the decubitus ulcer," *J. Am. Acad. Dermatol.*, vol. 6, no. 6, pp. 1014–1021, 1982, doi: 10.1016/S0190-9622(82)70085-4.

[30] Z. Moore *et al.*, "Pressure ulcer prevalence and prevention practices: A cross-sectional comparative survey in Norway and Ireland," *J. Wound Care*, vol. 24, no. 8, pp. 333–339, 2015, doi: 10.12968/jowc.2015.24.8.333.

[31] B. Barrois, D. Colin, and F. A. Allaert, "Prevalence, characteristics and risk factors of pressure ulcers in public and private hospitals care units and nursing homes in France," *Hosp. Pract. (1995)*, vol. 46, no. 1, pp. 30–36, 2018, doi: 10.1080/21548331.2018.1418139.

[32] E. Park-Lee and C. Caffrey, "Pressure ulcers among nursing home residents: United States, 2004.," *NCHS Data Brief*, no. 14, pp. 1–8, 2009.

[33] J. S. Mervis and T. J. Phillips, "Pressure ulcers: Pathophysiology, epidemiology, risk factors, and presentation," *J. Am. Acad. Dermatol.*, vol. 81, no. 4, pp. 881–890, 2019, doi: 10.1016/j.jaad.2018.12.069.

[34] J. C. Gardiner, P. L. Reed, J. D. Bonner, D. K. Haggerty, and D. G. Hale, "Incidence of hospital-acquired pressure ulcers - a population-based cohort study," *Int. Wound J.*, vol. 13, no. 5, pp. 809–820, 2016, doi: 10.1111/iwj.12386.

[35] J. S. Krause and L. Broderick, "Patterns of recurrent pressure ulcers after spinal cord injury: Identification of risk and protective factors 5 or more years after onset," *Arch. Phys. Med. Rehabil.*, vol. 85, no. 8, pp. 1257–1264, 2004, doi: 10.1016/j.apmr.2003.08.108.

[36] D. Jackson, A. M. Sarki, R. Betteridge, and J. Brooke, "Medical device-related pressure ulcers: A systematic review and meta-analysis," *Int. J. Nurs. Stud.*, vol. 92, pp. 109–120,

2019, doi: 10.1016/j.ijnurstu.2019.02.006.

[37] M. Kaşıkçı, M. Aksoy, and E. Ay, “Investigation of the prevalence of pressure ulcers and patient-related risk factors in hospitals in the province of Erzurum: A cross-sectional study,” *J. Tissue Viability*, vol. 27, no. 3, pp. 135–140, 2018, doi: 10.1016/j.jtv.2018.05.001.

[38] M. Koivunen, A. Hjerppe, E. Luotola, T. Kauko, and P. Asikainen, “Risks and prevalence of pressure ulcers among patients in an acute hospital in Finland,” *J. Wound Care*, vol. 27, no. 2, 2018.

[39] A. Tubaishat, P. Papanikolaou, D. Anthony, and L. Habiballah, “Pressure Ulcers Prevalence in the Acute Care Setting: A Systematic Review, 2000-2015,” *Clin. Nurs. Res.*, vol. 27, no. 6, pp. 643–659, 2018, doi: 10.1177/1054773817705541.

[40] M. W. van Leen, J. M. Schols, S. E. Hovius, and R. J. Halfens, “A Secondary Analysis of Longitudinal Prevalence Data to Determine the Use of Pressure Ulcer Preventive Measures in Dutch Nursing Homes, 2005–2014,” *Ostomy Wound Manag.*, vol. 63, no. 09, pp. 10–20, 2017, doi: 10.25270/owm.2017.09.1020.

[41] M. I. González-Méndez, M. Lima-Serrano, C. Martín-Castaño, I. Alonso-Araujo, and J. S. Lima-Rodríguez, “Incidence and risk factors associated with the development of pressure ulcers in an intensive care unit,” *J. Clin. Nurs.*, vol. 27, no. 5–6, pp. 1028–1037, 2018, doi: 10.1111/jocn.14091.

[42] P. García-Molina, E. Balaguer-López, F. P. García-Fernández, M. de los Á. Ferrera-Fernández, J. M. Blasco, and J. Verdú, “Pressure ulcers’ incidence, preventive measures, and risk factors in neonatal intensive care and intermediate care units,” *Int. Wound J.*, vol. 15, no. 4, pp. 571–579, 2018, doi: 10.1111/iwj.12900.

[43] M. Artico *et al.*, “Prevalence, incidence and associated factors of pressure ulcers in home palliative care patients: A retrospective chart review,” *Palliat. Med.*, vol. 32, no. 1, pp. 299–307, 2018, doi: 10.1177/0269216317737671.

[44] E. Zarei, E. Madarshahian, A. Nikkhah, and S. Khodakarim, “Incidence of pressure ulcers in intensive care units and direct costs of treatment: Evidence from Iran,” *J. Tissue Viability*, vol. 28, no. 2, pp. 70–74, 2019, doi: 10.1016/j.jtv.2019.02.001.

[45] H. I. Sarsak, “Review of pressure ulcers management in pediatrics: assessment, prevention, and intervention,” *J. Pediatr. Neonatal Care*, vol. 8, no. 5, 2018, doi: 10.15406/jpnc.2018.08.00350.

[46] D. Anthony, D. Alosoumi, and R. Safari, “Prevalence of pressure ulcers in long-term care: A global review,” *J. Wound Care*, vol. 28, no. 11, pp. 702–709, 2019, doi: 10.12968/jowc.2019.28.11.702.

[47] X. Deng, T. Yu, and A. Hu, “Predicting the risk for hospital-acquired pressure ulcers in critical care patients,” *Crit. Care Nurse*, vol. 37, no. 4, pp. e1–e11, 2017, doi: 10.4037/ccn2017548.

[48] Y. Amir, C. Lohrmann, R. J. G. Halfens, and J. M. G. A. Schols, “Pressure ulcers in four Indonesian hospitals: prevalence, patient characteristics, ulcer characteristics, prevention and treatment,” *Int. Wound J.*, vol. 14, no. 1, pp. 184–193, 2017, doi: 10.1111/iwj.12580.

[49] C. Joseph and L. Nilsson Wikmar, “Prevalence of secondary medical complications and risk factors for pressure ulcers after traumatic spinal cord injury during acute care in South Africa,” *Spinal Cord*, vol. 54, no. 7, pp. 535–539, 2016, doi: 10.1038/sc.2015.189.

[50] D. Becker *et al.*, “Pressure ulcers in ICU patients: Incidence and clinical and epidemiological features: A multicenter study in southern Brazil,” *Intensive Crit. Care Nurs.*, vol. 42, pp. 55–61, 2017, doi: 10.1016/j.iccn.2017.03.009.

[51] F. Coyer *et al.*, “Pressure injury prevalence in intensive care versus non-intensive care patients: A state-wide comparison,” *Aust. Crit. Care*, vol. 30, no. 5, pp. 244–250, 2017, doi: 10.1016/j.aucc.2016.12.003.

[52] A. C. Kwok, A. M. Simpson, J. Willcockson, D. P. Donato, I. A. Goodwin, and J. P. Agarwal, “Complications and their associations following the surgical repair of pressure ulcers,” *Am. J. Surg.*, vol. 216, no. 6, pp. 1177–1181, 2018, doi: 10.1016/j.amjsurg.2018.01.012.

[53] D. Engels, M. Austin, L. McNichol, J. Fencl, S. Gupta, and H. Kazi, “Pressure Ulcers: Factors Contributing to Their Development in the OR,” *AORN J.*, vol. 103, no. 3, pp. 271–281, 2016, doi: 10.1016/j.aorn.2016.01.008.

[54] W. H. Donovan, R. Edward Carter, G. M. Bedbrook, J. S. Young, and E. R. Griffiths, “Incidence of medical complications in spinal cord injury: Patients in specialised, compared with non-specialised centres,” *Paraplegia*, vol. 22, no. 5, pp. 282–290, 1984, doi: 10.1038/sc.1984.46.

[55] C. Vangilder, S. Amlung, P. Harrison, and S. Meyer, “Results of the 2008 – 2009 International Pressure Ulcer Prevalence™ Survey and a3-Year, Acute Care, Unit-Specific Analysis.,” *Ostomy Wound Manag.*, no. November, pp. 39–46, 2009, doi: 10.1016/j.scijus.2009.06.001.

[56] The national SCI statistical center., “Spinal cord injury facts and figures at a glance.,” *J. Spinal Cord Med.*, vol. 34, no. 6, pp. 620–1, 2017, doi: 10.1179/204577212X13237783484262.

[57] National Spinal Cord InjuryStatistical Center, “Spinal Cord Injury Facts and Figures at a Glance.,” *J. Spinal Cord Med.*, vol. 37, no. 3, pp. 355–6, 2014.

[58] N. B. Jain *et al.*, “Traumatic spinal cord injury in the United States, 1993-2012,” *JAMA - J. Am. Med. Assoc.*, vol. 313, no. 22, pp. 2236–2243, 2015, doi: 10.1001/jama.2015.6250.

[59] Y. Chen, M. J. DeVivo, and A. B. Jackson, “Pressure ulcer prevalence in people with spinal cord injury: Age-period-duration effects,” *Arch. Phys. Med. Rehabil.*, vol. 86, no. 6, pp. 1208–1213, 2005, doi: 10.1016/j.apmr.2004.12.023.

[60] W. O. McKinley, A. B. Jackson, D. D. Cardenas, and M. J. DeVivo, “Long-term medical

complications after traumatic spinal cord injury: a regional model systems analysis.," *Arch. Phys. Med. Rehabil.*, vol. 80, no. 11, pp. 1402–1410, 1999, doi: 10.1016/S0003-9993(99)90251-4.

[61] M. Hubli *et al.*, "Feedback improves compliance of pressure relief activities in wheelchair users with spinal cord injury," *Spinal Cord*, 2020, doi: 10.1038/s41393-020-0522-7.

[62] D. M. Brienza, P. E. Karg, M. Jo Geyer, S. Kelsey, and E. Trefler, "The relationship between pressure ulcer incidence and buttock-seat cushion interface pressure in at-risk elderly wheelchair users," *Arch. Phys. Med. Rehabil.*, vol. 82, no. 4, pp. 529–533, 2001, doi: 10.1053/apmr.2001.21854.

[63] C. Vangilder, G. D. Macfarlane, and S. Meyer, "Results of Nine International Pressure Ulcer Prevalence Surveys : 1989 to 2005," *Ostomy Wound Manag.*, vol. 54, no. 2, 2008.

[64] W. D. Spector, R. Limcangco, P. L. Owens, and C. A. Steiner, "Marginal Hospital Cost of Surgery-related Hospital-acquired Pressure Ulcers," *Med. Care*, vol. 54, no. 9, pp. 845–851, 2016, doi: 10.1097/MLR.0000000000000558.

[65] D. M. Smith, "Pressure ulcers in the nursing home," *Ann. Intern. Med.*, vol. 123, no. 6, pp. 433–442, 1995, doi: 10.7326/0003-4819-123-6-199509150-00008.

[66] K. Vanderwee, M. Clark, C. Dealey, L. Gunningberg, and T. Defloor, "Pressure ulcer prevalence in Europe: A pilot study," *J. Eval. Clin. Pract.*, vol. 13, no. 2, pp. 227–235, 2007, doi: 10.1111/j.1365-2753.2006.00684.x.

[67] E. W. Tam, A. F. Mak, W. N. Lam, J. H. Evans, and Y. Y. Chow, "Pelvic movement and interface pressure distribution during manual wheelchair propulsion," *Arch. Phys. Med. Rehabil.*, vol. 84, no. 10, pp. 1466–1472, 2003, doi: 10.1016/S0003-9993(03)00269-7.

[68] E. M. Giesbrecht, K. D. Ethans, and D. Staley, "Measuring the effect of incremental angles of wheelchair tilt on interface pressure among individuals with spinal cord injury," *Spinal Cord*, vol. 49, no. 7, pp. 827–831, 2011, doi: 10.1038/sc.2010.194.

[69] M. Makhsous *et al.*, "Measuring tissue perfusion during pressure relief maneuvers: Insights into preventing pressure ulcers," *J. Spinal Cord Med.*, vol. 30, no. 5, pp. 497–507, 2007, doi: 10.1080/10790268.2007.11754584.

[70] A. C. Ljung, M. C. Stenius, S. Bjelak, and J. F. Lagergren, "Surgery for pressure ulcers in spinal cord-injured patients following a structured treatment programme: a 10-year follow-up," *Int. Wound J.*, vol. 14, no. 2, pp. 355–359, 2017, doi: 10.1111/iwj.12609.

[71] E. Jaul, "Cohort study of atypical pressure ulcers development," *Int. Wound J.*, vol. 11, no. 6, pp. 696–700, 2014, doi: 10.1111/iwj.12033.

[72] K. Ozer, O. Colak, F. B. Goktas, N. Sungur, and U. Kocer, "A rare location for a common problem: Popliteal pressure ulcer," *Int. Wound J.*, vol. 13, no. 2, pp. 287–288, 2016, doi: 10.1111/iwj.12257.

[73] J. C. Y. Ong, F. C. Chan, and J. McCann, "Pressure ulcers of the popliteal fossae caused

by thromboembolic deterrent stockings (TEDS)," *Ir. J. Med. Sci.*, vol. 180, no. 2, pp. 601–602, 2011, doi: 10.1007/s11845-009-0384-7.

[74] K. Kataria, S. Sagar, M. Singhal, and R. Yadav, "Pressure sore at an unusual site- the bilateral popliteal fossa: A case report," *Oman Med. J.*, vol. 27, no. 3, 2012, doi: 10.5001/omj.2012.65.

[75] M. Makhsous, F. Lin, J. Bankard, R. W. Hendrix, M. Hepler, and J. Press, "Biomechanical effects of sitting with adjustable ischial and lumbar support on occupational low back pain: Evaluation of sitting load and back muscle activity," *BMC Musculoskelet. Disord.*, vol. 10, pp. 1–11, 2009, doi: 10.1186/1471-2474-10-17.

[76] M. J. Castro, D. F. Apple, E. A. Hillegass, and G. A. Dudley, "Influence of complete spinal cord injury on skeletal muscle cross-sectional area within the first 6 months of injury," *Eur. J. Appl. Physiol. Occup. Physiol.*, vol. 80, no. 4, pp. 373–378, 1999, doi: 10.1007/s004210050606.

[77] P. K. Shah *et al.*, "Lower-Extremity Muscle Cross-Sectional Area After Incomplete Spinal Cord Injury," *Arch. Phys. Med. Rehabil.*, vol. 87, no. 6, pp. 772–778, 2006, doi: 10.1016/j.apmr.2006.02.028.

[78] G. A. Wu and K. M. Bogie, "Not just quantity: Gluteus maximus muscle characteristics in able-bodied and SCI individuals - Implications for tissue viability," *J. Tissue Viability*, vol. 22, no. 3, pp. 74–82, 2013, doi: 10.1016/j.jtv.2013.03.003.

[79] C. D. Moore *et al.*, "Lower-extremity muscle atrophy and fat infiltration after chronic spinal cord injury," *J. Musculoskelet. Neuronal Interact.*, vol. 15, no. 1, pp. 32–41, 2015.

[80] A. S. Gorgey and G. A. Dudley, "Skeletal muscle atrophy and increased intramuscular fat after incomplete spinal cord injury," *Spinal Cord*, vol. 45, no. 4, pp. 304–309, 2007, doi: 10.1038/sj.sc.3101968.

[81] S. Carda, C. Cisari, and M. Invernizzi, "Sarcopenia or Muscle Modifications in Neurologic Diseases: A Lexical o Pathophsiological Difference?," *Eur. J. Phys. Rehabil. Med.*, vol. 49, 2013.

[82] E. Linder-Ganz, N. Shabshin, Y. Itzchak, Z. Yizhar, I. Siev-Ner, and A. Gefen, "Strains and stresses in sub-dermal tissues of the buttocks are greater in paraplegics than in healthy during sitting," *J. Biomech.*, vol. 41, no. 3, pp. 567–580, 2008, doi: 10.1016/j.jbiomech.2007.10.011.

[83] D. Brienza, J. Vallely, P. Karg, J. Akins, and A. Gefen, "An MRI investigation of the effects of user anatomy and wheelchair cushion type on tissue deformation," *J. Tissue Viability*, vol. 27, no. 1, pp. 42–53, 2018, doi: 10.1016/j.jtv.2017.04.001.

[84] J. A. Bulcke, J. L. Termote, Y. Palmers, and D. Crolla, "Computed tomography of the human skeletal muscular system.," *Neuroradiology*, vol. 17, no. 3, pp. 127–136, 1979.

[85] C. M. Nascimento, M. Ingles, A. Salvador-Pascual, M. R. Cominetti, M. C. Gomez-Cabrera, and J. Viña, "Sarcopenia, frailty and their prevention by exercise," *Free Radic.*

Biol. Med., vol. 132, no. August 2018, pp. 42–49, 2019, doi: 10.1016/j.freeradbiomed.2018.08.035.

[86] T. J. Doherty, "Invited review: Aging and sarcopenia.," *J. Appl. Physiol.*, vol. 95, no. 4, pp. 1717–27, 2003, doi: 10.1152/japplphysiol.00347.2003.

[87] H. Jee and J. Lim, "Discrepancies between Skinned Single Muscle Fibres and Whole Thigh Muscle Function Characteristics in Young and Elderly Human Subjects," vol. 2016, 2016, doi: 10.1155/2016/6206959.

[88] L. Larsson, B. Sjödin, and J. Karlsson, "Histochemical and biochemical changes in human skeletal muscle with age in sedentary males, age 22–65 years," *Acta Physiol. Scand.*, vol. 103, no. 1, pp. 31–39, 1978, doi: 10.1111/j.1748-1716.1978.tb06187.x.

[89] M. T. Korhonen *et al.*, "Aging, muscle fiber type, and contractile function in sprint-trained athletes," *J. Appl. Physiol.*, vol. 101, no. 3, pp. 906–917, 2006, doi: 10.1152/japplphysiol.00299.2006.

[90] M. D. Gordon, M. M. Gottschlich, E. I. Helvig, J. A. Marvin, and R. L. Richard, "Review of evidenced-based practice for the prevention of pressure sores in burn patients," *J. Burn Care Rehabil.*, vol. 25, no. 5, pp. 388–410, 2004, doi: 10.1097/01.BCR.0000138289.83335.F4.

[91] N. Bergstrom, B. Braden, A. Laguzza, and V. Holman, "The Braden Scale for Predicting Pressure Sore Risk," *Nurs. Res.*, vol. 36, no. 4, 1987.

[92] B. G. (VU U. Raijmakers, M. G. (Amsterdam R. R. C.-R. Nieuwenhuizen, H. (VU U. Beckerman, and S. A. R. R. C.-R. de Groot, "Differences in the Course of Daily Activity Level Between Persons with and Without Chronic Pain," *Am. J. Phys. Med. Rehabil.*, vol. 94, no. 2, pp. 101–113, 2014, doi: 10.1097/PHM.0000000000000206.

[93] L. Gagliese and R. Melzack, "Chronic pain in elderly people," *Pain*, vol. 70, no. 1, pp. 3–14, 1997, doi: 10.1016/S0304-3959(96)03266-6.

[94] P. J. Siddall and J. D. Loeser, "Pain following spinal cord injury," *Spinal Cord*, vol. 39, no. 2, pp. 63–73, 2001, doi: 10.1038/sj.sc.3101116.

[95] R. J. Hartke, T. R. Prohaska, and S. E. Furner, "Older Adults and Assistive Devices: Use, Multiple Use, and Need," *J. Aging Health*, vol. 10, no. 1, pp. 99–116, 1998.

[96] I. K. Crombie *et al.*, "Why older people do not participate in leisure time physical activity: A survey of activity levels, beliefs and deterrents," *Age Ageing*, vol. 33, no. 3, pp. 287–292, 2004, doi: 10.1093/ageing/afh089.

[97] K. A. Martin Ginis *et al.*, "Leisure Time Physical Activity in a Population-Based Sample of People With Spinal Cord Injury Part I: Demographic and Injury-Related Correlates," *Arch. Phys. Med. Rehabil.*, vol. 91, no. 5, pp. 722–728, 2010, doi: 10.1016/j.apmr.2009.12.027.

[98] S. M. Reichel, "Shearing force as a factor in decubitus ulcers in paraplegics," *J. Am. Med.*

Assoc., vol. 166, no. 7, pp. 762–763, 1958, doi: 10.1001/jama.1958.62990070004010a.

[99] B. P. J. A. Keller and B. Van Ramshorst, "Pressure ulcers in intensive care patients : a review of risks and prevention," *Intensive Care Med.*, vol. 28, pp. 1379–1388, 2002, doi: 10.1007/s00134-002-1487-z.

[100] A. A. Manorama, S. Baek, J. Vorro, A. Sikorskii, and T. R. Bush, "Blood perfusion and transcutaneous oxygen level characterizations in human skin with changes in normal and shear loads - Implications for pressure ulcer formation," *Clin. Biomech.*, vol. 25, no. 8, pp. 823–828, 2010, doi: 10.1016/j.clinbiomech.2010.06.003.

[101] A. Manorama, R. Meyer, R. Wiseman, and T. R. Bush, "Quantifying the effects of external shear loads on arterial and venous blood flow: Implications for pressure ulcer development," *Clin. Biomech.*, vol. 28, no. 5, pp. 574–578, 2013, doi: 10.1016/j.clinbiomech.2013.04.001.

[102] W. Pan, J. P. Drost, M. D. Basson, and T. R. Bush, "Skin perfusion responses under normal and combined loadings: Comparisons between legs with venous stasis ulcers and healthy legs," *Clin. Biomech.*, vol. 30, no. 10, pp. 1218–1224, 2015, doi: 10.1016/j.clinbiomech.2015.08.001.

[103] M. Kosiak, "Etiology of decubitus ulcers.," *Archives of physical medicine and rehabilitation*, vol. 42. pp. 19–29, 1961.

[104] S. Dinsdale, "Decubitus Ulcers: Role of Pressure and Friction in Causation," *Arch. Phys. Med. Rehabil.*, vol. 55, no. 4, pp. 147–152, 1974.

[105] T. HUSAIN, "An experimental study of some pressure effects on tissues, with reference to the bed-sore problem," *J. Pathol. Bacteriol.*, vol. 66, no. 2, pp. 347–358, 1953, doi: 10.1002/path.1700660203.

[106] E. Linder-Ganz, S. Engelberg, M. Scheinowitz, and A. Gefen, "Pressure-time cell death threshold for albino rat skeletal muscles as related to pressure sore biomechanics," *J. Biomech.*, vol. 39, no. 14, pp. 2725–2732, 2006, doi: 10.1016/j.jbiomech.2005.08.010.

[107] E. M. H. Bosboom, C. V. C. Bouten, C. W. J. Oomens, H. W. M. Van Straaten, F. P. T. Baaijens, and H. Kuipers, "Quantification and localisation of damage in rat muscles after controlled loading; a new approach to study the aetiology of pressure sores," *Med. Eng. Phys.*, vol. 23, no. 3, pp. 195–200, 2001, doi: 10.1016/S1350-4533(01)00034-0.

[108] D. A. Hobson, "Comparative effects of posture on pressure and shear at the body-seat interface," *J. Rehabil. Res. Dev.*, vol. 29, no. 4, p. 21, 1992, doi: 10.1682/JRRD.1992.10.0021.

[109] J. Berthold, B. E. Dicianno, and R. A. Cooper, "Pressure mapping to assess seated pressure distributions and the potential risk for skin ulceration in a population of sledge hockey players and control subjects," *Disabil. Rehabil. Assist. Technol.*, vol. 8, no. 5, pp. 387–391, 2013, doi: 10.3109/17483107.2013.769123.

[110] F. Gijsen, A. van der Giessen, A. van der Steen, and J. Wentzel, "Shear stress and

advanced atherosclerosis in human coronary arteries," *J. Biomech.*, vol. 46, no. 2, pp. 240–247, 2013, doi: 10.1016/j.jbiomech.2012.11.006.

[111] T. H. Bui, D. Pradon, P. Lestriez, K. Debray, R. Taiar, and B. Guillon, "Influence of Different Types of Wheelchair Cushions for Pressure Ulcers in View of the Experimental Approach," *Proc. LASTED Int. Conf.*, pp. 164–167, 2017, doi: 10.2316/p.2017.852-043.

[112] S. D. Darrah, B. E. Dicianno, J. Berthold, A. McCoy, M. Haas, and R. A. Cooper, "Measuring static seated pressure distributions and risk for skin pressure ulceration in ice sledge hockey players," *Disabil. Rehabil. Assist. Technol.*, vol. 11, no. 3, pp. 241–246, 2016, doi: 10.3109/17483107.2014.921939.

[113] M. Klaassen, D. J. Schipper, and M. A. Masen, "Influence of the relative humidity and the temperature on the in-vivo friction behaviour of human skin," *Biotribology*, vol. 6, pp. 21–28, 2016, doi: 10.1016/j.biotri.2016.03.003.

[114] L. C. Gerhardt, V. Strässle, A. Lenz, N. D. Spencer, and S. Derler, "Influence of epidermal hydration on the friction of human skin against textiles," *J. R. Soc. Interface*, vol. 5, no. 28, pp. 1317–1328, 2008, doi: 10.1098/rsif.2008.0034.

[115] D. Schwartz, Y. K. Magen, A. Levy, and A. Gefen, "Effects of humidity on skin friction against medical textiles as related to prevention of pressure injuries," *Int. Wound J.*, vol. 15, no. 6, pp. 866–874, 2018, doi: 10.1111/iwj.12937.

[116] J. Kottner, J. Black, E. Call, A. Gefen, and N. Santamaria, "Microclimate: A critical review in the context of pressure ulcer prevention," *Clin. Biomech.*, vol. 59, no. September, pp. 62–70, 2018, doi: 10.1016/j.clinbiomech.2018.09.010.

[117] G. J. Hodges, M. M. Mallette, A. Rigby, P. Klentrou, S. S. Cheung, and B. Falk, "Comparison of different wheelchair seating on thermoregulation and perceptual responses in thermoneutral and hot conditions in children," *J. Tissue Viability*, vol. 28, no. 3, pp. 144–151, 2019, doi: 10.1016/j.jtv.2019.04.003.

[118] C. M. Olney *et al.*, "Microclimate evaluation of strap-based wheelchair seating systems for persons with spinal cord injury: A pilot study," *J. Tissue Viability*, vol. 27, no. 3, pp. 181–187, 2018, doi: 10.1016/j.jtv.2018.06.001.

[119] E. C. Herrman, C. F. Knapp, J. C. Donofrio, and R. Salcido, "Skin perfusion responses to surface pressure-induced ischemia: implication for the developing pressure ulcer.," *J. Rehabil. Res. Dev.*, vol. 36, no. 2, pp. 109–120, 1999, doi: 10.1086/250095.

[120] E. Linder-Ganz and A. Gefen, "The effects of pressure and shear on capillary closure in the microstructure of skeletal muscles," *Ann. Biomed. Eng.*, vol. 35, no. 12, pp. 2095–2107, 2007, doi: 10.1007/s10439-007-9384-9.

[121] C. W. J. Oomens, D. Bader, S. Loerakker, and F. Baaijens, "Pressure Induced Deep Tissue Injury Explained," *Ann. Biomed. Eng.*, vol. 43, no. 2, pp. 297–305, 2015, doi: 10.1007/s10439-014-1202-6.

[122] I. Hoogendoorn, J. Reenalda, B. F. J. M. Koopman, and J. S. Rietman, "The effect of

pressure and shear on tissue viability of human skin in relation to the development of pressure ulcers: a systematic review," *J. Tissue Viability*, vol. 26, no. 3, pp. 157–171, 2017, doi: 10.1016/j.jtv.2017.04.003.

[123] P. Kaewprag, C. Newton, B. Vermillion, S. Hyun, K. Huang, and R. Machiraju, "Predictive models for pressure ulcers from intensive care unit electronic health records using Bayesian networks," *BMC Med. Inform. Decis. Mak.*, vol. 17, no. Suppl 2, 2017, doi: 10.1186/s12911-017-0471-z.

[124] Ming Zhang and V. C. Roberts, "The effect of shear forces externally applied to skin surface on underlying tissues," *J. Biomed. Eng.*, vol. 15, no. 6, pp. 451–456, 1993, doi: 10.1016/0141-5425(93)90057-6.

[125] T. Kamegaya, "Influence of sacral sitting in a wheelchair on the distribution of contact pressure on the buttocks and back and shear force on the ischial region," *J. Phys. Ther. Sci.*, vol. 28, no. 10, pp. 2830–2833, 2016, doi: 10.1589/jpts.28.2830.

[126] X. Wang, M. Cardoso, and G. Beurier, "Effects of seat parameters and sitters' anthropometric dimensions on seat profile and optimal compressed seat pan surface," *Appl. Ergon.*, vol. 73, no. December 2017, pp. 13–21, 2018, doi: 10.1016/j.apergo.2018.05.015.

[127] I. A. Hunter and K. J. Edwards, "Managing pressure sores," *Surg. (United Kingdom)*, vol. 35, no. 9, pp. 505–510, 2017, doi: 10.1016/j.mpsur.2017.06.008.

[128] S. Bhattacharya and R. K. Mishra, "Pressure Ulcers: Current Understanding and Newer Modalities of Treatment," *Indian J. Plast. Surg.*, vol. 48, no. 1, pp. 4–16, 2015, doi: 10.4103/0970.

[129] J. S. Mervis and T. J. Phillips, "Pressure ulcers: Prevention and management," *J. Am. Acad. Dermatol.*, vol. 81, no. 4, pp. 893–902, 2019, doi: 10.1016/j.jaad.2018.12.068.

[130] J. F. Graumlich *et al.*, "Healing pressure ulcers with collagen or hydrocolloid: A randomized, controlled trial," *J. Am. Geriatr. Soc.*, vol. 51, no. 2, pp. 147–154, 2003, doi: 10.1046/j.1532-5415.2003.51051.x.

[131] A. Linthwaite and E. Bethell, "Managing pressure ulcers and moisture lesions with new hydrocolloid technology," *Br. J. Nurs.*, vol. 25, no. 8, pp. 443–448, 2016, doi: 10.12968/bjon.2016.25.8.442.

[132] R. M. Walker, B. M. Gillespie, L. Thalib, N. S. Higgins, and J. A. Whitty, "Foam dressings for treating pressure ulcers (Review)," *Cochrane Database Syst. Rev.*, vol. 2017, no. 10, 2017, doi: 10.1002/14651858.CD011332.pub2.

[133] R. A. Atkinson and N. A. Cullum, "Interventions for pressure ulcers: A summary of evidence for prevention and treatment," *Spinal Cord*, vol. 56, no. 3, pp. 186–198, 2018, doi: 10.1038/s41393-017-0054-y.

[134] H. Yamanaka, S. Okada, and H. Sanada, "A multicenter, randomized, controlled study of the use of nutritional supplements containing collagen peptides to facilitate the healing of

pressure ulcers," *J. Nutr. Intermed. Metab.*, vol. 8, pp. 51–59, 2017, doi: 10.1016/j.jnim.2017.05.001.

[135] B. Smith *et al.*, "Pressure Ulcer Treatment Strategies, A Systematic Comparative Effectiveness Review," *Ann. Intern. Med.*, vol. 159, no. 1, 2013.

[136] W. V Padula *et al.*, "Improving the Quality of Pressure Ulcer Care With Prevention: A Cost-Effectiveness Analysis," *Med. Care*, vol. 49, no. 4, pp. 385–392, 2011.

[137] S. Gaspar, M. Peralta, A. Marques, A. Budri, and M. Gaspar de Matos, "Effectiveness on hospital-acquired pressure ulcers prevention: a systematic review," *Int. Wound J.*, vol. 16, no. 5, pp. 1087–1102, 2019, doi: 10.1111/iwj.13147.

[138] L. Gunningberg, I. M. Sedin, S. Andersson, and R. Pingel, "Pressure mapping to prevent pressure ulcers in a hospital setting: A pragmatic randomised controlled trial," *Int. J. Nurs. Stud.*, vol. 72, no. March, pp. 53–59, 2017, doi: 10.1016/j.ijnurstu.2017.04.007.

[139] S. Chapman, "Preventing and Treating Pressure Ulcers," *Community Wound Care*, no. March, pp. 155–165, 2017, doi: 10.1002/9781118281796.ch12.

[140] S. Mäki-Turja-Rostedt, M. Stolt, H. Leino-Kilpi, and E. Haavisto, "Preventive interventions for pressure ulcers in long-term older people care facilities: A systematic review," *J. Clin. Nurs.*, vol. 28, no. 13–14, pp. 2420–2442, 2019, doi: 10.1111/jocn.14767.

[141] A. Mitchell, "Adult pressure are care: preventing pressure ulcers," *Br. J. Nurs.*, vol. 27, no. 18, pp. 29–31, 2018.

[142] T. V. Boyko, M. T. Longaker, and G. P. Yang, "Review of the Current Management of Pressure Ulcers," *Adv. Wound Care*, vol. 7, no. 2, pp. 57–67, 2018, doi: 10.1089/wound.2016.0697.

[143] T. G. Reuler, J. B., & Cooney, "The pressure sore: Pathophysiology and principle of management," *Ann. Intern. Med.*, no. 94, pp. 661–666, 1981.

[144] V. Lopez *et al.*, "Skin tear prevention and management among patients in the acute aged care and rehabilitation units in the Australian Capital Territory: A best practice implementation project," *Int. J. Evid. Based. Healthc.*, vol. 9, no. 4, pp. 429–434, 2011, doi: 10.1111/j.1744-1609.2011.00234.x.

[145] A. Levy, M. B. O. Frank, and A. Gefen, "The biomechanical efficacy of dressings in preventing heel ulcers," *J. Tissue Viability*, vol. 24, no. 1, pp. 1–11, 2015, doi: 10.1016/j.jtv.2015.01.001.

[146] A. Tannen, T. Dassen, and R. Halfens, "Differences in prevalence of pressure ulcers between the Netherlands and Germany - Associations between risk, prevention and occurrence of pressure ulcers in hospitals and nursing homes," *J. Clin. Nurs.*, vol. 17, no. 9, pp. 1237–1244, 2008, doi: 10.1111/j.1365-2702.2007.02225.x.

[147] R. F. Edlich *et al.*, "Pressure Ulcer Prevention," vol. 14, no. December 2003, pp. 285–304,

2004.

[148] N. Shoham, A. Levy, K. Kopplin, and A. Gefen, “Contoured Foam Cushions Cannot Provide Long-term Protection Against Pressure-Ulcers for Individuals with a Spinal Cord Injury: Modeling Studies,” *Adv. Ski. Wound Care*, vol. 28, no. 7, pp. 303–316, 2015, doi: 10.1097/01.ASW.0000465300.99194.27.

[149] L. Stockton and S. Rithalia, “Is dynamic seating a modality worth considering in the prevention of pressure ulcers?,” *J. Tissue Viability*, vol. 17, no. 1, pp. 15–21, 2008, doi: 10.1016/j.jtv.2007.09.011.

[150] T. Freeto, S. J. Mitchell, and K. M. Bogie, “Preliminary development of an advanced modular pressure relief cushion: Testing and user evaluation,” *J. Tissue Viability*, vol. 27, no. 1, pp. 2–9, 2018, doi: 10.1016/j.jtv.2017.03.001.

[151] S. P. Burns and K. L. Betz, “Seating Pressures With Conventional Cushions in Tetraplegia,” *Arch. Phys. Med. Rehabil.*, vol. 80, pp. 566–571, 1999.

[152] S. H. Lee, J. S. Park, B. K. Jung, and S. A. Lee, “Effects of different seat cushions on interface pressure distribution: A pilot study,” *J. Phys. Ther. Sci.*, vol. 28, no. 1, pp. 227–230, 2016, doi: 10.1589/jpts.28.227.

[153] B. Crane, M. Wininger, and E. Call, “Orthotic-Style Off-Loading Wheelchair Seat Cushion Reduces Interface Pressure Under Ischial Tuberosities and Sacrococcygeal Regions,” *Arch. Phys. Med. Rehabil.*, vol. 97, no. 11, pp. 1872–1879, 2016, doi: 10.1016/j.apmr.2016.04.004.

[154] P. Nuthi, W. Carrigan, C. Pande, and M. B. J. Wijesundara, “Control implementation for real-time pressure adjusting seat cushion to prevent pressure ulcers,” *Proc. ASME Des. Eng. Tech. Conf.*, vol. 6, pp. 1–7, 2018, doi: 10.1115/DETC2018-86210.

[155] W. Carrigan *et al.*, “Design and operation verification of an automated pressure mapping and modulating seat cushion for pressure ulcer prevention,” *Med. Eng. Phys.*, vol. 69, pp. 17–27, 2019, doi: 10.1016/j.medengphy.2019.06.006.

[156] M. O. Park and S. H. Lee, “Effects of seating education and cushion management for adaptive sitting posture in spinal cord injury: Two case reports,” *Med. (United States)*, vol. 98, no. 4, 2019, doi: 10.1097/MD.0000000000014231.

[157] C. D. Hepburn, S. C. Anand, and C. Wood, “Recent advances in three-dimensional pressure relieving cushions for the prevention of pressure ulcers,” *J. Text. Inst.*, vol. 108, no. 11, pp. 1940–1948, 2017, doi: 10.1080/00405000.2017.1301019.

[158] P. Mendes, D. Paulisso, C. Caro, and D. Cruz, “Comparison of wheelchair cushion calibration by users with spinal cord injury and by occupational therapists, using a pressure mapping system. Differences in cushion calibration by the user and occupational therapist,” *Eur. Int. J. Sci. Technol.*, vol. 5, no. 6, pp. 77–85, 2016.

[159] H. K. Yuen and D. Garrett, “Comparison of three wheelchair cushions for effectiveness of pressure relief,” *Am. J. Occup. Ther.*, vol. 55, no. 4, pp. 470–475, 2001, doi:

10.5014/ajot.55.4.470.

[160] V. Mooney, M. J. Einbund, J. E. Rogers, and E. S. Stauffer, “Comparison of Pressure Distribution Qualities in Seat Cushions,” *Bull. Prosthet. Res.*, pp. 129–143, 1971.

[161] R. Zemp, J. Rhiner, S. Plüss, R. Togni, J. A. Plock, and W. R. Taylor, “Wheelchair Tilt-in-Space and Recline Functions: Influence on Sitting Interface Pressure and Ischial Blood Flow in an Elderly Population,” *Biomed Res. Int.*, vol. 2019, 2019, doi: 10.1155/2019/4027976.

[162] T. R. Bush and R. P. Hubbard, “Support force measures of midsized men in seated positions,” *J. Biomech. Eng.*, vol. 129, no. 1, pp. 58–65, 2007, doi: 10.1115/1.2401184.

[163] N. Shabshin, V. Ougortsin, G. Zoizner, and A. Gefen, “Evaluation of the effect of trunk tilt on compressive soft tissue deformations under the ischial tuberosities using weight-bearing MRI,” *Clin. Biomech.*, vol. 25, no. 5, pp. 402–408, 2010, doi: 10.1016/j.clinbiomech.2010.01.019.

[164] M. J. Coggrave and L. S. Rose, “A specialist seating assessment clinic: Changing pressure relief practice,” *Spinal Cord*, vol. 41, no. 12, pp. 692–695, 2003, doi: 10.1038/sj.sc.3101527.

[165] K. Ebe and M. J. Griffin, “Factors affecting static seat cushion comfort,” *Ergonomics*, vol. 44, no. 10, pp. 901–921, 2001, doi: 10.1080/00140130110064685.

[166] S. Horn *et al.*, “The National Pressure Ulcer Long-Term Care Study: Pressure Ulcer Development in Long-Term Care Residents,” *J. Am. Geriatr. Soc.*, vol. 52, no. 3, pp. 359–367, 2004, doi: 10.1111/j.1532-5415.2004.52106.x.

[167] X. Wang, M. Cardosso, and I. Theodora-, “Does Preferred Seat Pan Inclination Minimize Shear Force?,” *Hum. Simul. Virtual Environ. Work With Comput. Syst. (WWCS), Process Control*, no. June, pp. 743–753, 2019, doi: 10.1007/978-3-319-96077-7.

[168] K. Kobara, H. Takahashi, Y. Nagata, H. Osaka, T. Suehiro, and D. Fujita, “Disability and Rehabilitation: Assistive Technology An investigation into the effectiveness of a novel wheelchair seat-cover assembly for the reduction of forces exerted onto the buttocks,” *Disabil. Rehabil. Assist. Technol.*, pp. 1–6, 2020, doi: 10.1080/17483107.2020.1780484.

[169] S. E. Sonenblum, J. Ma, S. H. Sprigle, T. R. Hetzel, and J. McKay Cathcart, “Measuring the impact of cushion design on buttocks tissue deformation: An MRI approach,” *J. Tissue Viability*, vol. 27, no. 3, pp. 162–172, 2018, doi: 10.1016/j.jtv.2018.04.001.

[170] D. A. Gayol-Mérida and G. Plascencia, “On the estimation of maximum stress in cushions for wheelchair patients who are prone to develop pressure injuries,” *Technol. Heal. Care*, vol. 25, no. 4, pp. 749–760, 2017, doi: 10.3233/THC-160803.

[171] T. H. Bui, P. Lestriez, D. Pradon, K. Debray, and R. Taiar, “The Prevention of Pressure Ulcers: Biomechanical Modelization and Simulation of Human Seat Cushion Contributions,” *Proc. Int. Conf. Adv. Comput. Mech.*, no. February, pp. 1271–1280, 2017, doi: 10.1007/978-981-10-7149-2.

[172] A. Levy, K. Kopplin, and A. Gefen, “An air-cell-based cushion for pressure ulcer protection remarkably reduces tissue stresses in the seated buttocks with respect to foams: Finite element studies,” *J. Tissue Viability*, vol. 23, no. 1, pp. 13–23, 2014, doi: 10.1016/j.jtv.2013.12.005.

[173] L. Peko Cohen and A. Gefen, “Deep tissue loads in the seated buttocks on an off-loading wheelchair cushion versus air-cell-based and foam cushions: finite element studies,” *Int. Wound J.*, vol. 14, no. 6, pp. 1327–1334, 2017, doi: 10.1111/iwj.12807.

[174] R. H. Setyabudhy, A. Ali, R. P. Hubbard, C. Beckett, and R. C. Averill, “Measuring and Modeling of Human Soft Tissue and Seat Interaction,” *SAE Tech. Pap. Ser.*, no. 412, pp. 135–142, 1997, doi: 10.4271/970593.

[175] M. M. Verver, J. van Hoof, C. W. J. Oomens, J. S. H. M. Wismans, and F. P. T. Baaijens, “A finite element model of the human buttocks for prediction of seat pressure distributions,” *Comput. Methods Biomech. Biomed. Engin.*, vol. 7, no. 4, pp. 193–203, 2004, doi: 10.1080/10255840410001727832.

[176] V. Luboz *et al.*, “Personalized modeling for real-time pressure ulcer prevention in sitting posture,” *J. Tissue Viability*, vol. 27, no. 1, pp. 54–58, 2018, doi: 10.1016/j.jtv.2017.06.002.

[177] W. A. Traa *et al.*, “MRI based 3D finite element modelling to investigate deep tissue injury,” *Comput. Methods Biomech. Biomed. Engin.*, vol. 21, no. 14, pp. 760–769, 2018, doi: 10.1080/10255842.2018.1517868.

[178] K. M. Moerman *et al.*, “On the importance of 3D, geometrically accurate, and subject-specific finite element analysis for evaluation of in-vivo soft tissue loads,” *Comput. Methods Biomech. Biomed. Engin.*, vol. 20, no. 5, pp. 483–491, 2017, doi: 10.1080/10255842.2016.1250259.

[179] S. Li, M. Yin, L. Gao, S. Qi, and J. Wang, “FINITE ELEMENT PREDICTION of SUB-DERMAL TISSUE STRESSES of the BUTTOCKS during WHEELCHAIR PROPULSION,” *J. Mech. Med. Biol.*, vol. 16, no. 4, pp. 1–15, 2016, doi: 10.1142/S0219519416500585.

[180] L. Savonnet, X. Wang, and S. Duprey, “Finite element models of the thigh-buttock complex for assessing static sitting discomfort and pressure sore risk : a literature review,” *Comput. Methods Biomech. Biomed. Engin.*, vol. 5842, pp. 1–10, 2018, doi: 10.1080/10255842.2018.1466117.

[181] A. Macron, H. Pillet, J. Doridam, A. Verney, and P. Y. Rohan, “Development and evaluation of a new methodology for the fast generation of patient-specific Finite Element models of the buttock for sitting-acquired deep tissue injury prevention,” *J. Biomech.*, vol. 79, pp. 173–180, 2018, doi: 10.1016/j.jbiomech.2018.08.001.

[182] S. E. Sonenblum, D. Seol, S. H. Sprigle, and J. M. K. Cathcart, “Seated buttocks anatomy and its impact on biomechanical risk,” *J. Tissue Viability*, vol. 29, no. 2, pp. 69–75, 2020, doi: 10.1016/j.jtv.2020.01.004.

[183] I. P. H. Leung, L. Fleming, K. Walton, S. Barrans, and K. Ousey, “Development of a model to demonstrate the effects of friction and pressure on skin in relation to pressure ulcer formation,” *Wear*, vol. 376–377, pp. 266–271, 2017, doi: 10.1016/j.wear.2016.11.026.

[184] I. P. H. Leung, L. T. Fleming, K. Walton, S. M. Barrans, and K. Ousey, “Finite element analysis to model ischemia experienced in the development of device related pressure ulcers,” *Proc. Inst. Mech. Eng. Part H J. Eng. Med.*, vol. 233, no. 7, pp. 745–753, 2019, doi: 10.1177/0954411919851387.

[185] H. Yamada, Y. Inoue, Y. Shimokawa, and K. Sakata, “Skin stiffness determined from occlusion of a horizontally running microvessel in response to skin surface pressure: a finite element study of sacral pressure ulcers,” *Med. Biol. Eng. Comput.*, vol. 55, no. 1, pp. 79–88, 2017, doi: 10.1007/s11517-016-1500-2.

[186] W. W. Chow and E. E. Odell, “Deformations and Stresses in Softbody Tissues of a Sitting Person,” *J. Biomech. Eng.*, vol. 100, no. 2, pp. 79–89, 1978.

[187] B. a Todd and J. G. Thacker, “Three-dimensional computer model of the human buttocks, in vivo.,” *J. Rehabil. Res. Dev.*, vol. 31, no. 2, pp. 111–119, 1994.

[188] R. Ragan, T. W. Kernozek, M. Bidar, and J. W. Matheson, “Seat-interface pressures on various thicknesses of foam wheelchair cushions: A finite modeling approach,” *Arch. Phys. Med. Rehabil.*, vol. 83, no. 6, pp. 872–875, 2002, doi: 10.1053/apmr.2002.32677.

[189] E. Linder-Ganz, G. Yarnitzky, Z. Yizhar, I. Siev-Ner, and A. Gefen, “Real-time finite element monitoring of sub-dermal tissue stresses in individuals with spinal cord injury: Toward prevention of pressure ulcers,” *Ann. Biomed. Eng.*, vol. 37, no. 2, pp. 387–400, 2009, doi: 10.1007/s10439-008-9607-8.

[190] H. Delingette, “Toward Realistic Soft-Tissue Modeling in Medical Simulation,” *Proc. IEEE*, vol. 86, no. 3, 1998.

[191] P. A. L. S. Martins, R. M. N. Jorge, and A. J. M. Ferreira, “A Comparative Study of Several Material Models for Prediction of Hyperelastic Properties: Application to Silicone-Rubber and Soft Tissues,” *Strain*, vol. 42, no. 3, pp. 135–147, 2006, doi: doi:10.1111/j.1475-1305.2006.00257.x.

[192] M. Makhsous, D. Lim, R. Hendrix, J. Bankard, W. Z. Rymer, and F. Lin, “Finite element analysis for evaluation of pressure ulcer on the buttock: development and validation.,” *IEEE Trans. Neural Syst. Rehabil. Eng.*, vol. 15, no. 4, pp. 517–525, 2007, doi: 10.1109/TNSRE.2007.906967.

[193] Q. Sun *et al.*, “Soft Tissue Stress in Buttock-Thigh of a Seated Individual Elucidated by a 3D FE Model,” *RESNA 28th Annu. Conf.*, pp. 1–7, 2005.

[194] M. Grujicic, B. Pandurangan, G. Arakere, W. C. Bell, T. He, and X. Xie, “Seat-cushion and soft-tissue material modeling and a finite element investigation of the seating comfort for passenger-vehicle occupants,” *Mater. Des.*, vol. 30, no. 10, pp. 4273–4285, 2009, doi:

10.1016/j.matdes.2009.04.028.

[195] R. Sopher, J. Nixon, C. Gorecki, and A. Gefen, “Exposure to internal muscle tissue loads under the ischial tuberosities during sitting is elevated at abnormally high or low body mass indices,” *J. Biomech.*, vol. 43, no. 2, pp. 280–286, 2010, doi: 10.1016/j.jbiomech.2009.08.021.

[196] E. Linder-Ganz and A. Gefen, “Stress Analyses Coupled With Damage Laws to Determine Biomechanical Risk Factors for Deep Tissue Injury During Sitting,” *J. Biomech. Eng.*, vol. 131, no. 1, p. 011003, 2009, doi: 10.1115/1.3005195.

[197] S. Chen, J. Scott, T. R. Bush, and S. Roccabianca, “A Subject Specific Model of the Human Thigh Informed by In Vivo Experimental Data,” in *World Congress of Biomechanics*, 2018.

[198] C. W. J. Oomens, O. F. J. T. Bressers, E. M. H. Bosboom, C. V. C. Bouten, and D. L. Bader, “Can loaded interface characteristics influence strain distributions in muscle adjacent to bony prominences?,” *Comput. Methods Biomech. Biomed. Engin.*, vol. 6, no. 3, pp. 171–180, 2003, doi: 10.1080/1025584031000121034.

[199] G. W. Schmid-Schonbein, S.-Y. Woo, and B. W. Zweifach, *Frontiers in Biomechanics*. New York, Berlin, Heidelberg, Tokyo: Springer-Verlag, 1986.

[200] A. F. T. Mak and L. D. Huang, “Biomechanical Model for Pressure Ulcers,” vol. 119, no. November 1997, pp. 406–408, 2015.

[201] E. L. Wagnac, C.-E. Aubin, and J. Dansereau, “A new method to generate a patient-specific finite element model of the human buttocks.,” *IEEE Trans. Biomed. Eng.*, vol. 55, no. 2 Pt 1, pp. 774–783, 2008, doi: 10.1109/TBME.2007.912640.

[202] C. Y. Tang, W. Chan, and C. P. Tsui, “Finite Element Analysis of Contact Pressures between Seat Cushion and Human Buttock-Thigh Tissue,” *Engineering*, vol. 02, no. 09, pp. 720–726, 2010, doi: 10.4236/eng.2010.29093.

[203] E. M. H. Bosboom, M. K. C. Hesselink, C. W. J. Oomens, C. V. C. Bouten, M. R. Drost, and F. P. T. Baaijens, “Passive transverse mechanical properties of skeletal muscle under in vivo compression,” *J. Biomech.*, vol. 34, no. 10, pp. 1365–1368, 2001, doi: 10.1016/S0021-9290(01)00083-5.

[204] S. Loerakker, L. R. Solis, D. L. Bader, F. P. T. Baaijens, V. K. Mushahwar, and C. W. J. Oomens, “How does muscle stiffness affect the internal deformations within the soft tissue layers of the buttocks under constant loading?,” *Comput. Methods Biomech. Biomed. Engin.*, vol. 16, no. 5, pp. 520–529, 2013, doi: 10.1080/10255842.2011.627682.

[205] J.-S. Affagard, S. F. Bensamoun, and P. Feissel, “Development of an Inverse Approach for the Characterization of In Vivo Mechanical Properties of the Lower Limb Muscles,” *J. Biomech. Eng.*, vol. 136, no. 11, p. 111012, 2014, doi: 10.1115/1.4028490.

[206] S. B. JS Affagard, P Feissel, “Characterization of Muscle Displacement Field Using Ultrasound Technique,” *19th Congr. Eur. Soc. Biomech.*, no. Vi, p. 7337, 2012.

[207] J.-S. Affagard, P. Feissel, and S. F. Bensamoun, “Measurement of the quadriceps muscle displacement and strain fields with ultrasound and Digital Image Correlation (DIC) techniques,” *IRBM*, vol. 36, pp. 170–177, 2015, doi: 10.1016/j.irbm.2015.02.002.

[208] C. Then *et al.*, “A method for a mechanical characterisation of human gluteal tissue.,” *Technol. Heal. Care*, vol. 15, no. 6, pp. 385–398, 2007.

[209] R. M. A. Al-Dirini, J. Nisyrios, M. P. Reed, and D. Thewlis, “Quantifying the in vivo quasi-static response to loading of sub-dermal tissues in the human buttock using magnetic resonance imaging,” *Clin. Biomech.*, vol. 50, no. October 2016, pp. 70–77, 2017, doi: 10.1016/j.clinbiomech.2017.09.017.

[210] M. Makhsous *et al.*, “Use of MRI images to measure tissue thickness over the ischial tuberosity at different hip flexion,” *Clin. Anat.*, vol. 24, no. 5, pp. 638–645, 2011, doi: 10.1002/ca.21119.

[211] Y. Tamura, I. Hatta, T. Matsuda, H. Sugi, and T. Tsuchiya, “Changes in muscle stiffness during contraction recorded using ultrasonic waves,” *Nature*, vol. 299, pp. 6–8, 1982.

[212] R. M. A. Al-Dirini, M. P. Reed, and D. Thewlis, “Deformation of the gluteal soft tissues during sitting,” *Clin. Biomech.*, vol. 30, no. 7, pp. 662–668, 2015, doi: 10.1016/j.clinbiomech.2015.05.008.

[213] C. W. J. Oomens, D. L. Bader, S. Loerakker, and F. Baaijens, “Pressure Induced Deep Tissue Injury Explained,” *Ann. Biomed. Eng.*, vol. 43, no. 2, pp. 297–305, 2015, doi: 10.1007/s10439-014-1202-6.

[214] R. Salcido *et al.*, “Histopathology of pressure ulcers as a result of sequential computer-controlled pressure sessions in a fuzzy rat model.pdf,” *Advances in skin & wound care*, vol. 7, no. 5. pp. 25–34, 1980.

[215] V. D. Sree, M. K. Rausch, and A. B. Tepole, “Linking microvascular collapse to tissue hypoxia in a multiscale model of pressure ulcer initiation,” *Biomech. Model. Mechanobiol.*, vol. 18, no. 6, pp. 1947–1964, 2019, doi: 10.1007/s10237-019-01187-5.

[216] D. Lim, F. Lin, R. W. Hendrix, B. Moran, C. Fasanati, and M. Makhsous, “Evaluation of a new sitting concept designed for prevention of pressure ulcer on the buttock using finite element analysis,” *Med. Biol. Eng. Comput.*, vol. 45, no. 11, pp. 1079–1084, 2007, doi: 10.1007/s11517-007-0261-3.

[217] E. Linder-Ganz, “Mechanical compression-induced pressure sores in rat hindlimb: muscle stiffness, histology, and computational models,” *J. Appl. Physiol.*, vol. 96, no. 6, pp. 2034–2049, 2004, doi: 10.1152/japplphysiol.00888.2003.

[218] Y. C. Fung, *Biomechanics: Mechanical Properties of Living Tissue*. Springer-Verlag, 1993.

[219] T. J. Vogl *et al.*, “Mechanical soft tissue property validation in tissue engineering using magnetic resonance imaging experimental research,” *Acad Radiol*, vol. 17, no. 12, pp. 1486–1491, 2010, doi: 10.1016/j.acra.2010.08.010.

[220] H. M. Clarkson, *Musculoskeletal Assessment: Joint Range of Motion and Manual Muscle Strength*. Lippincott Williams & Wilkins, 2000.

[221] Z. Sadler, J. Scott, J. Drost, S. Chen, S. Roccabianca, and T. R. Bush, "Initial estimation of the in vivo material properties of the seated human buttocks and thighs," *Int. J. Non. Linear. Mech.*, vol. 107, no. July, pp. 77–85, 2018, doi: 10.1016/j.ijnonlinmec.2018.09.007.

[222] S. E. Sonenblum, S. H. Sprigle, J. M. Cathcart, and R. J. Winder, "3D anatomy and deformation of the seated buttocks," *J. Tissue Viability*, vol. 24, no. 2, pp. 51–61, 2015, doi: 10.1016/j.jtv.2015.03.003.

[223] R. H. R.W. Ogden, "Large deformation isotropic elasticity — on the correlation of theory and experiment for incompressible rubberlike solids," *Proc. R. Soc. London. Math. Phys. Sci.*, vol. 326, no. 1567, pp. 565–584, 1972.

[224] J. Guo, S. Hirsch, M. Scheel, J. Braun, and I. Sack, "Three-parameter shear wave inversion in MR elastography of incompressible transverse isotropic media: Application to in vivo lower leg muscles," *Magn. Reson. Med.*, vol. 75, no. 4, pp. 1537–1545, 2016, doi: 10.1002/mrm.25740.

[225] "SigmaStat." Systat Software, Inc., 2018.

[226] "MATLAB and Statistics Toolbox Release 2015b." The MathWorks, Inc., Natick, Massachusetts, USA, 2015.

[227] S. D. Darrah *et al.*, "Measuring static seated pressure distributions and risk for skin pressure ulceration in ice sledge hockey players Measuring static seated pressure distributions and risk for skin pressure ulceration in ice sledge hockey players," *Disabil. Rehabil. Assist. Technol.*, vol. 11, no. 3, 2016, doi: 10.3109/17483107.2014.921939.

[228] I. Janssen, S. B. Heymsfield, Z. M. Wang, and R. Ross, "Skeletal muscle mass and distribution in 468 men and women aged 18-88 yr," *J. Appl. Physiol.*, vol. 89, pp. 81–88, 2000, doi: 10.1152/jappl.2000.89.1.81.

[229] A. Macron, H. Pillet, J. Doridam, A. Verney, and P. Y. Rohan, "Development and evaluation of a new methodology for the fast generation of patient-specific Finite Element models of the buttock for sitting-acquired deep tissue injury prevention," *J. Biomech.*, vol. 79, pp. 173–180, 2018, doi: 10.1016/j.jbiomech.2018.08.001.

[230] N. Kadono and M. J. Pavol, "Effects of aging-related losses in strength on the ability to recover from a backward balance loss," *J. Biomech.*, vol. 46, no. 1, pp. 13–18, 2013, doi: 10.1016/j.jbiomech.2012.08.046.

[231] L. Demarré *et al.*, "The cost of prevention and treatment of pressure ulcers: A systematic review," *Int. J. Nurs. Stud.*, vol. 52, no. 11, pp. 1754–1774, 2015, doi: 10.1016/j.ijnurstu.2015.06.006.

[232] C. Wann-Hansson, P. Hagell, and A. Willman, "Risk factors and prevention among patients with hospital-acquired and pre-existing pressure ulcers in an acute care hospital,"

J. Clin. Nurs., vol. 17, no. 13, pp. 1718–1727, 2008, doi: 10.1111/j.1365-2702.2008.02286.x.

[233] T. H. Bup, P. Lestriez, K. Debrayl, and R. Taiarl, "Influence of Different Types of Wheelchair Cushions for Pressure Ulcers in View of the Experimental Approach," *Proc. IASTED Int. Conf.*, pp. 164–167, 2017, doi: 10.2316/P.2017.852-043.

[234] D. Zbogar, J. J. Eng, W. C. Miller, A. V. Krassioukov, and M. C. Verrier, "Physical activity outside of structured therapy during inpatient spinal cord injury rehabilitation," *J. Neuroeng. Rehabil.*, vol. 13, no. 1, pp. 1–11, 2016, doi: 10.1186/s12984-016-0208-8.

[235] D. Schmid and M. F. Leitzmann, "Television viewing and time spent sedentary in relation to cancer risk: A meta-analysis," *J. Natl. Cancer Inst.*, vol. 106, no. 7, 2014, doi: 10.1093/jnci/dju098.

[236] J. Scott, S. Chen, S. Roccabianca, and T. R. Bush, "The effects of body position on the material properties of soft tissue in the human thigh," *J. Mech. Behav. Biomed. Mater.*, vol. 110, 2020, doi: 10.1016/j.jmbbm.2020.103964.

[237] C. J. Richards, J. R. Steele, and G. M. Spinks, "Experimental Evaluation and Analytical Model of the Pressure Generated by Elastic Compression Garments on a Deformable Human Limb Analogue," *Med. Eng. Phys.*, 2020, doi: 10.1016/j.medengphy.2020.05.015.

[238] S. E. Sonenblum and S. H. Sprigle, "Buttock tissue response to loading in men with spinal cord injury," *PLoS One*, vol. 13, no. 2, pp. 1–15, 2018, doi: 10.1371/journal.pone.0191868.

[239] J. R. Basford, T. R. Jenkyn, K.-N. An, R. L. Ehman, G. Heers, and K. R. Kaufman, "Evaluation of healthy and diseased muscle with magnetic resonance elastography," *Arch. Phys. Med. Rehabil.*, vol. 83, no. 11, pp. 1530–1536, 2002, doi: https://doi.org/10.1053/apmr.2002.35472.

[240] L. Giangregorio and N. McCartney, "Bone Loss and Muscle Atrophy in Spinal Cord Injury : Epidemiology , Fracture Prediction , and Bone Loss and Muscle Atrophy in Spinal Cord Injury :," *J. Spinal Cord Med.*, vol. 29, no. 5, pp. 489–500, 2006, doi: 10.1080/10790268.2006.11753898.

[241] D. P. Lemmer *et al.*, "What Lies Beneath: Why Some Pressure Injuries May Be Unpreventable for Individuals With Spinal Cord Injury," *Arch. Phys. Med. Rehabil.*, vol. 100, no. 6, pp. 1042–1049, 2019, doi: 10.1016/j.apmr.2018.11.006.

[242] A. Gefen, "Tissue Changes in Patients Following Spinal Cord Injury and Implications for Wheelchair Cushions and Tissue Loading: A Literature Review," *Ostomy Wound Manag.*, vol. 60, no. 2, pp. 34–45, 2014.

[243] K. Ozer, O. Colak, F. B. Goktas, N. Sungur, and U. Kocer, "A rare location for a common problem: Popliteal pressure ulcer," *Int. Wound J.*, vol. 13, no. 2, pp. 287–288, 2016, doi: 10.1111/iwj.12257.

[244] D. P. Apatsidis, S. E. Solomonidis, and S. M. Michael, "Pressure Distribution at the

Seating Interface of Custom- Molded Wheelchair Seats : Effect of Various Materials," *Arch. Phys. Med. Rehabil.*, vol. 83, pp. 1151–1156, 2002, doi: 10.1053/apmr.2002.33987.

[245] C. M. Modlesky *et al.*, "Assessment of skeletal muscle mass in men with spinal cord injury using dual-energy X-ray absorptiometry and magnetic resonance imaging," *J. Appl.*, vol. 96, pp. 561–565, 2004.

[246] A. Mehta *et al.*, "Biplanar flap reconstruction for pressure ulcers: Experience in patients with immobility from chronic spinal cord injuries," *Am. J. Surg.*, vol. 203, no. 3, pp. 303–307, 2012, doi: 10.1016/j.amjsurg.2011.10.007.

[247] Y. K. Jan, M. A. Jones, M. H. Rabadi, R. D. Foreman, and A. Thiessen, "Effect of wheelchair tilt-in-space and recline angles on skin perfusion over the ischial tuberosity in people with spinal cord injury," *Arch. Phys. Med. Rehabil.*, vol. 91, no. 11, pp. 1758–1764, 2010, doi: 10.1016/j.apmr.2010.07.227.

[248] T. R. Bush and R. P. Hubbard, "Support Force Measures of Mid-Sized Men in Seated Positions," *J. Biomech. Eng. Asme*, vol. 129, no. 1, pp. 58–65, 2007, doi: 10.1115/1.2401184.

[249] J. Harrand and K. Bannigan, "Do tilt-in-space wheelchairs increase occupational engagement: A critical literature review," *Disabil. Rehabil. Assist. Technol.*, vol. 11, no. 1, pp. 3–12, 2016, doi: 10.3109/17483107.2014.932021.

[250] S. T. Leitkam, T. R. Bush, and M. Li, "A methodology for quantifying seated lumbar curvatures," *J. Biomech. Eng.*, vol. 133, no. 11, 2011, doi: 10.1115/1.4005400.

[251] H. L. Bartlett, L. H. Ting, and J. T. Bingham, "Accuracy of force and center of pressure measures of the Wii Balance Board," *Gait Posture*, vol. 39, no. 1, pp. 224–228, 2014, doi: 10.1016/j.gaitpost.2013.07.010.

[252] G. V. Zammit, H. B. Menz, and S. E. Munteanu, "Reliability of the TekScan MatScan® system for the measurement of plantar forces and pressures during barefoot level walking in healthy adults," *J. Foot Ankle Res.*, vol. 3, no. 1, pp. 1–9, 2010, doi: 10.1186/1757-1146-3-11.

[253] Y. Jan, D. M. Brienza, M. L. Boninger, and G. Brenes, "Comparison of skin perfusion response with alternating and constant pressures in people with spinal cord injury," *Spinal Cord*, vol. 49, pp. 136–141, 2011, doi: 10.1038/sc.2010.58.

[254] I. A. Braga, C. C. N. S. Pirett, R. M. Ribas, P. P. G. Filho, and A. D. Filho, "Bacterial colonization of pressure ulcers: Assessment of risk for bloodstream infection and impact on patient outcomes," *J. Hosp. Infect.*, vol. 83, no. 4, pp. 314–320, 2013, doi: 10.1016/j.jhin.2012.11.008.

[255] S. E. Sonenblum, S. H. Sprigle, and J. S. Martin, "Everyday sitting behavior of full-time wheelchair users," *J. Rehabil. Res. Dev.*, vol. 53, no. 5, pp. 585–598, 2016, doi: 10.1682/JRRD.2015.07.0130.

[256] S. E. Sonenblum, S. Sprigle, F. H. Harris, and C. L. Maurer, "Characterization of Power

Wheelchair Use in the Home and Community," *Arch. Phys. Med. Rehabil.*, vol. 89, no. 3, pp. 486–491, 2008, doi: 10.1016/j.apmr.2007.09.029.

[257] M. Makhsous *et al.*, "Periodically Relieving Ischial Sitting Load to Decrease the Risk of Pressure Ulcers," *Arch. Phys. Med. Rehabil.*, vol. 88, no. 7, pp. 862–870, 2007, doi: 10.1016/j.apmr.2007.03.017.

[258] C. L. Maurer and S. Sprigle, "Effect of Seat Inclination on Seated Pressures of Individuals With Spinal Cord Injury," *Phys. Ther.*, vol. 84, no. 3, pp. 255–261, 2004, doi: 10.1093/ptj/84.3.255.

[259] V. D. Sree, M. K. Rausch, and A. B. Tepole, "Linking microvascular collapse to tissue hypoxia in a multiscale model of pressure ulcer initiation," *Biomech. Model. Mechanobiol.*, vol. 18, no. 6, pp. 1947–1964, 2019, doi: 10.1007/s10237-019-01187-5.

[260] J. A. Whitney *et al.*, "Guidelines for the treatment of pressure ulcers," *Wound Repair Regen.*, vol. 14, no. 6, pp. 663–679, 2006, doi: 10.1111/j.1524-475X.2006.00175.x.

[261] D. Hanson, D. K. Langemo, J. Anderson, P. Thompson, and S. Hunter, "Friction and shear considerations in pressure ulcer development.," *Adv. Skin Wound Care*, vol. 23, no. 1, pp. 21–24, 2010, doi: 10.1097/01.asw.0000363489.38996.13.

[262] T. R. Bush, "Support Force Measures of Midsized Men in Seated Positions," *J. Biomech. Eng.*, vol. 129, no. 1, p. 58, 2006, doi: 10.1115/1.2401184.

[263] K. Kobara, H. Osaka, H. Takahashi, T. Ito, D. Fujita, and S. Watanabe, "Effect of rotational axis position of wheelchair back support on shear force when reclining," *J. Phys. Ther. Sci.*, vol. 26, no. 5, pp. 701–706, 2014, doi: 10.1589/jpts.26.701.

[264] B. E. Dicianno *et al.*, "RESNA position on the application of tilt, recline, and elevating legrests for wheelchairs," *Assist. Technol.*, vol. 21, no. 1, pp. 13–22, 2009, doi: 10.1080/10400430902945769.

[265] L. C. Gerhardt, N. Mattle, G. U. Schrade, N. D. Spencer, and S. Derler, "Study of skin-fabric interactions of relevance to decubitus: Friction and contact-pressure measurements," *Ski. Res. Technol.*, vol. 14, no. 1, pp. 77–88, 2008, doi: 10.1111/j.1600-0846.2007.00264.x.

[266] S. Sprigle, W. Dunlop, and L. Press, "Reliability of Bench Tests of Interface Pressure," *Assist. Technol.*, vol. 15, no. 1, pp. 49–57, 2003, doi: 10.1080/10400435.2003.10131889.

[267] L. R. Alejano, J. González, and J. Muralha, "Comparison of different techniques of tilt testing and basic friction angle variability assessment," *Rock Mech. Rock Eng.*, vol. 45, no. 6, pp. 1023–1035, 2012, doi: 10.1007/s00603-012-0265-7.

[268] R. Ulusay and H. Karakul, "Assessment of basic friction angles of various rock types from Turkey under dry, wet and submerged conditions and some considerations on tilt testing," *Bull. Eng. Geol. Environ.*, vol. 75, no. 4, pp. 1683–1699, 2016, doi: 10.1007/s10064-015-0828-4.